

**Molecular and physiological characterization  
of a novel PHYA mutant allele in  
*Arabidopsis thaliana***

**Inaugural-Dissertation**

zur Erlangung des Doktorgrades  
der Mathematisch-Naturwissenschaftlichen Fakultät  
der Universität zu Köln

vorgelegt von

**Vladyslava Sokolova**  
aus Kiev, Ukraine

Köln, 2011

Diese Arbeit wurde am  
Biological Research Centre in Szeged  
in der Institute of Plant Biology  
durchgeführt

Prüfungsvorsitzender: **Prof. Dr. Martin Hülskamp**

Berichterstatter: **Prof. Dr. George Coupland**  
**Prof. Dr. Ute Höcker**

Tag der mündlichen Prüfung: 05.12.2011

## TABLE OF CONTENTS

<b>TABLE OF CONTENTS</b> .....	3
<b>ABBREVIATIONS</b> .....	5
<b>1 INTRODUCTION</b> .....	7
1.1 Light perception .....	7
1.2 Phytochromes overview .....	8
1.2.1 Properties and functions .....	8
1.2.2 Molecular structure .....	9
1.2.3 Photoconversion .....	10
1.2.4 Phytochrome-mediated responses .....	11
1.2.5 Intracellular accumulation and distribution .....	12
1.3 Regulation of phytochrome A nuclear transport .....	14
1.4 Phytochrome signaling .....	16
1.4.1 Phytochrome kinase activity .....	16
1.4.2 Phytochrome interacting factors .....	17
1.4.3 Signal integration .....	18
1.5 Aim of this study .....	19
<b>2. MATERIALS AND METHODS</b> .....	20
2.1. MATERIALS .....	20
2.1.1 Chemicals, enzymes, oligonucleotides, cloning vectors .....	20
2.1.2 Buffers, solutions, media, antibiotics .....	20
2.1.3 Bacterial and yeast strains .....	21
2.1.4 Plant materials .....	22
2.1.5 Oligonucleotides .....	22
2.1.6 Softwares and databases .....	26
2.1.7 Databases accession numbers .....	26
2.2. METHODS .....	27
2.2.1 Molecular techniques .....	27
2.2.1.1 Plant total DNA isolation .....	27
2.2.1.2 Bacterial plasmid DNA isolation .....	27
2.2.1.3 Plant total RNA isolation .....	28
2.2.1.4 Polymerase chain reaction (PCR) amplification .....	28
2.2.1.5 Digestion and ligation .....	29
2.2.1.6 Cloning of PHYA and constructs generation .....	30
2.2.1.7 Molecular mapping .....	31
2.2.1.8 Quantitative RT-PCR .....	31
2.2.1.9 Plant total protein extraction .....	32
2.2.1.10 Protein level analysis .....	32
2.2.2 Bacterial and yeast applied methods .....	33
2.2.2.1 <i>E. coli</i> transformation .....	33

2.2.2.2 <i>Agrobacterium tumefaciens</i> transformation.....	34
2.2.2.3 Yeast transformation.....	34
2.2.3 Plant applied methods.....	35
2.2.3.1 Plant growth and light conditions.....	35
2.2.3.2 Hypocotyl length and cotyledon angle measurement.....	35
2.2.3.3 Crossing.....	36
2.2.3.4 Segregation analysis.....	36
2.2.3.5 <i>Agrobacterium</i> -mediated transformation of <i>Arabidopsis thaliana</i> .....	36
2.2.3.6 Epifluorescence microscopy.....	36
<b>3. RESULTS</b> .....	<b>38</b>
3.1 Identification of the <i>psm</i> mutation.....	38
3.1.1 Genetic mapping to define the mutant locus.....	38
3.1.2 Confirmation of the position of mutation by transgenic plants.....	42
3.2 Physiological characterization of <i>phyA-5</i> .....	43
3.2.1 Photomorphogenic responses.....	43
3.2.2 High Irradiation Response and action spectrum.....	46
3.2.3 Very Low Fluence Response.....	48
3.3 <i>PhyA-5</i> transcription analysis.....	52
3.4 <i>PhyA-5</i> protein level analysis.....	54
3.5 Subcellular localization of <i>phyA-5</i> protein.....	56
3.6 Molecular interaction of <i>PHYA-5</i> with nuclear transport facilitators.....	59
3.7 Complementation of the <i>phyA-201</i> mutant by <i>phyA-5</i> -YFP-NLS and <i>phyA</i> -YFP-NLS fusion proteins.....	63
<b>4. DISCUSSION</b> .....	<b>66</b>
<b>5. SUMMARY - ZUSAMMENFASSUNG</b> .....	<b>74</b>
5.1 Summary.....	74
5.2 Zusammenfassung.....	75
<b>6. REFERENCES</b> .....	<b>77</b>
<b>APPENDIX</b> .....	<b>90</b>
<b>ACKNOWLEDGMENTS</b> .....	<b>91</b>
<b>LEBENS LAUF</b> .....	<b>92</b>
<b>EIDESSTATTLICHE ERKLÄRUNG</b> .....	<b>93</b>

## ABBREVIATIONS

A. tumefaciens	<i>Agrobacterium tumefaciens</i>
bp	basepair
bHLH	basic helix-loop-helix
CAPS	cleaved amplified polymorphic sequences
cDNA	complementary deoxyribonucleic acid
Chr	chromosome
Col	Columbia ecotype
CTAB	cetyltrimethylammoniumbromid
dCAPS	derived cleaved amplified polymorphic sequences
DNA	deoxyribonucleic acid
E. coli	<i>Escherichia coli</i>
EDTA	ethylenediaminetetraacetic acid
FHL	FHY1-LIKE
FHY1	FAR-RED ELONGATED HYPOCOTYL 1
FP	forward primer
FR	far-red
FRC	fluence rate curve
GAF	cGMP-specific phosphodiesterases, adenylyl cyclases and FhlA domain
h	hour
HFR1	LONG HYPOCOTYL IN FAR-RED 1
HIR	high irradiance response
HKRD	histidin kinase related domain
kb	kilobasepair
kDa	kiloDalton
LAF1	LONG AFTER FAR-RED LIGHT 1
Ler	Landsberg erecta ecotype
LFR	low fluence response
Mbp	megabasepair
mRNA	messenger ribonucleic acid
NB	nuclear body
NES	nuclear export sequence

## ABBREVIATIONS

NLS	nuclear localization signal
NTE	amino terminal extension domain
PAS	PER/ARNT/SIM domains
PCR	polymerase chain reaction
PEG	polyethylene glycol
Pfr	far-red light absorbing form
PHY	phytochrome domain
PHYA-E	PHYTOCHROME A-E
PIF	phytochrome-interacting factor
Pr	red light absorbing form
PVDF	polyvinylidene fluoride
PVP-40	polyvinylpyrrolidone
qRT-PCR	real-time quantitative reverse transcription PCR
R	red
RNA	ribonucleic acid
RP	reverse primer
RT-PCR	reverse transcribed polymerase chain reaction
SDS-PAGE	sodium dodecyl sulphate polyacrylamide gel electrophoresis
SSLP	simple sequence length polymorphism
Ta	annealing temperature
UTR	untranslated region
VLFR	very low fluence response
Ws	Wassilewskija ecotype
WT	wild-type
YFP	yellow fluorescent protein

## 1. INTRODUCTION

### 1.1 Light perception

Plants are photoautotrophic sessile organisms, whose immobility requires constant monitoring and precise synchronization of physiological events with environmental conditions throughout the plants' life cycle. Light is a major environmental factor, serving not only as an energy source, but also as a regulation signal of multiple physiological processes through a wide range of signaling pathways. Light delivers information about time and seasons, mediates induction or inhibition of developmental processes (flowering, breaking of bud dormancy, induction or inhibition of germination), regulates circadian events (opening and closing of stomata and flowers), provides positional information, influences directional growth and adult architecture (Chen *et al.*, 2004). Generally, light affects plants in several different ways: (i) providing the energy source via photosynthesis; (ii) directing the movement of plants and their parts, called phototropic response; (iii) controlling and regulating plant development, called photomorphogenesis (Schaefer and Nagy, 2005).

Plants have developed a set of light-sensing molecules – photoreceptors, which allow plants to sense the quantity, quality, direction and duration of light. The interaction of the light stimulus via photoreceptors with the internal plant processes initiates and regulates multiple signaling pathways, resulting in the appropriate physiological response.

Photoreceptors are categorized into three different classes according to the light wavelength which they perceive. Red and far-red light is absorbed by the phytochromes (phy) (Furuya and Schäfer, 1996; Batschauer, 1999). Blue and ultraviolet-A light is perceived by the cryptochromes (*CRY*) and the phototropins (*PHOT*) (Cashmore *et al.*, 1999; Christie and Briggs, 2001). Also, it has been recently shown that ultraviolet-B light in plants is perceived by *UV RESISTANCE LOCUS8 (UVR8)* (Rizzini *et al.*, 2011).

In *Arabidopsis thaliana*, two cryptochrome genes have been characterized: *CRY1* and *CRY2* (Ahmad and Cashmore, 1993, Ahmad *et al.*, 1995, Lin *et al.*, 1996, 1998). The phototropin family consists of two members, *PHOT1* and *PHOT2* (Huala *et al.*, 1997; Christie *et al.*, 1998; Sakai *et al.*, 2001).

The phytochrome gene family has five members, named phytochrome A (*PHYA*) through *PHYE* in *Arabidopsis thaliana* (Sharrock and Quail, 1989; Clack *et al.*, 1994).

## 1.2 Phytochromes overview

### 1.2.1 Properties and functions

Phytochromes have been discovered in all flowering plants, ferns, mosses and cyanobacteria (Mathews *et al.*, 1997). They perceive the red and far-red region of the light spectrum (650 - 750 nm). Phytochromes regulate the majority of plant developmental transitions, including seed germination, inhibition of hypocotyl growth, cotyledon opening, anthocyanin production, flavonoid and chlorophyll synthesis, apical dominance, detection of neighbors and timing of flowering (Nagy and Schäfer, 2002).

The classical approach divides phytochromes to “light-labile” Type I (phyA) and “light-stable” Type II (phyB-E) (Sharrock and Quail, 1989). The dominant phytochrome of etiolated plants is phyA, which highly accumulates in darkness (Clough *et al.*, 1999), and whose extreme photosensitivity allows perceiving the weakest light, for example in the soil under ground level. Phytochrome A is quickly degraded upon R light irradiation, and thereby phyB becomes the dominant PHY of light-grown plants (Sharrock and Clack, 2002). Because of the difference in stability in response to light, the relative abundance of phyA and phyB changes during de-etiolation, growth and development of plants. This leads in some cases to phyA/phyB antagonizing each other, for example during the shade-avoidance response (Franklin *et al.*, 2005). Additionally, it has been shown that phyA has a role in the perception of day length both in young seedlings and in mature *Arabidopsis* (Emma *et al.*, 1994); phyD and phyE are more closely related to phyB, and mediate shade avoidance responses (petiole elongation and flowering time) together (Franklin *et al.*, 2005; Devlin *et al.*, 1999.). phyE has specific roles in regulating internode elongation (Devlin *et al.*, 1998) and seed germination (Hennig *et al.*, 2002). phyC was shown to regulate leaf expansion (Qin *et al.*, 1997) and to participate in the modulation of blue light sensing (Franklin *et al.*, 2003).

The importance of phytochromes was demonstrated by studying the phytochrome quintuple mutant. Seed germination of the quintuple phytochrome mutants failed to respond to light, indicating that no other photoreceptors are able to break seed dormancy (Strasser *et al.*, 2010). If germination problems are bypassed by the addition of gibberellins (Yamaguchi *et al.*, 1998), continuous red light failed to inhibit hypocotyl

growth and promote proper plant architecture in the quintuple phytochrome mutant. The quintuple phytochrome mutant was also unable to develop under red light beyond a few rudimentary leaves. In white-light-grown plants, no response to red/far-red ratio was observed, confirming the role of phytochromes as the only sensors of red/far-red ratio. After growth under white light, returning the quintuple phytochrome mutant to red light resulted in rapid senescence of already expanded leaves and severely impaired expansion of new leaves (Strasser *et al.*, 2010)

### 1.2.2 Molecular structure

Functional phytochrome acts as a dimer, and its monomers are large (about 124 kDa) water-soluble proteins, each of them covalently binding an open tetrapyrrole chain by a thioether bond. All phytochromes were shown to form heterodimers, except for phyA which forms homodimers only (Sharrock and Clack, 2004).

Monomers of plant phytochromes consist of two structural domains - globular N-terminal and C-terminal domains - that are connected by a proteolytically vulnerable hinge region (Quail, 1997).

The C-terminal domain is responsible for the dimerization of phytochrome molecules (Edgerton and Jones, 1992) via PAS (PER-ARNT-SIM) domains. Besides two PAS domains, the C-terminal part also contains two histidine kinase-related domains (HKRD), which show homology to bacterial histidine kinases (Schneider-Poetsch *et al.*, 1991; Yeh *et al.*, 1998). The region containing the first HKRD and the PAS motifs form a hot spot for missense mutations that lead to a reduction in light responses (Xu *et al.*, 1995; Yanovsky *et al.*, 2002). The C-terminal half of phyA has been shown to mediate interaction with several proteins, namely nucleoside diphosphate kinase 2 (Choi *et al.*, 1999), phytochrome kinase substrate 1 (Fankhauser *et al.*, 1999) and the basic helix-loop-helix transcription factor PIF3 (Ni *et al.*, 1998, 1999). As opposed to phyB, whose C-terminal part is not crucial for PHYB-directed photomorphogenesis (Matsushita *et al.*, 2003, Palágyi *et al.*, 2010), phyA requires it for HIR signaling (Cherry *et al.*, 1993; Wolf *et al.*, 2011).

The N-terminal domain is responsible for defining the functional characteristics of phytochromes (Wagner *et al.*, 1996a; Mateos *et al.*, 2006), determining whether a phytochrome molecule exhibits the functional characteristics of the light-labile phyA or the light-stable phyB photoreceptor. This part of the molecule carries a single covalently linked linear tetrapyrrole chromophore (phytochromobilin) (Wagner *et al.*, 1996a). The

N-terminal part of plant phytochromes contains three conserved domains: PAS domain, GAF and PHY domain. Together they form a core photosensory domain and exhibit bilin lyase activity, ligating the chromophore to a cysteine residue of the GAF domain (Wu and Lagarias, 2000).

The PHY domain is conserved in all phytochromes and required for proper modulations of phytochrome activity. Deletion of the PHY domain in PHYB causes the instability of the Pfr form and the shift in absorption to a blue spectrum by both Pr and Pfr (Oka *et al.*, 2004). Missense mutation in this domain of PHYB causes hypersensitivity to R light (Kretsch *et al.*, 2000). Natural variation of PHYA in this region displays reduction in PHYA activity and blue shift for Pfr absorption (Maloof *et al.*, 2001).

The extreme N-terminus (amino terminal extension domain (NTE)) is rich in serine residues, which are subjects of phosphorylation (Lapko *et al.*, 1997, 1999). It displays structural modifications during photoconversion from the red-light-absorbing Pr to Pfr form (Moller *et al.*, 2002). Experiments performed with modified N-terminal part of phyA suggest that this part of the protein plays a role in the stabilization of phytochrome and its Pfr conformation as well as in the regulation of phytochrome-mediated responses and signal attenuation (Cherry *et al.*, 1992; Stockhaus *et al.*, 1992; Jordan *et al.*, 1996, 1997; Wagner *et al.*, 1996b; Casal *et al.*, 2002; Trupkin *et al.*, 2007).

### 1.2.3 Photoconversion

Phytochromes are characterized by the presence of the bilin/tetrapyrrole chromophore (Smith, 2000, Quail, 2002), association of which with the phytochrome apoprotein enables detection of light. The molecular mechanism of light perception is driven by phototransformation between the two spectrally distinct forms of phytochromes, the red-light absorbing (Pr, absorption maximum ~660 nm) and the far-red light absorbing (Pfr, absorption maximum ~730 nm) forms (Butler *et al.*, 1959). Phytochrome proteins, which are synthesized in their red-light-absorbing form, are considered to be inactive. They can be phototransformed into the far-red-light absorbing active form by exposure to red light (Vierstra and Quail, 1983). Pfr formation triggers signal transduction, which in turn affects gene expression through the transcriptional network (Nagy and Schäfer, 2002). Since sunlight is enriched in red light (compared to far-red light), phytochromes predominantly exist in the Pfr form in the light, and can convert back to the Pr form during periods of darkness through a process known as dark reversion. Photoconversion back to Pr can also be mediated by pulses of far-red light

(Sineshchekov 1995; Braslavsky *et al.*, 1997). Despite different absorption maxima, the Pr and Pfr forms have overlapping absorption spectra. The Pfr and Pr forms of type II phytochromes (phyB-E) are stable in light, and levels of the two isoforms are proportional to the ratio of R and FR light perceived. This allows the light-stable phytochromes to work as sensors of light quality. The light-labile phyA works in a different way. In etiolated seedlings, phyA Pr accumulates in the very high levels, and because of the overlapping absorption spectra of the Pr and Pfr forms, even a small amount of R or FR light is sufficient to generate phyA-Pfr (Shinomura *et al.*, 1996). Taken together with the fact that plants are not generally exposed to simple monochromatic light, but to a wide light spectrum, accumulated data demonstrate that the phytochrome photosensing system works as a dynamic equilibrium between the Pr and Pfr forms, allowing plants to sense the red/far-red ratio of the light environment and to respond accordingly (reviewed by Schäfer and Bowler, 2002).

Upon photoconversion the domain conformation of phytochromes significantly changes through apoprotein–chromophore and inter–domain interactions. The N-terminal 6 kDa region forms an  $\alpha$ -helical conformation in Pfr, but exists in a random coil conformation in Pr. This conformational modification results in a more exposed chromophore in Pfr as compared to Pr (Deforce *et al.*, 1994; Singh *et al.*, 1989; Vierstra *et al.*, 1987). The 6 kDa-peptide seems to interact directly with the chromophore and possibly with other structural motifs, causing a series of conformational changes. The N-terminal domain is more exposed in the Pr form than in the Pfr form (Lapko *et al.*, 1998).

The hinge region, shielded in Pr form, is exposed in Pfr and Ser-598 may be phosphorylated (Quail 1997; Fankhause *et al.*, 1999). The Pr and Pfr phytochromes also exhibit differential exposure of tryptophan residues (Singh *et al.*, 1988, 1989, 1990).

Taken together, these observations suggest that conformational changes are an essential part of phytochrome photoactivation.

#### **1.2.4 Phytochrome-mediated responses**

Phytochrome responses have been divided into three categories, based on wavelength, fluence and intensity of the perceived light and reversibility of the effect: very low fluence responses (VLFRs), low fluence responses (LFRs) and high irradiance responses (HIRs). HIRs are now further subdivided into R- and FR-HIRs (Nagy and Schäfer, 2002).

The LFRs are induced by single short exposure to R light and are reversible by FR light. These responses are mediated by light-stable phytochromes (phyB,C,D,E), whose stable Pfr form results in high Pfr/Pr ratio.

The light-labile phyA mediates responses (HIR and VLFR) that are characterized by low Pfr/Pr ratio and are not R/FR reversible (Smith and Whitelam, 1990). High levels of phyA in the etiolated seedlings are responsible for the VLFR, which is triggered by extremely low amounts of light (Hennig *et al.*, 1999; Eichenberg *et al.*, 2000). Historically, it was observed that “safe” green light is sufficient to inhibit the growth of corn mesocotyles (Mandoli and Briggs, 1981). It was also described that a short pulse of irradiation with low intensity is sufficient to promote germination (Botto *et al.*, 1996). VLFRs are defined as induced by short pulses of irradiation with low intensity, which leads to very low levels of Pfr irrespective of wavelength (Casal *et al.*, 1997).

PhyA also controls the FR high irradiance response, which can be generated by continuous high-fluence FR light (Schäfer and Bowler, 2002). HIR was defined as a high energy reaction under prolonged irradiation of relatively high intensity (Smith and Whitelam 1990). Under such conditions the ratio of Pfr/Pr forms is extremely low. HIRs are not R/FR reversible and require continuous irradiation, because even short intermittent dark phases lead to the breakdown of the response (Mancinelli, 1994; Buche *et al.*, 2000; Dieterle *et al.*, 2001). The action spectrum of the FR-HIR reveals a maximum at about 730 nm, and under such conditions 3 to 7% of all phytochrome molecules remain in the Pfr form (Shinomura *et al.*, 2000). The necessity to maintain a low level of Pfr for long periods of time required for HIRs leads to the following conclusion. These responses are important for plant development in closed habitats, such as in deep shade or in the soil below the ground level, which are characterized by low ratios of R:FR (Yanovsky *et al.*, 1995). The responses induced by HIR and maintained by phyA are seed germination, anthocyanin production, axis elongation and flowering induction (Smith, 2000).

### **1.2.5 Intracellular distribution of phytochromes**

The intracellular distribution of the photoreceptor is a crucial condition for understanding light signal transduction. Accumulated data indicate that phytochrome signal transduction requires a combination of multiple processes and takes place in different subcellular compartments. Subcellular localization of the phytochromes changes dynamically and is regulated by light in a quality and quantity dependent manner at

multiple levels (Lorrain *et al.*, 2006; Nagatani, 2004). Multiple studies have revealed that phytochromes are located in the cytoplasm in darkness, and enter the nucleus in a light quality and quantity dependent manner (Sakamoto and Nagatani, 1996; Yamaguchi *et al.*, 1999; Kircher *et al.*, 1999, 2002; Hisada *et al.*, 2000).

In contrast to phyB, whose presence in the nucleus has been confirmed even in etiolated seedlings (Gil *et al.*, 2000), endogenous phyA in etiolated seedlings has been shown immunocytochemically to be dispersed throughout the cytosol (McCurdy and Pratt, 1986; Speth *et al.*, 1986; Pratt, 1994). These results have been confirmed by studying the distribution of the phyA-GFP fusion protein in the cytosol (Kircher *et al.*, 1999, 2002; Hisada *et al.*, 2000).

phyA Pr accumulates at very high levels in the dark (Sharrock and Clack 2002). When plants transition from the dark to an illuminated environment, phyA undergoes rapid proteasomal degradation, which is preceded by ubiquitination (Jabben *et al.*, 1989a, 1989b) and phosphorylation (Saijo *et al.*, 2008). The phyA protein level also decreases rapidly, when it is expressed under the control of the constitutive 35S promoter (Kim *et al.*, 2000). It has also been shown that dark-to-light transition decreases the level of *PHYA* mRNA and, consequently, the synthesis of phyA protein (Sharrock and Quail 1989).

It has been demonstrated that the photoconversion of phytochrome to the Pfr form triggers translocation of the photoreceptor to the nucleus (Sakamoto and Nagatani, 1996; Kircher *et al.*, 1999). However, a considerable amount of intracellular Pfr phytochromes is not transferred to the nucleus (Nagy and Schäfer, 2002).

The light quality necessary for the nuclear transfer of phytochromes correlates with the light specificities of phyA and phyB. The light-labile phyA translocates to the nucleus much faster than the light-stable phyB,C,D,E (Kircher *et al.*, 2002; Nagy and Schäfer, 2002). phyB is efficiently transported into the nucleus in response to R light and this response is reversible by FR light, like a typical LFR. Similar regulation of the subcellular localization has also been reported for phyC, phyD and phyE (Kircher, *et al.*, 1999; Yamaguchi *et al.*, 1999; Kircher *et al.*, 2002; Nagatani, 2004; reviewed Kevei *et al.*, 2007).

The nuclear import of phyA is a rapid process in etiolated seedlings. A single light pulse (5 min) of any light quality (FR, R, B) induces nuclear import of phyA (Hisada *et al.*, 2000; Kim *et al.*, 2000; Kircher *et al.*, 2002). These data suggest that nuclear import of phyA correlates with phyA-mediated VLFRs. In addition, continuous FR light also

initiates nuclear transport (Kircher *et al.*, 1999), suggesting that nuclear import of phyA also correlates with phyA-mediated HIRs.

Continuous FR light or brief R light pulses initiate the formation of phyA-containing nuclear bodies (NB) (Hisada *et al.*, 2000; Kim *et al.*, 2000; Kircher *et al.*, 1999, 2002). Such structures are considered to be sites of ubiquitin-mediated degradation of phyA. Several studies also support the idea that localization of phyA in NBs is important for its function (Chen *et al.*, 2003; Hiltbrunner *et al.*, 2005; Kevei *et al.*, 2007; Rösler *et al.*, 2007; Chen, 2008).

PhyA also forms light-induced cytoplasmic bodies (Speth *et al.*, 1986; Nagatani 2004; Kevei *et al.*, 2007). The study of a mutant, which shows no phyA nuclear import (Rösler *et al.*, 2007) has revealed that it still exhibits light-induced phyA degradation. The suggestion that phyA could be degraded not only in the nucleus, but also in the cytosol has been confirmed by studying phyA-GFP derivatives containing either nuclear localization (NLS) or export signal (NES) sequences (Toledo-Ortiz *et al.*, 2010). It has also been shown that the degradation rate of phyA is faster in the nucleus than in the cytoplasm (Debrieux and Fankhauser, 2010; Toledo-Ortiz *et al.*, 2010)

### 1.3 Regulation of phytochrome A nuclear transport

Nuclear translocation of phyA is a crucial part of phyA-mediated signaling. As opposed to phyB, which was postulated to enter the nucleus by the general nuclear import machinery after light-induced unmasking of an NLS (Chen *et al.*, 2005), no NLS motif has been identified in phyA, suggesting the existence of transport facilitators for phytochrome A nuclear translocation.

An early study led to the identification of the *FARRED ELONGATED HYPOCOTYL 1* and *3* (*FHY1* and *FHY3*) genes. Mutations in these genes cause pronounced hyposensitive phenotype in FR, indicating their essential role in phyA signaling (Whitelam *et al.*, 1993). Later, a homolog of the *FHY1*: *FHY1-LIKE* (*FHL*) (Zhou *et al.*, 2005) and of *FHY3*: *FAR RED IMPAIRED RESPONSE 1* (*FARI*) (Hudson *et al.*, 1999) were identified.

It has been shown that both HIR and VLFR are impaired in the *fhyl* mutant (Cerdan *et al.*, 1999), which supports the idea of *FHY1* playing an essential role in phyA signaling. Later it was demonstrated that nuclear accumulation of phyA is reduced in the

*fhy1* mutant, suggesting that *FHY1* may regulate nuclear accumulation of phyA (Hiltbrunner *et al.*, 2005). The phenotype of the *fhy1/fhl* double mutant is similar to the phyA null mutant (Rosler *et al.*, 2007), and nuclear accumulation of phyA in the mutant has not been detected (Rosler *et al.*, 2007; Hiltbrunner *et al.*, 2006). These results confirm that nuclear accumulation of phyA is crucial to phyA functioning and suggest that both *FHY1* and *FHL* are required for nuclear accumulation of the photoreceptor.

*FHY1* and *FHL* encode small (23 and 20 kDa, respectively) plant-specific proteins which have functional NLS and NES sequences, although it has been shown that the NLS, but not the NES, is required for the proper protein functioning (Desnos *et al.*, 2001; Zeidler *et al.*, 2004; Zhou *et al.*, 2005). *FHY1* and *FHL* have been shown to colocalize with phyA in early NBs and directly interact with light-activated phyA through their conserved carboxyl-terminal domains (Hiltbrunner *et al.*, 2005, 2006). This interaction requires the first 406 amino acids of phyA (Hiltbrunner *et al.*, 2006).

The first model stated that the Pfr form of phyA interacts with *FHY1/FHL* in the cytoplasm after light activation and the complex is imported into the nucleus, which was shown *in vitro* and supported by *in planta* microscopic studies (Hiltbrunner *et al.*, 2005, 2006; Genoud *et al.*, 2008).

Later the preferentiality (but not exclusivity) of *FHY1* and *FHL* binding to phyA Pr was demonstrated using *in vivo* co-immunoprecipitation approaches (Saijo *et al.*, 2008, Shen *et al.*, 2009, Yang *et al.*, 2009). Very recent data reveal that the phyA Pfr-*FHY1/FHL* complexes are more stable than the phyA Pr-*FHY1/FHL* complexes and phyA Pfr is necessary for nuclear import (Rausenberger *et al.*, 2011). Curiously, one of the studies have shown that phyA, *FHY1*, *FHL*, *LAF1*, and *HFR1* are components of protein complexes *in vivo*, suggesting that *FHY1* and *FHL* might have another role besides nuclear translocation of phyA (Yang *et al.*, 2009).

*FHY3* and *FAR1* are novel types of transcriptional regulators that have evolved from a mutator-like transposase. They were believed to participate in phyA signaling by regulation of gene expression (Wang and Deng, 2002; Hudson *et al.*, 2003). Later it was shown that *FHY3* and *FAR1* indirectly control phyA nuclear accumulation by promoting the expression of *FHY1* and *FHL*. These transcription factors directly bind to sequences upstream of the transcription start sites of *FHY1* and *FHL* (Lin *et al.*, 2007). The nuclear accumulation of phyA is slightly reduced in *fhy3* and strongly reduced in the *fhy3/far1* double mutant, confirming their role in phyA nuclear accumulation (Lin *et al.*, 2007).

It has been demonstrated that *FHY1/FHL* transcript levels are rapidly down-regulated in etiolated plants upon exposure to FR light (Desnos *et al.*, 2001; Lin *et al.*, 2007), suggesting that *FHY1/FHL* expression is subject of negative feedback regulation by phyA signaling. *ELONGATED HYPOCOTYL 5 (HY5)* is a well-characterized bZIP transcription factor involved in promoting photomorphogenesis (Oyama *et al.*, 1997; Osterlund *et al.*, 2000a; Ulm *et al.*, 2004; Lee *et al.*, 2007). HY5 has been recently identified as a regulator of *FHY1/FHL* expression (Li *et al.*, 2010). It has been demonstrated that *HY5* directly binds ACGT-containing elements a few base pairs away from the FHY3/FAR1 binding sites in the *FHY1/FHL* promoters by physically interacting with FHY3/FAR1 through their DNA binding domains, and negatively regulates FHY3/FAR1-activated *FHY1/FHL* expression under the FR light (Li *et al.*, 2010).

## 1.4 Phytochrome signaling

Phytochrome actions are divided into two parts at the molecular level, namely perception of the light signal and its transformation to biochemical signals. Thus, phytochromes exhibit dual molecular functions: a sensory function responsible for detecting relevant light signals, and a regulatory function in which the perceived information is transferred to downstream transduction pathways (reviewed Smith, 2000).

Current concepts of the phytochrome-mediated mechanism of gene expression regulation consist of three parts: (i) phytochromes act as kinases on multiple substrates, regulating the expression of genes differentially; (ii) phytochromes have several specific reaction partners that direct signal transduction towards the selective control of gene expression; (iii) both elements of the early pathway segment converge at several negative and positive regulators.

### 1.4.1 Phytochrome kinase activity

The C-terminal half of phytochromes contains two regions similar to the bacterial histidine kinases, and the possibility of plant phytochromes acting as light-regulated kinases and transferring light signals by transphosphorylation of interacting partners has been discussed for years. Phytochrome kinase substrate (PKS1), a cytosol located protein has been shown to be phosphorylated by the oat Pfr phyA in the serin or threonin residue (Fankhauser *et al.*, 1999). The kinase activity of phyA has been also suggested to act on cryptochromes (Ahmad *et al.*, 1998). A nucleoside diphosphate kinase (NDPK1), which

is located in both cytosol and nucleus, has been identified as interactor of phyA. NDPK1 has been shown to increase kinase activity after incubation with the recombinant oat Pfr phyA (Choi *et al.*, 1999).

The possible link between kinase activity and phytochrome signaling through interaction of phyA with PKS1 in the cytosol and with NDPK1 in the cytosol and the nucleus as well as the possible initiation of a kinase cascade remains unknown.

#### 1.4.2 Phytochrome interacting factors

The yeast two-hybrid library screen and co-immunoprecipitation methods have been used to identify the primary interaction partners of phytochromes. Several phytochrome-interacting factors (PIFs) have been discovered. PIF3, the first identified interacting partner (Ni *et al.*, 1998) belongs to the basic helix-loop-helix (bHLH) protein family. Subsequently, other members of this family such as PIF1, PIF4, PIF5, PIF6, and PIF7 were identified as interacting partners of phytochromes and were shown to participate in the regulation of various light responses (Khanna *et al.*, 2004; Lorrain *et al.*, 2008; Leivar *et al.*, 2008; reviewed Leivar and Quail, 2011).

PIFs contain a conserved N-terminal sequence necessary for phyB-specific binding (Khanna *et al.*, 2004; Zhu *et al.*, 2000), called the Active Phytochrome B (APB) motif. PIF1 and PIF3 also contain a separate domain, which is necessary for phyA binding (Al-Sady *et al.*, 2006; Shen *et al.*, 2008), called the Active Phytochrome A-binding (APA) motif.

Phytochromes act as inhibitors of PIF3, destabilizing this protein in the nucleus. Upon activation by light, phytochromes are transferred to the nucleus, where they bind to PIF3. The binding of phytochromes to PIF3 results in PIF3 phosphorylation (Al-Sady *et al.*, 2006) and subsequent degradation (Bauer *et al.*, 2004; Park *et al.*, 2004). This mechanism is suggested to be common to this class of signaling protein (Lorrain *et al.*, 2008; Shen *et al.*, 2008).

Previous studies demonstrated that PIF3 promoted hypocotyl elongation, suggesting that PIF3 is a negative regulator of seedling growth (Kim *et al.*, 2003). Also, PIF3 has been shown to act positively in the light regulation of chloroplast development (Monte *et al.*, 2004), which suggests that PIF3 has a dual function, acting early and positively as a transcription factor, but acting later to regulate phyB abundance and repress light-induced inhibition of hypocotyl elongation (Monte *et al.*, 2007; Al-Sady *et al.*, 2008).

Other members of the PIF family appear to function predominantly as negative regulators (Bae and Choi, 2008; Duek and Fankhauser, 2005). The effects of different PIFs could be additive; single *pif* mutants have weak effects, whereas quadruple *pif1pif3pif4pif5* (*pifq*) mutants have been shown to have constitutive photomorphogenetic phenotype (Leivar *et al.*, 2009).

### 1.4.3 Signal integration

A number of light responses are mediated by the coordinated action of several photoreceptors (Casal, 2000a), indicating the presence of shared signaling components. These include the negative regulators of the DET/COP/FUS class and the positive regulator HY5 (Quail, 2002; Saijo *et al.*, 2003).

*HY5* encodes a constitutively nuclear bZIP transcription factor, which positively regulates photomorphogenesis through binding to G-boxes within the promoters of light-inducible genes (Osterlund *et al.*, 2000a).

Several negative regulators of phytochrome signaling were identified from mutant screens. The mutants show constant photomorphogenesis: the etiolated seedlings resemble light-grown seedlings (Schwechheimer and Deng, 2000; Yi and Deng, 2005). Biochemically, the identified COP/DET/FUS proteins belong to three groups of protein complexes: the COP1 complex, the COP9 signalosome (CSN) complex, and the CDD complex (COP10, DDB1, and DET1). It has been suggested that all three complexes repress photomorphogenesis by participating in the ubiquitination/proteasome-mediated degradation of key photomorphogenesis-promoting transcription factors (Yanagawa *et al.*, 2004; Chen *et al.*, 2006). Among these proteins COP1 (CONSTITUTIVELY PHOTOMORPHOGENIC 1) is a point of convergence downstream of multiple light signals. COP1 functions as an E3 ubiquitin-protein ligase, targeting several proteins for degradation by assisting in their ubiquitylation (Osterlund *et al.*, 1999, 2000a). These proteins include HY5 (Osterlund *et al.*, 2000b), LONG AFTER FAR-RED LIGHT 1 (LAF1) (Seo *et al.*, 2003) and LONG HYPOCOTYL IN FAR-RED 1 (HFR1) (Duek *et al.*, 2004; Jang *et al.*, 2005) for degradation via the 26S proteasome. COP1 also acts as an E3 ligase to regulate phyA signaling by targeting the phyA photoreceptor itself for elimination (Seo *et al.*, 2004) and terminating signaling by desensitization of activated receptors.

Additional data support the proposed role of proteasome-mediated protein degradation in adjusting the phytochrome signaling point towards two other loci -

*EMPFINDLICHER IM DUNKELROTEN LICHT 1 (EID1)* and *SUPPRESSOR OF PHYA (SPA1)*, identified earlier as specific negative regulators of phyA signaling (Hoecker *et al.*, 1999; Dieterle *et al.*, 2001). EID1 was identified as a new F-box protein, a putative component of SCF (SKP1/Cullin1/F-box protein) complexes that function as E3 ubiquitin ligases (Dieterle *et al.*, 2001). SPA1 is a nuclear-localized WD-40-repeat-containing protein that has high sequence similarity to COP1 (Hoecker *et al.*, 2001). SPA1 has been shown to bind COP1 together with SPA-like proteins to form SPA-COP1 complexes, which exhibit E3 ligase activity (Zhu *et al.*, 2008).

## 1.5 Aim of this study

Mutant analysis is one of the major approaches for identifying novel phytochrome signaling components and discovering links between protein functions and domain structure. Multiple putative light signal transduction intermediates have been identified from mutant screens aimed at isolating mutants with impaired light sensing (Møller *et al.*, 2002). Analyses of phytochrome-deficient mutants provide understanding of the phytochrome functions throughout plant development. On the other hand, identification of phytochrome loss-of-function mutants provides comprehension of multiple separate functions of the different domains and establishes a link between protein structure and the mode of phytochrome action.

In this study *phyA-5*, a novel loss-of-function mutant allele has been investigated. The aim of the investigation has been to characterize the mutant and to identify the mutated gene; to describe the impact of the mutation on phytochrome-mediated responses, localization and protein-protein interaction; and to provide a new insight to the interconnection between phytochrome domain structure and function.

## 2. MATERIALS AND METHODS

### 2.1. MATERIALS

#### 2.1.1 Chemicals, enzymes, oligonucleotides, cloning vectors

Chemicals used in this study were purchased from Sigma, Reanal, Difco, Qbiogene and Aldrich Chem. Co. Enzymes were purchased from Fermentas, New England Biolabs and Invitrogen. Cloning vectors, used in this study were: pBluescriptII KS/SK (Stratagene); yeast vectors: pD153 (Shimizu-Sato *et al.*, 2002), pGADT7 (CLONTECH Laboratories, Inc.); plant cloning vector: pPCVB812, including the coding sequence of the yellow fluorescent protein (YFP) and the nopaline synthase (NOS3') terminator (Bauer *et al.*, 2004). Oligonucleotides were synthesized by Sigma or IDT (Integrated DNA Technologies).

#### 2.1.2 Buffers, solutions, media, antibiotics

Standard buffers and solutions and were prepared as described (Sambrook *et al.*, 1989).

Bacterial growth medium was prepared as follows:

LB (Luria-Bertani Medium) (pH = 7.0): 1% tryptone (Reanal), 0.5% yeast extract (Reanal), 1% NaCl (Reanal); solid medium: 1.5% agar (Reanal)

YEB (pH = 7.0): 0.5% beef extract (Difco), 0.1% yeast extract, 0.5% Bacto® peptone (Difco), 0.5% sucrose (Reanal), 2 mM MgSO<sub>4</sub> (sterile filtered, added after autoclaving; Sigma); solid medium: 1.5% Bacto® agar (Difco).

Yeast culture medium was prepared as follows:

YPAD (pH = 7.0), 1% yeast extract, 2% Bacto® peptone, 2% glucose, 0.01% adenine hemisulfate (Sigma); solid medium: 1.5% Bacto® agar

Synthetic Dropout medium (pH = 7.0): 2% glucose, 0.67% yeast nitrogen base w/o amino acids (Difco), 0.64 g/l Leu/Trp Complete Supplement mixture (CSM) or 0.63 g/l His/Leu/Trp CSM (both from Qbiogene); solid medium : 1.5% Bacto® agar.

Plant growth medium was prepared as follows:

MS3 (Murashige-Skoog Medium) (pH = 5.6): 4.3 g/l MS salt (Sigma), 3% sucrose, 1% agar (Difco).

AM (Arabidopsis Medium) (pH = 5.6): 2.16 g/l MS salt, 1% sucrose, 0.2% phytigel (Sigma).

Antibiotics in this study were used as follows for selective growth in sterile conditions:

**Table 1. List of antibiotics, used for selection.**

Organism	Antibiotic	Concentration
<i>Escherichia coli</i>	Ampicillin (Amp)	100 µg/ml
	Kanamycin (Km)	50 µg/ml
<i>Agrobacterium tumefaciens</i>	Carbenicillin (Cb)	100 µg/ml
	Kanamycin (Km)	50 µg/ml
	Rifampicine (Rif)	25 µg/ml
<i>Arabidopsis thaliana</i>	Hygromycin (Hyg)	15 µg/ml
	Claforan (Cf)*	200 µg/ml

\* Claforan was used in AM and MS medium not for the purpose of selection, but in order to reduce the chances of bacterial contamination.

### 2.1.3 Bacterial and yeast strains

<i>Escherichia coli</i> XL-1 Blue	recA1 endA1 gyrA96 thi-1 hsdR17 (rk <sup>-</sup> ,mk <sup>+</sup> ) supE44 relA1 lac [F' proAB lacI <sup>q</sup> ZΔM15 Tn10 (Tet <sup>R</sup> )]
<i>Escherichia coli</i> S17-1	F <sup>-</sup> recA pro hsdR RP4-2 Tc <sup>r</sup> ::Mu Tn <sup>r</sup> ::Tn7 (Tnp <sup>R</sup> , Spc <sup>R</sup> , Str <sup>R</sup> )
<i>Agrobacterium tumefaciens</i> GV3101	rpoH <sup>+</sup> hrcA <sup>+</sup> pMP90RK (Gm <sup>R</sup> , Km <sup>R</sup> , Rif <sup>R</sup> ) (Koncz and Schell, 1986)

## MATERIALS AND METHODS

*Saccharomyces cerevisiae* Y187

MATa ura3-52, his3-200, Ade2-101, trp1-901, leu2-3, 112, gal4Δ, gal80Δ, met-, URA3::GAL1<sub>UAS</sub>-GAL1<sub>TATA</sub>-lacZ MEL1

*Saccharomyces cerevisiae* AH109

MATa, trp1-901, leu2-3,112, ura3-52, his3-200, gal4Δ, gal80Δ, LYS2::GAL1<sub>UAS</sub>-GAL1<sub>TATA</sub>-HIS3, GAL2<sub>UAS</sub>-GAL2<sub>TATA</sub>-ADE2 URA3::MEL1<sub>TATA</sub>-lacZ MEL1

### 2.1.4 Plant materials

*Arabidopsis thaliana* wild-type:

Columbia ecotype (Col-0), Wassilevskaya ecotype (Ws), Landsberg erecta ecotype (Ler).

*Arabidopsis thaliana* mutants:

*phyA-201* (Ler) (Nagatani *et al.*, 1993), *phyA-5* (renamed *psm*) (Ws), kindly provided by late Prof. Gary Whitelam.

### 2.1.5 Oligonucleotides

**Table 2. List of PCR markers used for rough mapping.**

Chr.	Marker	location (cM)	Type, enzyme	Primer sequence
I	NCC1	12.6	dCAPS RsaI	FP: TACTATCACATTTAATTAAGGGAACC RP: ATTCTTTTAATTAACTCATCATTTC
	Ciw12	41.3	SSLP	FP: AGGTTTTATTGCTTTTCACA RP: CTTTCAAAGCACATCACA
	F5J5	60	dCAPS SspI	FP: TTTTAAAACCGGATAGAAAGGAT RP: AAAGATTTTGTATTTAAGTGCATCA
	nga280	83.8	SSLP	FP: GGCTCCATAAAAAGTGCACC RP: CTGATCTCACGGACAATAGTGC
	nga111	115.5	SSLP	FP: TGTTTTTTAGGACAAATGGCG RP: CTCCAGTTGGAAGCTAAAGGG
	F16J10	13.4	CAPS	FP: TTTCAACTTCAAGTGTTTTCCAC

MATERIALS AND METHODS

II	F16J10	13.4	HinfI	RP: AACTTATAAAGGTTTGTAAAGCGTAT
	F16F14	30.8	CAPS RsaI	FP: TGTTCTCTTCTCCATACCCTTTTGCTA RP: AGGCTCTGAAGCAAGTGTAGTGGT
	ELF3	46	dCAPS EcoRI	FP: TGAGCAAACGATGACAACAACC RP: ACGTTCTTCTTGTATTGACTGGAG
	T9D9	61	dCAPS TaqI	FP: CCGCGGATGCAAAACAGACTC RP: TCTTCAAGGCTAATCACCTCCCTTATC
	nga168	73.8	SSLP	FP: GAGGACATGTATAGGAGCCTCG RP: TCGTCTACTGCACTGCCG
	T8I13	86.5	dCAPS SspI	FP: TCACCGCAGTGTAATCATGAAAC RP: TCGATATATGTCTTGGAATCTGGAAT
III	GAPC	8.4	CAPS EcoRV	FP: ACAAATTTCCACCTATAGGCAAGCAAG RP: GTCTCCAACGCTAGCTGCACCACT
	nga162	20.6	SSLP	FP: CTCTGTCACTCTTTTCCTCTGG RP: CATGCAATTTGCATCTGAGG
	GL1	48.4	CAPS TaqI	FP: CTCCTAGATTGTAATAGTGGTAG RP: ATATTGAGTACTGCCTTTAG
	T6H20	60.6	dCAPS EcoRI	FP: TGAAGAATATGCTCAGGAGAATCTCGAATT RP: TCTCATCCAATCTCACAATGGTTCG
	F4P12	75	CAPS AluI	FP: CTTCCATGGACGCCGTCAC RP: ATTTTCGGGTAAATTACCAAATTGAGA
IV	F6N15	1.5	dCAPS HindIII	FP: GAAAAGGCAAGTGGGTTTGGA RP: ACACCCATGTCCCTCTATTTTATTATAAA
	T14P8	13	CAPS HincII	FP: GTCCGAACAAACAGCTCAGATCAGT RP: CCCCAAGTCTTTTACAATTAATTCCAT
	nga8	26.6	SSLP	FP: TGGCTTTCGTTTATAAACATCC RP: GAGGGCAAATCTTTATTTTCGG
	F25G1 3	46	dCAPS RsaI	FP: CACACGTTGGTAAGTGATTTCTCTTTGG RP: GGCACAAAAGGATTTTCGCAAACAT
	AG	63.2	CAPS XbaI	FP: CAACAGGTTTCTTCTTCTTCTC RP: AAGGGAAAATTAATATACACATGA
	T19K4	86	dCAPS PstI	FP: TTCCAAACGCGCCGCTACT RP: CGCCGGAAACTGTACGACAACC
	DHS1	108.6	CAPS BsaAI	FP: GATTCAGTGTGTGTGTTAGGT RP: NTTTATGTTTGTAACTTAATTTATGC

V	CTR1.2	9.3	SSLP	FP: CCACTTGTTTCTCTCTCTAG RP: TATCAACAGAAACGCACCGAG
	nga106	33.3	SSLP	FP: TGCCCCATTTTGTCTTCTC RP: GTTATGGAGTTTCTAGGGCACG
	nga139	50.5	SSLP	FP: GGTTTCGTTTCACATTCCAGG RP: AGAGCTACCAGATCCGATGG
	snp164	84	dCAPS HinfI	FP: GCATACTCCAATTGCTCAGGCAG RP: TTCGGTGATCGGCTTAATGGTT
	nga129	105.4	SSLP	FP: CCACTGAAGATGGTCTTGAGG RP: TCAGGAGGAACTAAAGTGAGG
	LFY3	116.9	CAPS RsaI	FP: AAGGTTTCACGAGTGGCTTATTCC RP: CCTCGTCCTTCATACCCACAAGC
	cer4358 65	136	CAPS HinfI	FP: CGACTCCTCCTCCTGACTATAACAA RP: GAAAGTAGTGGAATCGTGGAAGAAA

**Table 3. List of PCR markers used for fine mapping.**

Marker name	Marker type/ enzyme	Position	Primer sequence
Nga59	SSLP	Chr1 8 kb	FP: TAAAACAGTAGCCCAGACCCG RP: GCATCTGTGTTCACTCGCC
T21E18	dCAPS SspI	Chr1 1845 kb	FP: GCCGAAGTTGGAAGACTAATGACAC RP: CCTCTCATTTCACCAATTTAAGTAACAA
F24B9	dCAPS SpeI	Chr1 2409 kb	FP: GAAATATTCAGAAGTGTGAGATAGCTACTA RP: CAGACAAAATAGAGCTAAGACTGACTAATT
phyA-M	dCAPS AccI	Chr1 3098 kb	FP: TTGTTTACTTGCCTTGGATGA RP: AGGGCTTTCTGCAATGTAGA
PSM	dCAPS TaqI	Chr1 3099 kb	FP: TCATTGCGCAGACCACTGTAGATT RP: TAAACAACCGAAGGGCTGAATCAG
F14N23	dCAPS BseGI	Chr1 3359 kb	FP: GAATCATGCGAGTTTTATTGAA RP: CCGATAATGGCAATTACAGGAT
NCC1	dCAPS RsaI	Chr1 4106 kb	FP: TACTATCACATTTAATTAAGGGAACC RP: ATTCTTTTAATTAACATCATTTTGC
Ciw12	SSLP	Chr1 9621kb	FP: AGGTTTATTGCTTTTCACA RP: CTTTCAAAGCACATCACA

**Table 4. List of PCR primers used for cloning and sequencing.**

Primer name	Used for	Primer sequence
PHYA-F(full) PhyA-R(full) PHYA-R(stop-)	Cloning a full-sized <i>PHYA</i> gene with promoter	5'-AAACTCGAGGAGAAGAAGAAAGAGATAAC-3' 5'-CAAGATATCTTGCAACATAGTCACGAATC-3' 5'- CCCGGGCTTGTTTGCTGCAGCGAGTTCCG-3'
PHYA406-F PHYA406-R	Cloning first part of the <i>PHYA</i> gene	5'-TTTGGATCCATATGTCAGGCTCTAGGCCGAC-3' 5'-TTTCCCGGGTGGTTATCGAGTTCCACCTCC-3'
PHYAseq1 PHYAseq2 PHYAseq3 PHYAseq4 PHYAseq5 PHYAseq6 PHYAseq7 PHYAseq8 PHYAseq9 PHYAseq10 PHYAseq11 PHYAseq12 PHYAseq13	Sequencing of the <i>PHYA</i> gene	5'-CATTAAAAACCGAGAAAACACAT-3' 5'-TGACGAAAAAAAAATAAACCTT-3' 5'-TTAAGCCCACTGTTCTGTTTTAG -3' 5'-TTTGTGTAGTGGATTTACCCTGTAA-3' 5'-CTGAGGGCTCAAGGCGATCA-3' 5'-TTGCAGAAAGCCCTTGGATTT-3' 5'-ATCCCTCAAGCAGCCCGTTTTCT-3' 5'-GCTGATGCGTGATGCTCCACTGGG-3' 5'-GGCAGCTGTGAGGATATCATCGA-3' 5'-GTATCGTGGTCGAAGAACTTGATGCAA-3' 5'-AGAGGAAGTGATTGACAAAATGCT-3' 5'-ATAACAAATGAGACCGGAGAAGAAGT-3' 5'-CAAGTAGTCCCCAAAAGAAAAGG-3'

**Table 5. List of PCR primers used for analysis of transcript level.**

Primer name	Primer sequence
PHYA-RT-F PHYA-RT-R	5'-ATCTAGAGATCAGGTTAACGCA-3' 5'-CCTTCTTCTGACACATCTTCC-3'
TUB2/3-F TUB2/3-R	5'-CCAGCTTTGGTGATTTGAAC-3' 5'-CCAGCTTTCGGAGGTCAGAG-3'
PRR9-RT-F PRR9-RT-R	5'-CCTTCTCAAGATTTGAGGAAAGC-3' 5'-TTTGGCTCACCTGAAGTACTCTC-3'

### 2.1.6 Software and databases

Chromas ( <a href="http://www.technelysium.com.au/chromas.html">http://www.technelysium.com.au/chromas.html</a> )	Analyzing the abi files obtained from sequencing
TAIR database ( <a href="http://www.arabidopsis.org">www.arabidopsis.org</a> )	Obtaining gene sequences, polymorphisms and mapping markers
BLAST ( <a href="http://www.ncbi.nih.gov/blast">www.ncbi.nih.gov/blast</a> )	Analyzing and comparing sequences
ClustalW2 ( <a href="http://www.ebi.ac.uk/Tools/msa/clustalw2/">http://www.ebi.ac.uk/Tools/msa/clustalw2/</a> )	
Oligo 4.1	Designing oligonucleotide sequences
Webcutter 2.0 ( <a href="http://rna.lundberg.gu.se/cutter2/">http://rna.lundberg.gu.se/cutter2/</a> )	Obtaining information about restriction sites, preparing restriction maps of a gene
IrfanView 4.25, CorelDraw X3	Image processing
Microsoft Excel 2003	Data analysis
ImageJ 1.42q	Image analysing
dCAPS Finder 2.0 ( <a href="http://helix.wustl.edu/dcaps/dcaps.html">http://helix.wustl.edu/dcaps/dcaps.html</a> )	Creation of PCR-based dCAPS markers
Clone Manager 9	Protein sequences alignment
RaptorX ( <a href="http://raptorx.uchicago.edu/">http://raptorx.uchicago.edu/</a> )	Protein structure prediction program

### 2.1.7 Databases accession numbers

Arabidopsis\_PHYA: NM\_100828; Arabidopsis\_PHYB: NP\_179469; Arabidopsis\_PHYC: ABG21336; Arabidopsis\_PHYD: AAW56595; Arabidopsis\_PHYE: CAB53654; Nicotiana\_PHYA: CAA47284; Cucurbita\_PHYA: P06592; Glycine\_PHYA: P42500; Pisum\_PHYA: AAT97643; Populus\_PHYA: O49934; Solanum\_PHYA: P30733; Solanum\_PHYB1: CAA05293; Oryza\_PHYA: A2XLG5; Avena\_PHYA: P06593; Sorghum\_PHYA: AAB41397; Triticum\_PHYA: CAC85512; Picea\_PHYA: Q40762; Pinus\_PHYA: CAA65510; Adiantum\_PHY2: BAA33775; Selaginella\_PHY1: Q01549; Ceratodon\_PHY3: AAM94956; Physcomitrella\_PHY5a: XP\_001761145; Physcomitrella\_PHY5b3: XP\_001767224; Physcomitrella\_PHY5c: XP\_001754366; Marchantia\_PHY: BAB39687.

## 2.2. METHODS

### 2.2.1 Molecular techniques

#### 2.2.1.1 Plant total DNA isolation

**CTAB method** for plant DNA isolation was used to obtain high quality DNA, suitable for PCR amplification of long fragments (up to 10 kb). 40-60 mg of plant tissue (about 1 cm<sup>2</sup> leaf of adult plants, or 20-30 4-day-old seedlings) were put in a 1.5 ml centrifuge tube (Eppendorf), frozen in liquid nitrogen and ground by vigorous shaking with a 3 mm stainless steel ball for 2 min. 500 µl of 2×CTAB buffer (2% CTAB, 100 mM Tris-HCl pH 8.0, 20 mM EDTA pH 8.0, 1.4 M NaCl, 1% PVP-40, 0.5% β-mercaptoethanol), preheated to 65°C was added to each sample. Samples were incubated at 65°C for 30 minutes, centrifuged briefly (13000g, 30 sec). The supernatant was transferred to another tube, shaken with an equal volume of chloroform and subsequently centrifuged (13000g, 5 min). The aqueous phase (top layer) was transferred into a new tube, followed by addition of 0.75 volumes of 2-propanol. After incubation at room temperature, the tubes were centrifuged (13000g) for 10 minutes. The supernatant was discarded; the pellet was washed with cold 70% ethanol, and dried before it was dissolved in 100 µl of sterile water. The samples were incubated with 10 µg RNase at 37°C for 1 hour followed by phenol-chloroform (1:1 mixture) extraction, chloroform extraction and 2-propanol precipitation as described above. The pellets were washed by cold 70 % ethanol, dried and dissolved in 100 µl of sterile water. 1-2 µl of DNA solution was used in a PCR reaction.

**Rapid DNA extraction** protocol was used as described (Berendzen *et al.*, 2005) for simple preparation of multiple DNA samples in order to amplify short PCR fragments (up to 500bp). This method was used in genotyping recombinants during the mapping procedure.

#### 2.2.1.2 Bacterial plasmid DNA isolation

Bacterial plasmid DNA isolation was performed by alkaline lysis method (Birnboim and Doly, 1979).

If higher quality DNA was required (for samples intended for sequencing), 20 U RNase I (Fermentas) was added to each sample, incubated at 37°C for 1 hour, followed by phenol/chloroform (1:1) extraction, chloroform extraction and 2-propanol

precipitation. The concentration of isolated plasmids was evaluated by comparing via electrophoresis with  $\lambda$ -DNA standard.

### 2.2.1.3 Plant total RNA isolation

Plant total RNA isolation was performed using RNeasy Plant Mini Kit (QIAGEN) according to the manufacturer's protocol. The concentration of isolated RNA was determined by standard spectrophotometer measurement (Sambrook *et al.*, 1989).

### 2.2.1.4 Polymerase chain reaction (PCR) amplification

Standard PCR amplifications were performed with Taq polymerase (Fermentas) for short fragment amplification (100-1000 bp), or with Pfu Ultra polymerase (Stratagene) for amplifying DNA fragments longer than 1kb.

#### Amplification of long fragments (over 1000 bp)

Components:	
10X Pfu Buffer with MgSO <sub>4</sub>	4 $\mu$ l
2 mM dNTPs mix	4 $\mu$ l
10 $\mu$ M forward primer	1 $\mu$ l
10 $\mu$ M reverse primer	1 $\mu$ l
DNA template	2 $\mu$ l
Pfu polymerase (2.5 U/ $\mu$ l)	1 $\mu$ l
Water	up to 40 $\mu$ l

Thermal cycle profile:	
1.	95°C - 5 min
2.	[95°C - 30 sec, Ta - 30 sec, 72°C - X min] x 30
3.	72°C - 5 min
4.	4°C - $\infty$

This protocol was used for amplifying fragments, meant to be cloned. Usually, values for Ta were 55-60n°C, sometimes optimized for individual reactions; an elongation time X was calculated as 1 min per kb of amplified fragment.

**Amplification of short DNA fragments**


---

Components:

---

10x Buffer	1 $\mu$ l
25 mM MgCl <sub>2</sub>	1 $\mu$ l
2 mM dNTPs mix	1.5 $\mu$ l
5 $\mu$ M forward primer	0.5 $\mu$ l
5 $\mu$ M reverse primer	0.5 $\mu$ l
DNA template	1 $\mu$ l
Dye Red*	1 $\mu$ l
Taq polymerase (5 U/ $\mu$ l)	0.2 $\mu$ l
Water	up to 10 $\mu$ l

\* Dye Red is the sodium salt of Cresol Red (Aldrich Chem. Co) dissolved in 30% sucrose water solution.

---

Thermal cycle profile:

---

1. 95°C - 2 min
2. [95°C - 30 sec, Ta - 30 sec, 72°C - 1 min] x 50
3. 72°C - 3 min
4. 4°C -  $\infty$

This protocol was used for dCAPS and SSPL genetic marker-based mapping procedure. Usually, values for Ta were 55-60°C, sometimes optimized for individual reactions.

**2.2.1.5 Digestion and ligation**

Digestion of DNA fragments, PCR products and vectors with restriction enzymes was performed according to the manufacturers' instructions. The DNA fragments were electrophoretically separated on 1% agarose (SeaKem® LE, Cambrex) gel and extracted from the gel using the phenol extraction method (Sambrook *et al.*, 1989). The concentration of purified DNA fragments was determined by comparison to a  $\lambda$ -DNA standard.

Ligation of DNA fragments was performed using T4 DNA Ligase (Fermentas) according to the manufacturer's instructions. The vector/fragment ratio in a ligation mixture was 1:7.

#### 2.2.1.6 Cloning of PHYA and constructs generation

Genomic DNA from mutant (*psm*) and corresponding wild-type (Ws) plants, including the 1555 bp promoter and UTR regions of Arabidopsis *PHYA* (At1g09570) was amplified by PCR using primers PhyA-F(full) and PhyA-R(full) and inserted into pBluescript SK vector using *XhoI* and *EcoRV* restriction enzymes. The sequence of these clones was obtained by automated sequencing, and analyzed by ClustalW2 web-based software.

Genomic DNA fragment, including the 1555 bp promoter sequence of Arabidopsis *PHYA* gene from Ws and *psm* (*phyA-5*) was amplified using primers PHYA-F(full) and PHYA-R(stop-). The PCR products obtained were inserted into pBluescript SK (pBSK) vector after digestion with *XhoI* and *SmaI* restriction enzymes resulting PHYA pBSK and PHYA-5 pBSK, respectively. pPCVB812 including the coding sequence of the yellow fluorescent protein (YFP) and nopaline synthase (NOS3') terminator (Bauer *et al.*, 2004) was digested with *Sall* and *SmaI* restriction endonucleases. *XhoI-SmaI* fragments of PHYA pBSK or PHYA-5 pBSK were inserted into this vector resulting PHYA:PHYA-YFP pPCVB and PHYA:PHYA-5-YFP pPCVB, respectively.

Cloning of the SV40 NLS (nuclear localization signal, Kalderon *et al.*, 1984) sequence was described by Wolf *et al.* (2011). *XhoI-SmaI* fragments of PHYA pBSK or PHYA-5 pBSK were inserted into the YFP-NLS pPCV vector resulting in PHYA:PHYA-YFP-NLS pPCVB and PHYA:PHYA-5-YFP-NLS pPCVB, respectively.

The following yeast two-hybrid plasmid constructs were already described previously: PHYA pD153 (Shimizu-Sato *et al.*, 2002), PHYA(1-406) pD153, FHY1 pGADT7, FHL pGADT7 (Hiltbrunner *et al.*, 2006).

PHYA-5 pD153 and PHYA-5(1-406) pD153 constructs were created as follows: PHYA-5 pBSK was used as a template in a PCR reaction performed using PHYA406-F and PHYA406-R primers. The resulting product was digested with *BamHI-HindIII* and inserted into PHYA pD153 to *BamHI-HindIII* sites. The same PCR product was cloned as a *BamHI-SmaI* fragment into PHYA(1-406) pD153 to obtain PHYA-5(1-406) pD153.

Every construct containing a PCR product was verified by automated sequencing.

### 2.2.1.7 Molecular mapping

PCR-based molecular markers such as CAPS, dCAPS and SSPL were used during this study. The sequences of markers used for rough mapping were obtained from the TAIR database. Markers, used for fine mapping, were created with dCAPS Finder 2.0 online software, based on polymorphisms between Col-0 and Ws ecotypes, obtained from the TAIR database.

PCR-based analysis was performed, following the short DNA fragment amplification protocol (see 2.2.1.4.), using the DNA of selected recombinants as template. In case of dCAPS markers, after completing the PCR reaction, overnight digestion was performed as follows:

Components:	
PCR mixture	10 $\mu$ l
Water	7.8 $\mu$ l
10X Buffer	2 $\mu$ l
Restriction endonuclease enzyme (10 U/ $\mu$ l)	0.2 $\mu$ l

Electrophoretic separation of DNA fragments was performed according to standard procedures (Sambrook *et al.*, 1989), using 4% agarose (SeaKem® LE, Cambrex) gel.

The differentiation between ecotypes was performed by visual comparison of fragments obtained, compared to Col-0 and Ws controls.

### 2.2.1.8 Quantitative RT-PCR

Plant total RNA was isolated (see 2.2.1.3) from seedlings collected under the appropriate conditions. First strand cDNA synthesis was performed on 1  $\mu$ g of total plant RNA using RevertAid™ First Strand cDNA Synthesis Kit (Fermentas) and random primers (Fermentas) following the manufacturer's protocol.

The product of cDNA synthesis was diluted five times in RNase-free water and 1.5  $\mu$ l aliquots were used for each reaction. The reaction was set up in 15  $\mu$ l, using ABI SYBR® Green PCR Master Mix (Applied Biosystems) following the manufacturer's

instruction. mRNA level of target genes was continuously measured by an ABI PRISM® 7700 (Applied Biosystems) PCR machine.

---

Thermal cycle profile:

---

1. 95°C - 2.5 min
2. [95°C - 15 sec, 60°C - 1 min] x 40
3. 95°C - 15 sec
4. 60°C - 1 min

A series of cDNA dilutions was created in each experiment: samples of a WT cDNA were mixed and 1-, 10-, 100- and 1000-fold dilutions were made. Data from each dilution were plotted against log dilution values. This calibration line was used to identify values from experimental samples. *TUB2/3* mRNA level was identified for each sample as a constitutively expressed control. Values of genes of interest were normalized to the corresponding *TUB2/3* data. Each sample was measured three times.

### **2.2.1.9 Plant total protein extraction**

50-100 mg of plant material, frozen in liquid nitrogen was homogenized in a microcentrifuge tube using hot extraction buffer (65 mM Tris-HCl, pH 7.8, 4M urea, 5% (w/v) SDS, 14 mM 2-mercaptoethanol, 15% (v/v) glycerol, 0.05% (w/v) bromophenol blue). Samples were ground until homogeneity. The homogenate was heated for 5 min at 95°C and centrifuged (15 min at 13000 g), and the supernatant was transferred to a fresh microcentrifuge tube. 10µl from the protein sample was used to quantify the protein concentration applying the amidoblack assay (Schäffner and Weissmann, 1973). Samples were stored at -20°C till further analysis.

### **2.2.1.10 Protein level analysis**

20 µg of total plant protein extract was denaturated at 95°C before separation on 10% SDS-PAGE gel in Tris/glycine/SDS running buffer (2.5 mM TRIS; 192 mM glycine; 0.01 % SDS). Separated proteins were transferred onto PVDF membrane (Millipore) using a Bio Rad wet blot device according to the manufacturer's instructions.

The PVDF membrane was blocked for 1 h at room temperature in the blocking buffer (0.1 M Tris/HCl pH 7.4, 0.2 M NaCl, 0.05 % (v/v) Tween 20, 2.5 % milk powder), then washed with washing buffer (0.05M Tris/HCl pH 7.4, 0.2M NaCl, 0.05 % (v/v) Tween20) for 10 minutes.

The membrane was incubated in 1000 times diluted primary antibody raised against the N-terminal half of *Arabidopsis* PHYA (kindly provided by Prof. E. Schäfer) or against actin (Sigma) for 2 h at room temperature, washed 3 times for 10 minutes in washing buffer. Subsequently, membranes were incubated in diluted alkaline phosphatase-coupled secondary antibodies: anti-rabbit antiserum (Bio-Rad) for PHYA and anti-mouse antiserum for actin (Sigma). After 1.5 h incubation at room temperature, 3 times for 10 minutes washing in the washing buffer was performed.

The membrane was washed in developing buffer (0.1 M Tris/HCl pH 9.7, 0.1 M NaCl, 0.05 M MgCl<sub>2</sub>) for 2 min, and incubated in developing solution (10 ml developing buffer containing 44 µl NBT\* and 33 µl BCIP\*\*) till clear bands appeared.

The membrane was washed with distilled water, dried overnight at room temperature in dark, then scanned for image processing.

\*7.5% (w/v) NBT (p-Nitro blue tetrazolium chloride) in 70% (v/v) dimethylformaldehyde.

\*\*5% (w/v) BCIP (5-Bromo-4-chloro-3-indolyl phosphate-p-toluidinsalt) in 100% dimethylformaldehyde.

### **2.2.2 Bacterial and yeast methods applied**

#### **2.2.2.1 *E. coli* transformation**

Chemically competent *E. coli* cells were prepared as described (Sambrook *et al.*, 1989), and stored at -80°C. The ligation mixture or the plasmid was put into a sterile plastic tube and kept on ice. Melted competent cells (100 µl) were added to the mixture, mixed gently and incubated on ice for 10-15 minutes, followed by a heat shock at 42 °C for 1-2 minutes. Subsequently the mixture was placed on ice immediately for 2-3 minutes, followed by plating the transformation mixtures onto LB-agar plates containing ampicillin. 40 µl of 0.1M IPTG (isopropyl beta-D-thiogalactopyranoside, Sigma) and 40 µl of 20 mg/ml Xgal (5-bromo-4-chloro-3-indolyl-beta-D-galactopyranoside, Sigma) were spread and dried on LB-agar plates before plating the transformation mixture for

blue/white colour positive clones selection in case if pBSk plasmids were used. Plates were incubated at 37 °C for 16 h.

*Escherichia coli* XL-1 Blue strain was used for molecular cloning, whereas the S17 strain was used for *A. tumefaciens* transformation.

#### **2.2.2.2 *Agrobacterium tumefaciens* transformation**

*Escherichia coli* strain S17, containing the target construct in binary vector and *Agrobacterium tumefaciens* GV3101 strain were inoculated from single colony and propagated in 2 ml of liquid LB and YEB medium for 16 h at 37°C or at 28°C, respectively. Cells were centrifuged (5000g, 3 min) and resuspended in 20 µl YEB medium. Resuspended *E. coli* and *A. tumefaciens* were mixed and pipetted on YEB-agar plates, and incubated at 28 °C for 24 h. Grown colonies were dispersed with inoculation loop on the surface of YEB-agar plates containing 100 µg/ml carbenicillin, 50 µg/ml kanamycin and 25 µg/ml rifampicine.

#### **2.2.2.3 Yeast transformation**

Yeast cells (strain AH109 or Y187) were incubated with constant shaking in 5 ml YPAD medium at 30°C for 16-18 h. Overnight cultures were transferred into fresh 50 ml YPAD medium and incubated for another 4-5 h at 30°C until OD<sub>600</sub>=0.4-0.6 was reached. Yeast cells were collected by brief centrifugation (1000 g, 5 min) and resuspended in 30 ml sterile water and centrifugated again. The cell pellet was resuspended in 1 ml of freshly prepared, sterile 1X TE/LiAc (0.1 M lithium acetate, 0.01 M Tris-HCl, 1 mM EDTA, pH 7.5) and incubated for 15 min at 30°C.

The transformation mixture (150 µl PEG/TE/LiAc solution (50% polyethylene glycol in 1X TE/LiAc; 7.5 µl 10 mg/ml autoclaved herring sperm DNA; 25 µl yeast suspension) was added to the plasmid DNA mixture and incubated at 30°C for 30 min, followed by a heat shock at 42°C for 20 min.

The mixture was centrifuged (5000g, 1 min), the supernatant was removed and cells were resuspended in 100 µl of sterile water. This cell suspension was spread onto Synthetic Dropout Medium, lacking Leu and Trp plates and incubated at 30°C for 4 days.

### 2.2.3 Plant methods applied

#### 2.2.3.1 Plant growth and light conditions

Plants were routinely grown in greenhouse on soil at 22°C under long-day conditions of 16 hrs light and 8 h darkness after 4 days of dark-cold treatment at 4°C. Sterile growth was executed in growth chambers (Sanyo MLR-350) on MS or AM medium under long-day conditions. Seeds were surface sterilized in 30% bleach for 10 min and subsequently washed 3 times with sterile water.

Seedlings, intended for hypocotyl length, cotyledons angle measurement and microscopic experiments were grown on 4-layers of water-wet filter paper (0.1 ml water per 1 cm<sup>2</sup> of filter paper). Seeds were sown on wet filter paper, incubated in dark at 4°C for 3 days. Cold-treated seeds were exposed to 6 h white light for germination induction, then transferred to 22°C and darkness for an additional 12 h and were grown at different light conditions for 4 days.

White light illumination was provided by cool-white fluorescent tubes. For growth in red, far-red, and blue light custom-made LED panels were used (Table 6).

**Table 6. Wavelengths of maximum emission and emission range for light-panels used in this study.**

Light	Emission range, nm	Maximum emission, nm
Red	645-675	660
Fred	715-745	730
Blue	455-480	470

#### 2.2.3.2 Hypocotyl length and cotyledon angle measurement

40-50 seedlings were used for each measurement. Seedlings were placed on a 1% agar plate and scanned with a flatbed scanner (Canon) at 600 dots per inch resolution. Hypocotyl length and cotyledon angle values were measured with ImageJ software and calculations were performed in Microsoft Excel 2003. Hypocotyl lengths of light-grown seedlings were normalized to the corresponding dark-grown hypocotyl length.

### 2.2.3.3 Crossing

Crossing was performed with plants starting to flower. A mature but unopened flower bud was opened using a pair of forceps, followed by removal of the all anthers without damaging the pistil. This procedure was performed under low magnification on a stereo microscope. A mature open flower from the donor plant was selected and its anthers were brushed on the stigma of the emasculated flower. Seed-buds were protected with plastic cylinders. The heterozygous F1 plants and F2 segregants were studied.

### 2.2.3.4 Segregation Analysis

F1 seed resulting from backcross of the mutant (*psm*) and wild-type (Ws) were grown under selective light conditions (weak FR) and the phenotype of the F1 seedlings was observed. To obtain F2 generations, the F1 seeds were planted, self-pollinated and harvested individually. Hypocotyl measurement for the F2 population grown under selective light conditions was performed and the number of plants with each phenotype was determined.

### 2.2.3.5 Agrobacterium-mediated transformation of *Arabidopsis thaliana*

A single *Agrobacterium* colony, transformed with the desired plasmid was inoculated in 2 ml liquid YEB medium, supplied with 100 µg/ml carbenicilin, 50 µg/ml kanamycin and 25 µg/ml rifampicine. After 20 h of constant shaking at 28°C, this culture was used to inoculate 300 ml YEB medium supplemented with the same antibiotics. When the OD<sub>600</sub> of the 300 ml liquid culture reached 0.5, cells were harvested by centrifugation (3500g, 20min) and resuspended in 300 ml 3% (w/v) sucrose solution. This solution, supplemented with 60 µl Silwet L-77 (Lehle Seeds) was used to transform *Arabidopsis* plants according to Clough and Bent, 1998.

### 2.2.3.6 Epifluorescence microscopy

Epifluorescence microscopy setup and observation techniques were described previously (Bauer *et al.*, 2004). Semi-quantitative epifluorescence microscopy was performed as follows: 4-day-old etiolated seedlings were irradiated with 1 minute long R

## MATERIALS AND METHODS

light pulses of different light intensities. After a 5-minute incubation in the dark at 25°C, 12-bit TIFF images, not containing any saturated pixels were taken of the observed nuclei. In order to minimize the effect of the microscopic light the image was taken within the first 30 seconds after switching on the excitation light source. The same exposure time and excitation light, intensity setting were applied throughout the whole experiment. The average intensity of pixels was calculated in the examined nuclei using the ImageJ software. After subtraction of the signal from the vacuole background in each image, the mean value of data obtained from at least 15 independent nuclei was normalized to the corresponding dark control.

### 3. RESULTS

#### 3.1 Identification of the *psm* mutation

##### 3.1.1 Genetic mapping of the mutated locus

The *psm* (Phytochrome Signaling Mutant) mutant, studied in this work, was isolated from an EMS-mutagenized population of *A. thaliana* ecotype Wassilewskaya (Ws) in the laboratory of Prof. Garry Whitelam as hyposensitive to FR light.

The special light-intensity-dependent mutant phenotype has been revealed as a result of this work (Figure 1).

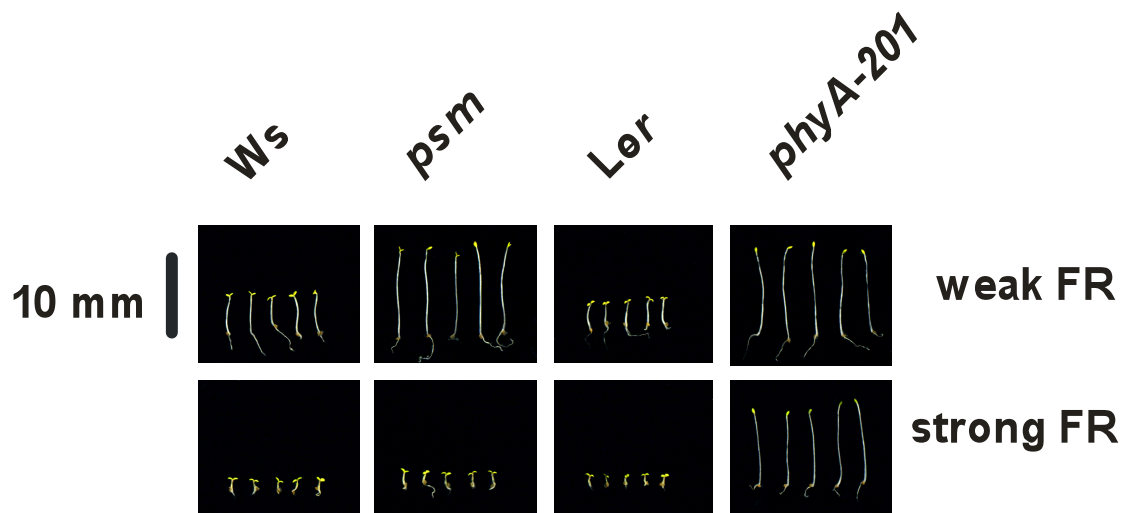


**Figure 1.** Light dependent phenotype of *psm* mutant.

Comparison of 4-day-old seedlings grown under constant irradiation; weak FR:  $1 \mu\text{mol m}^{-2} \text{s}^{-1}$  far-red light; strong FR:  $10 \mu\text{mol m}^{-2} \text{s}^{-1}$  far-red light. Analyzed genotypes: Ws: Wassilewskaya; *psm* mutant (ecotype Ws); Ler: Landsberg erecta, *phyA-201* (ecotype Ler).

The Arabidopsis *phyA* null mutants, containing no active *phyA* photoreceptor grown under continuous FR, exhibit long hypocotyl and closed, unexpanded cotyledon phenotype (Parks and Quail 1993, Nagatani *et al.*, 1993, Whitelam *et al.*, 1993). *psm* mutant seedlings, grown in continuous weak FR light ( $1 \mu\text{mol m}^{-2} \text{s}^{-1}$ ) exhibit a phenotype

that was nearly indistinguishable from the *phyA-201* null mutant (Ler ecotype), whereas no difference in seedling phenotypes was observed between the *psm* mutant and wild-type plants under strong FR light ( $10 \mu\text{molm}^{-2}\text{s}^{-1}$ ).

In order to analyze the nature of mutation and to identify the mutated locus, the *psm* mutant was backcrossed with WT (Ws) and analysis of the F1 and F2 generation was performed. F1 seedlings from the backcross exhibited wild-type phenotype in weak FR light, which indicates the mutation is recessive. The F2 generation of the backcross with WT exhibited 3:1 (212:75) segregation of the mutant phenotype, indicating monogenic inheritance.

Molecular mapping (Lukowitz *et al.*, 2000; Jander *et al.*, 2002) was performed to identify the mutated locus, using DNA polymorphisms between Ws and Columbia (Col) ecotypes of Arabidopsis. The mapping population was created by crossing *psm* with Col wild-type plants. The F1 generation plants of this cross between mutant and wild-type plants were grown, self-pollinated and used as a source of seeds for F2 mapping population. Taking into account that Ws genotype in the F2 mapping population represents mutant, and Col genotype represents wild-type, accurate characterization of the phenotype was performed followed by determination of the genotype and their correlation.

Subsequently, seedlings from the F2 population grown for 4 days under weak FR light were screened for mutant phenotype (long hypocotyls). As a result, 100 individual plants were selected. Genomic DNA samples were prepared from each chosen plant. Mapping was performed using PCR-based analysis of molecular markers based on polymorphic microsatellites, also named simple sequence length polymorphisms (SSLP), and simple nucleotide polymorphisms (SNP) (Table 2). The mutation was roughly mapped by this method to upper arm of chromosome 1 (marker NCC1).

To determine the position of the mutation more precisely, 50 plants from the F2 generation were selected as recombinants between markers, surrounding NCC1 (NGA59 and *ciw12*). These recombinants were self-pollinated, seeds were harvested and their phenotypes were determined by examination of F3 population. Additional dCAPS markers were generated inside the analyzed region (Table 3).

Positional mapping with newly designed markers revealed the position of the mutation in close proximity to the *PHYA* gene (Figure 2). The original background of mutant is Ws, so in the mapping population Ws represents mutant and Col represents wild-type genotype.

No recombination was detected with *PHYA* dCAPS marker. Results of the genetic mapping strongly suggested that the observed phenotype is caused by a mutation in the *PHYA* gene.

Marker, position	NGA59 0.01 Mbp	T21E18 1.8 Mbp	F24B9 2.4 Mbp	phyA-M 3.1 Mbp	F14N23 3.3 Mbp	NCC1 4 Mbp
Phenotype						
mut	het	het	het	ws	ws	ws
mut	het	het	het	ws	ws	ws
mut	het	ws	ws	ws	ws	ws
mut	het	ws	ws	ws	ws	ws
mut	ws	ws	ws	ws	het	het
mut	ws	ws	ws	ws	ws	het
mut	ws	ws	ws	ws	ws	het
mut	ws	ws	ws	ws	ws	het
wt	col	col	col	col	het	het
wt	col	col	col	col	het	het
wt	col	col	col	col	col	het
wt	col	col	col	col	col	het
wt	het	het	col	col	col	het
wt	het	het	col	col	col	col
wt	het	het	col	col	col	col
wt	het	het	col	col	col	col
wt	het	het	het	col	col	col
wt	het	het	het	col	col	col

**Figure 2.** Genetic recombination of F2 mapping population.

The two upper rows describe genetic markers, used in molecular mapping: first row: markers' name, second row: physical position on chromosome 1. The first column contains the phenotypes of the selected recombinants. The colored boxes show the genotype of corresponding recombinants determined at the specified markers. The marked area indicates localization of the potential mutation.

The endogenous *PHYA*, including introns, UTR and 1550 bp promoter was amplified three times independently to exclude PCR errors and cloned into pBSK vector. Sequencing was carried out with uniformly distributed sequencing primers (see Table 4), providing high quality sequences across the entire region. *PHYA* was also amplified from Ws, cloned and sequenced. This sequence was used as reference.

Sequence analysis revealed a single cytosine to thymine nucleotide substitution, which causes exchange of alanine to valine in the NTE domain of the mutant *PHYA* at the amino acid position 30 (Figure 3A). A cleavable amplified polymorphic sequence marker was created using the identified sequence polymorphism (PSM, see Table 3).

No recombination was detected between this genetic marker and the mutation after the analysis of 120 F2 plants that displayed the mutant phenotype. This fact further supports the sequence data indicating that the *PHYA* gene of the *psm* mutant is altered at this position.

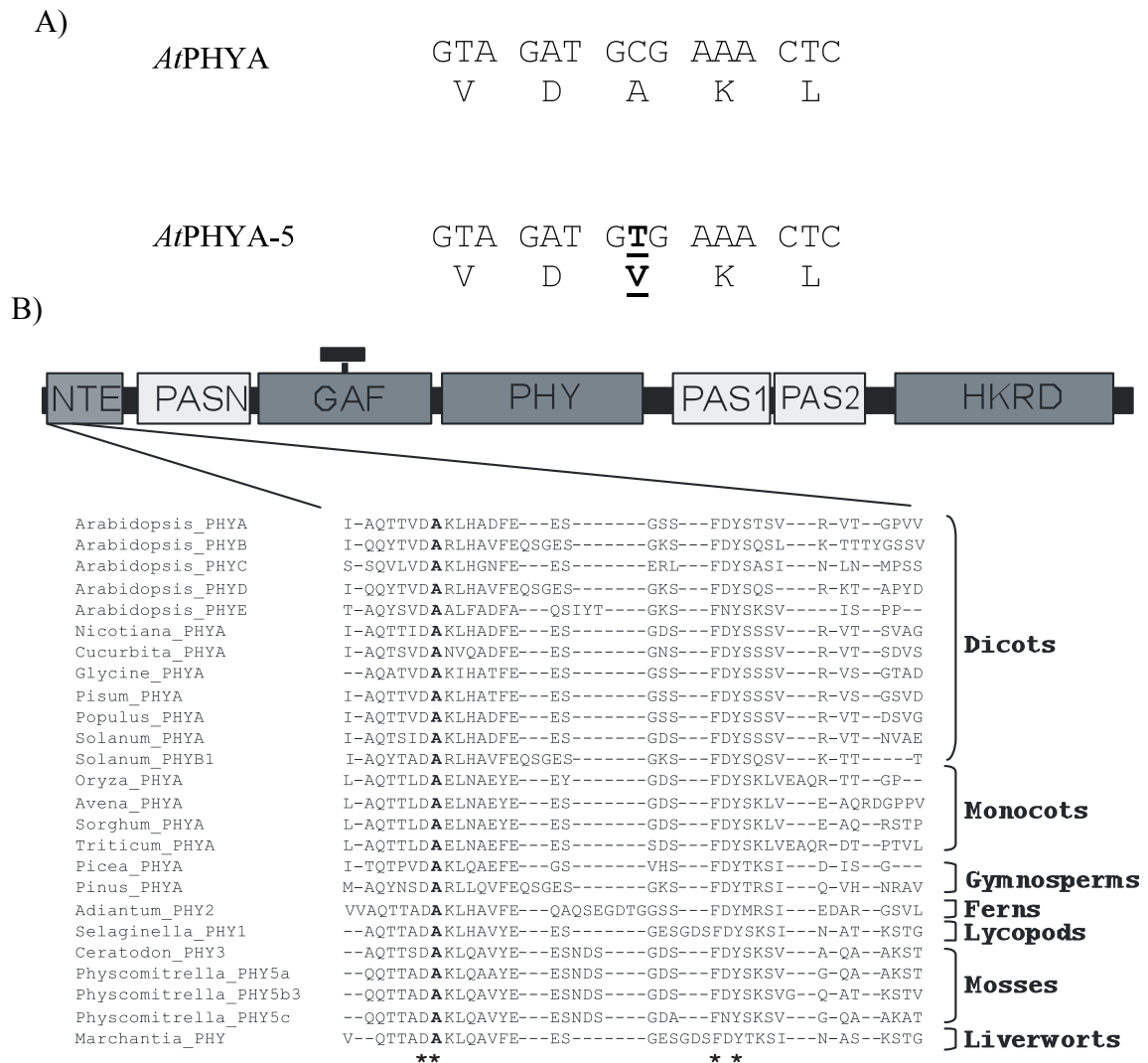


**Figure 3.** Location of the *phyA-5* mutation.

A) Nucleotide and protein sequence of the wild-type and mutated *PHYA* gene.

B) Diagram of the phytochrome domains together with the sequence alignment of the corresponding region. The position of the missense mutation is indicated (bold letter). NTE - amino terminal extension; PASN, N-terminal PER/ARNT/SIM domain; GAF, cGMP-specific phosphodiesterases, adenylyl cyclases and FhlA domain; PHY, phytochrome domain; PAS1 and PAS2, two additional PER/ARNT/SIM domains; HKRD, histidine kinase-related domain; small black rectangle attached to the GAF represents the chromophore.

The mutant was named *phyA-5* following the guidelines described by Quail *et al.*, 1994.

Sequence alignment of different phytochromes revealed that the mutated alanine is highly conserved throughout plant evolution and could be identified in phytochrome sequences derived from diverse taxa (etc. dicots, monocots, ferns, mosses), and also conserved amongst other *Arabidopsis* phytochromes (Figure 3B).

### 3.1.2 Confirmation of the position of mutation by transgenic plants

Transgenic plants, expressing *phyA-5* fused to the yellow fluorescent protein (YFP) under the control of the *PHYA* promoter in *phyA-201* background were generated (PHYA:PHYA-5-YFP) in order to validate that the observed phenotype of the *phyA-5* mutant is caused by the identified mutation. WT *PHYA* was also expressed in the same background (PHYA:PHYA-YFP) as a control. Resistance-based selection of transformants was performed, and selected plants (T1 generation) were self-pollinated to generate a homozygous T2 population.

About 100 T2 seeds of several transformed T1 lines were grown under selective conditions and the ratio of resistant to sensitive seedlings was determined. Lines exhibiting a 1:3 resistance ratio (resistant: sensitive) were proved to contain a single copy of the transgene. Resistant T2 plants were fully grown and T3 seeds examined for segregation of the selectable marker to identify a homozygous transformed line.

Protein levels of PHYA-YFP and PHYA-5-YFP in the selected homozygous single copy transgenic lines were compared to Ws by western blot analysis. Lines exhibiting transgenic *phyA* levels similar to that of the endogenous *phyA* were chosen for further experiments.

The transgenic line PHYA:PHYA-YFP fully complemented the hyposensitive *phyA-201* mutant, exhibiting short wild-type-like hypocotyls under both strong and weak FR light (Figure 4). The transgenic line PHYA:PHYA-5-YFP re-established the *phyA-5* flunce-depended phenotype in *phyA-201*. Weak FR light-grown seedlings showed hyposensitivity, whereas strong FR light diminished the difference between PHYA:PHYA-YFP and PHYA:PHYA-5-YFP (Figure 4).

These results confirm that the A30V mutation in *PHYA* is indeed responsible for the observed phenotype.

### 3.2 Physiological characterization of *phyA-5*

#### 3.2.1 Photomorphogenic responses

No difference in 4-day-old seedling phenotypes was observed between the wild-type (Ws and Ler), *phyA-5*, and PHYA-5-YFP or PHYA-YFP expressing transgenic lines under strong FR light (Figure 4). Similarly, all tested lines exhibited similar hypocotyl elongation inhibition under continuous red or white light and remained etiolated in darkness.

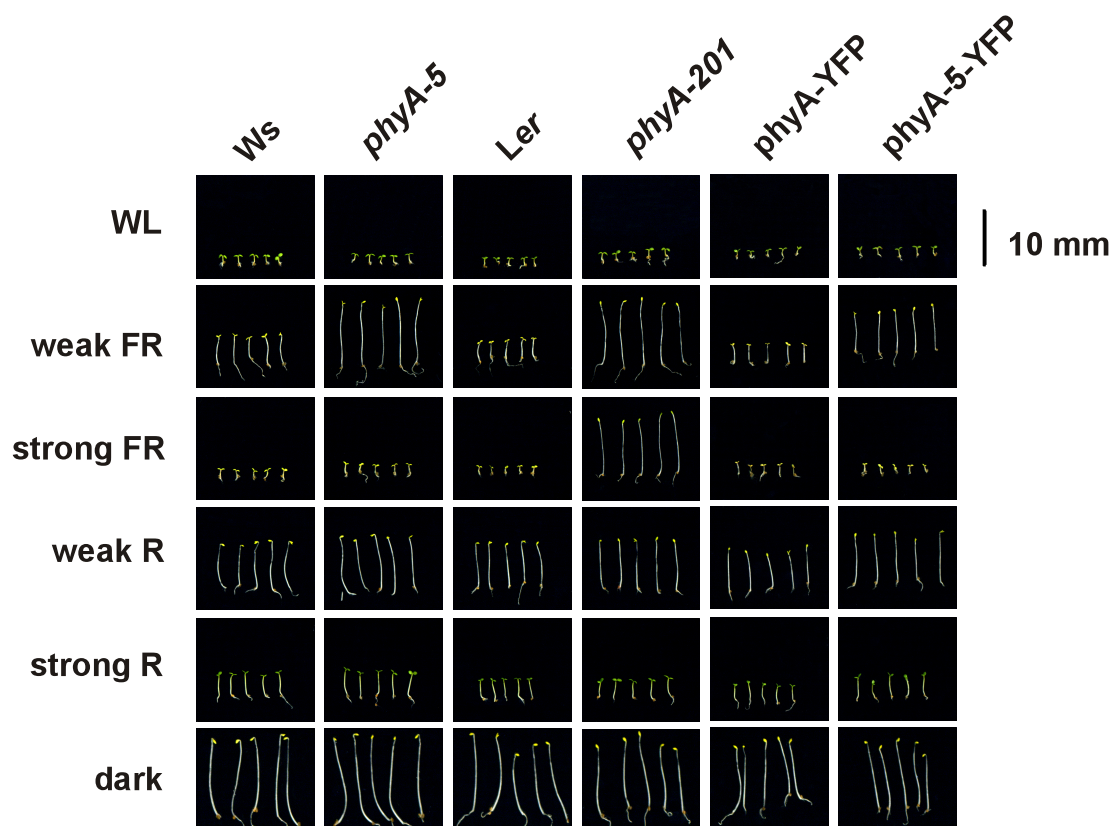


**Figure 4.** Effect of constant illumination on the inhibition of hypocotyl elongation of 4-day-old seedlings

WL:  $100 \mu\text{mol m}^{-2}\text{s}^{-1}$  fluorescent white light; weak FR:  $1 \mu\text{mol m}^{-2}\text{s}^{-1}$  far-red light; strong FR:  $10 \mu\text{mol m}^{-2}\text{s}^{-1}$  far-red light; weak R:  $0.002 \mu\text{mol m}^{-2}\text{s}^{-1}$  red light; strong R:  $20 \mu\text{mol m}^{-2}\text{s}^{-1}$  red light; dark: etiolated seedlings.

Analyzed genotypes: Ws: Wassilewskaya; *phyA-5* mutant (ecotype Ws); Ler: Landsberg erecta, *phyA-201* (ecotype Ler); *phyA*-YFP: *PHYA:PHYA-YFP* in *phyA-201* background; *phyA-5*-YFP: *PHYA:PHYA-5-YFP* in *phyA-201* background.

Seedlings expressing the mutant phyA-5 photoreceptor (*phyA-5*, *PHYA:PHYA-5-YFP*) and grown in continuous weak FR light, however, exhibited a hyposensitive phenotype similar to the *phyA-201* null mutant.

The fluence rate dependent response of hypocotyl elongation and cotyledon expansion was determined in order to investigate the observed light-dependent phenotype.

4-day-old seedlings were grown under different intensities of light with the appropriate wavelength. Hypocotyl lengths were determined as inhibition relative to the length of dark-grown seedlings for each line (Figure 5A, B). Cotyledon expansion was determined as an angle between cotyledons (Figure 5C, D).

The *phyA-5* mutant showed hyposensitive hypocotyl elongation inhibition response under constant weak FR irradiation (Figure 5A). The difference between *phyA-5* and wild-type (Ws) remains constant over the wide range of the applied fluence rates ( $0.1-1 \mu\text{mol m}^{-2}\text{s}^{-1}$ ). However, the *phyA-5* mutant displayed an increased light sensitivity, exhibiting a phenotype undistinguishable from the wild-type under  $10 \mu\text{mol m}^{-2}\text{s}^{-1}$  of FR light.

These results correlate with the cotyledon angle measurements, which also demonstrate hyposensitivity of *phyA-5* under low intensity of far-red light (Figure 5C).

The *phyA-5* mutation, however, does not affect the inhibition of hypocotyl elongation in seedlings grown under constant R light (Figure 2B).

The phyA-YFP fusion protein, expressed under the control of the PHYA promoter in *phyA-201* background complemented phyA deficiency in the mutant in terms of the classical photomorphogenic response (Figure 5A,D), indicating that the YFP tag does not reduce the physiological activity of phyA and that phyA-YFP is a fully functional photoreceptor, mimicking the properties of native phyA.

Transgenic lines, expressing the fusion protein phyA-5-YFP under the control of the PHYA promoter in *phyA-201* background displayed equally reduced light sensitivity similarly to *phyA-5*.

The obtained data indicate that phyA-5 encodes a partially active photoreceptor with altered far-red light sensing.

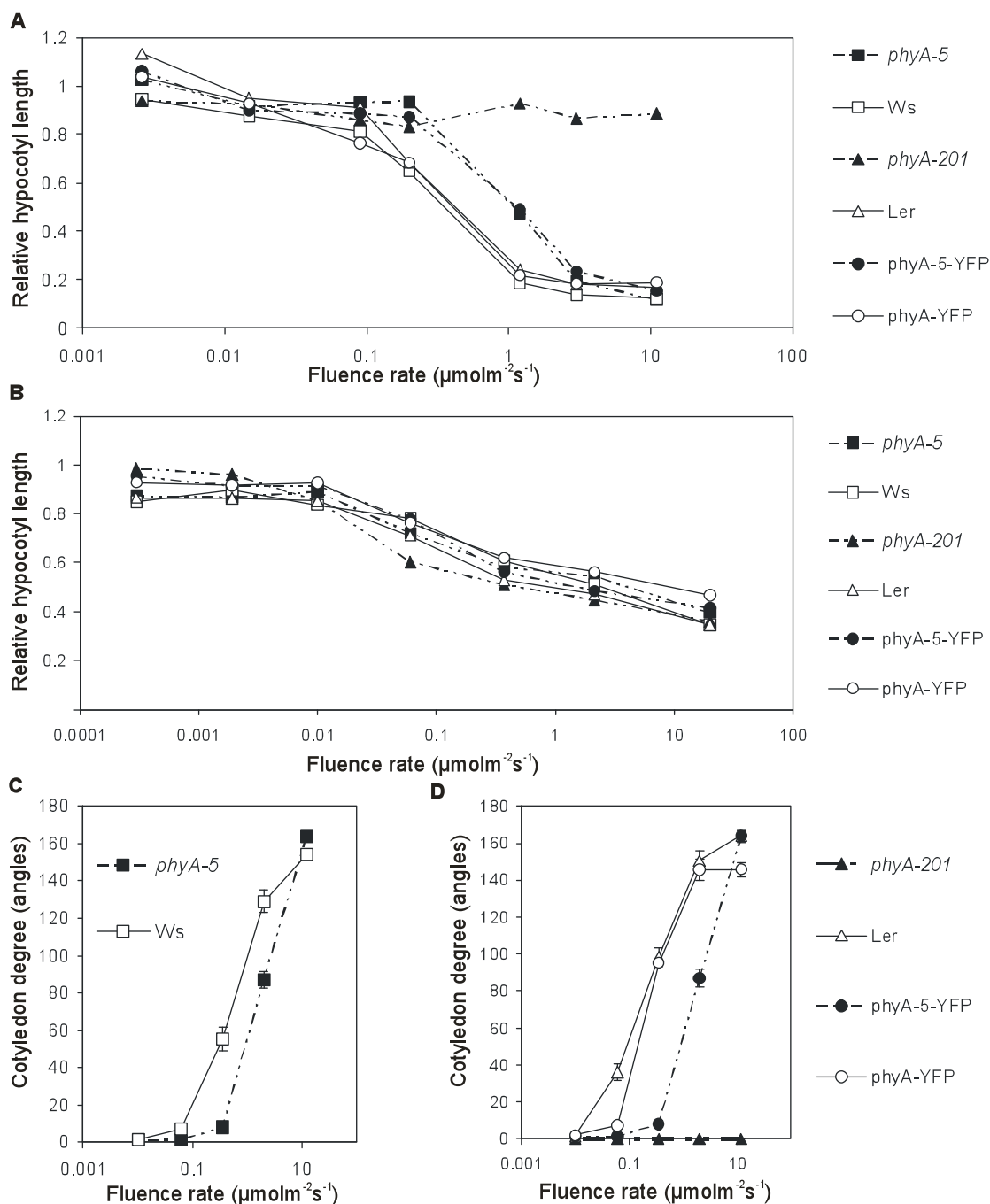


**Figure 5.** Physiological characterization of light responses.

**A, B:** Fluence rate dependent inhibition of hypocotyl elongation, measured on 4-day-old seedlings grown in far-red light and red light respectively. The obtained values were normalized to the hypocotyl length of the corresponding dark-grown seedlings.

**C, D:** Fluence rate dependency of hypocotyl angle, measured on 4-day-old seedlings grown in far-red light, cotyledon angles were measured immediately after the light treatment.

Analyzed genotypes: Ws: Wassilewskaya; *phyA-5* mutant (ecotype Ws); Ler: Landsberg erecta, *phyA-201* mutant (ecotype Ler); *phyA-YFP*: *PHYA:PHYA-YFP* in *phyA-201* background; *phyA-5-YFP*: *PHYA:PHYA-5-YFP* in *phyA-201* background.

### 3.2.2 High Irradiation Response and action spectrum

The High Irradiation Response was studied thoroughly as photoinhibition of hypocotyl elongation. This response requires continues irradiation and depends on fluence rate (Casal *et al.*, 2000b). The action spectrum constructed for HIR defines the spectral characteristics of the photoreceptor.

Additional fluence rate curves of hypocotyl elongation were constructed, in order to analyze the spectral sensitivity as relative efficiency of different wavelengths of light for induction of hypocotyl inhibition response.

Different wavelengths of irradiation were obtained by using different narrow banded DEPIL interference filters. Hypocotyl lengths of seedlings grown under these light fields were measured on the fourth day of the light treatment. The obtained values were normalized to the corresponding dark control value (Figure 6A, B).

The reciprocal value of the fluence rate resulting in 60% inhibition of hypocotyl elongation compared to the corresponding dark controls was determined; the highest obtained value in each line was set to 1, and all corresponding data were normalized to this value (Figure 6C).

Analyses were performed for the wild-type (Ws) and *phyA-5* mutant. The wild-type exhibited a typical HIR action spectrum, with maximum light sensitivity at 718 nm (Figure 6C). Although the maximum in light sensitivity remained at 718 nm in *phyA-5*, the overall shape of the action spectrum was changed. The light sensitivity of the *phyA-5* mutant is strongly reduced in the entire wavelength range examined, especially at higher wavelengths. The most pronounced reduction was observed at 742 nm resulting in complete insensitivity (Figure 6 B).

This experiment confirmed that the *phyA-5* mutation causes severe reduction in HIR. This effect is more pronounced at higher FR wavelengths.

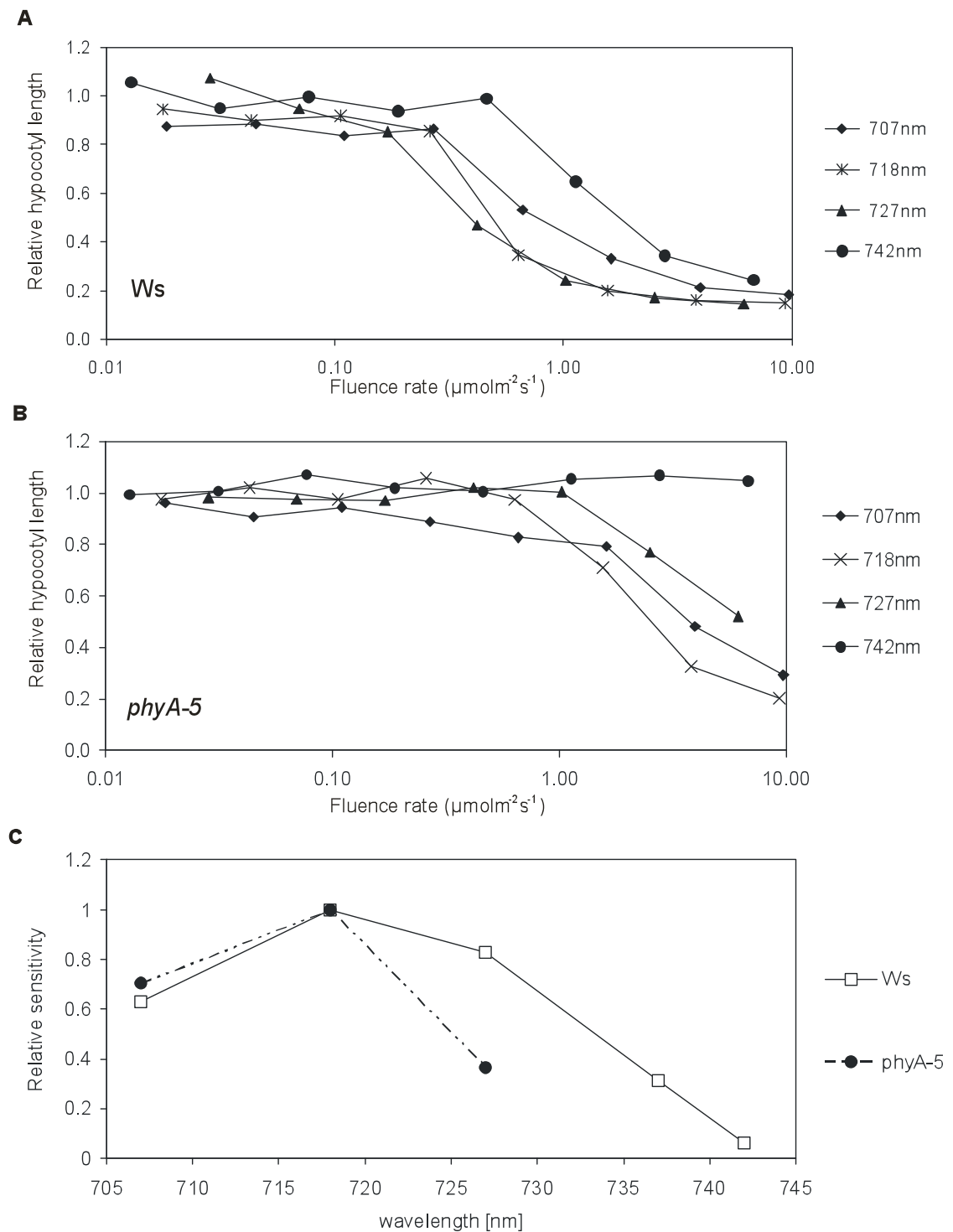


**Figure 6.** Hypocotyl elongation inhibition at different wavelengths.  
**A, B:** Relative hypocotyl lengths of 4-day-old seedlings, grown under constant FR light irradiation of different wavelengths. **A:** *Ws*, **B:** *phyA-5*.  
**C:** Action spectra for hypocotyl elongation in wild-type (*Ws*) and *phyA-5* seedlings.

### 3.2.3 Very Low Fluence Response

*phyA* accumulates in darkness and gets degraded rapidly in red light (Hennig *et al.*, 1999; Eichenberg *et al.*, 2000). Highly accumulated in the dark, *phyA* can perceive extremely low amounts of light and regulate very-low-fluence responses (VLFRs). This *phyA* mode of action is involved in regulating a number of processes during seedling development, including the inhibition of stem elongation by FR pulses (Casal *et al.*, 2000b).

In order to characterize *phyA*-mediated VLFR, seedlings grown in darkness were treated with 2.5-min repeated far-red light pulses followed by dark phases of variable lengths (Figure 7, Figure 8).

FR light pulses (DAL 715 nm filter) of  $0.6 \mu\text{mol m}^{-2}\text{s}^{-1}$  and  $6 \mu\text{mol m}^{-2}\text{s}^{-1}$  were applied every 7.5 min. The hypocotyl lengths were measured after 4 days of growth, and each obtained value was normalized to the corresponding etiolated control

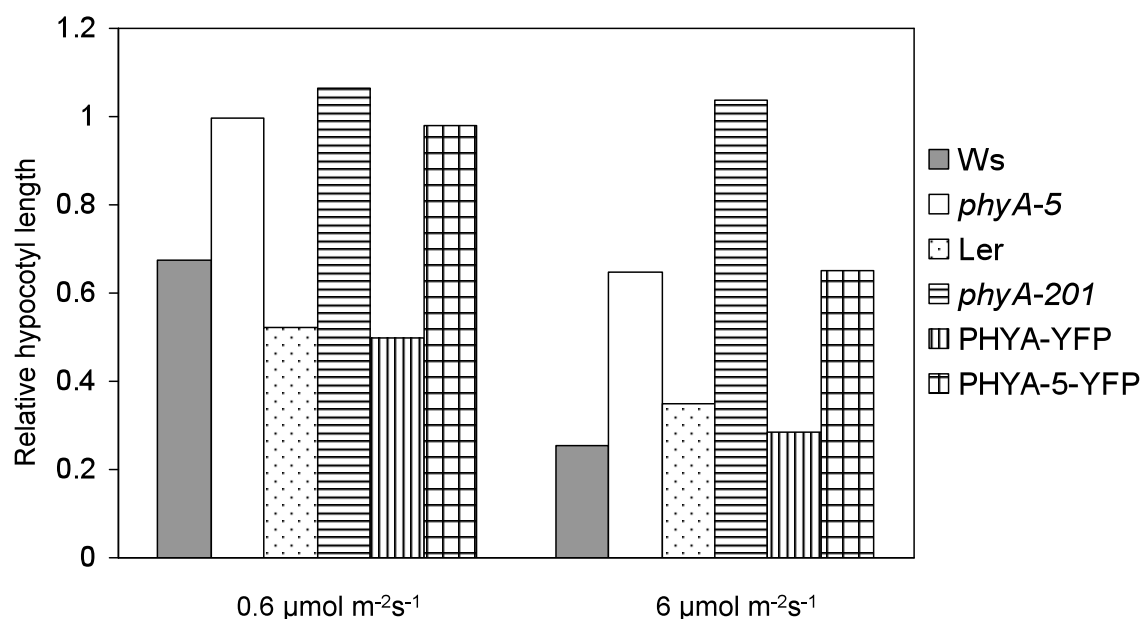


**Figure 7.** Relative hypocotyl elongation inhibition, induced by frequent FR pulses. 2.5 min pulses of FR light were applied every 7.5 minutes. The left and right panels represent the results of treatment with  $0.6 \mu\text{mol m}^{-2}\text{s}^{-1}$  and  $6 \mu\text{mol m}^{-2}\text{s}^{-1}$  pulses, respectively.

Analyzed genotypes: Ws: Wassilewskaya; *phyA-5* mutant (ecotype Ws); Ler: Landsberg erecta, *phyA-201* (ecotype Ler); PHYA-YFP: *PHYA:PHYA-YFP* in *phyA-201* background; PHYA-5-YFP: *PHYA:PHYA-5-YFP* in *phyA-201* background.

(Figure 7).

Weak and frequent FR pulses ( $0.6 \mu\text{mol m}^{-2}\text{s}^{-1}$ ) could induce the inhibition of hypocotyl elongation only in genotypes in which wild-type *phyA* is present (e.g. Ws, Ler, *PHYA:PHYA-YFP* in *phyA-201*) (Figure 7).

*PhyA-5*, just like the *phyA-201* null mutant exhibited complete loss of HIR.

Strong ( $6 \mu\text{mol m}^{-2} \text{s}^{-1}$ ) 7.5 min FR pulses can induce a *phyA-5*-driven response which is less pronounced than in the case of *phyA* (Figure 7). *PhyA-201* showed no response at this intensity either.

The second part of the experiment includes repeated FR pulses, interrupted by long dark phases – 30 and 60 min (Figure 8).

FR light pulses (DAL715 filter) of  $6 \mu\text{mol m}^{-2}\text{s}^{-1}$  were given once in every 60 or 30 min. Hypocotyl length was measured after 4 days of growth and normalized to the corresponding dark-grown control.

Seedlings, containing *phyA-5* (*phyA-5* mutant, *PHYA:PHYA-5-YFP* in *phyA-201* background), exhibited highly reduced hypocotyl elongation inhibition, mimicking the *phyA-201* null mutant. These observations are supported by results obtained from transgenic seedlings expressing *phyA-YFP* and *phyA-5-YFP*.

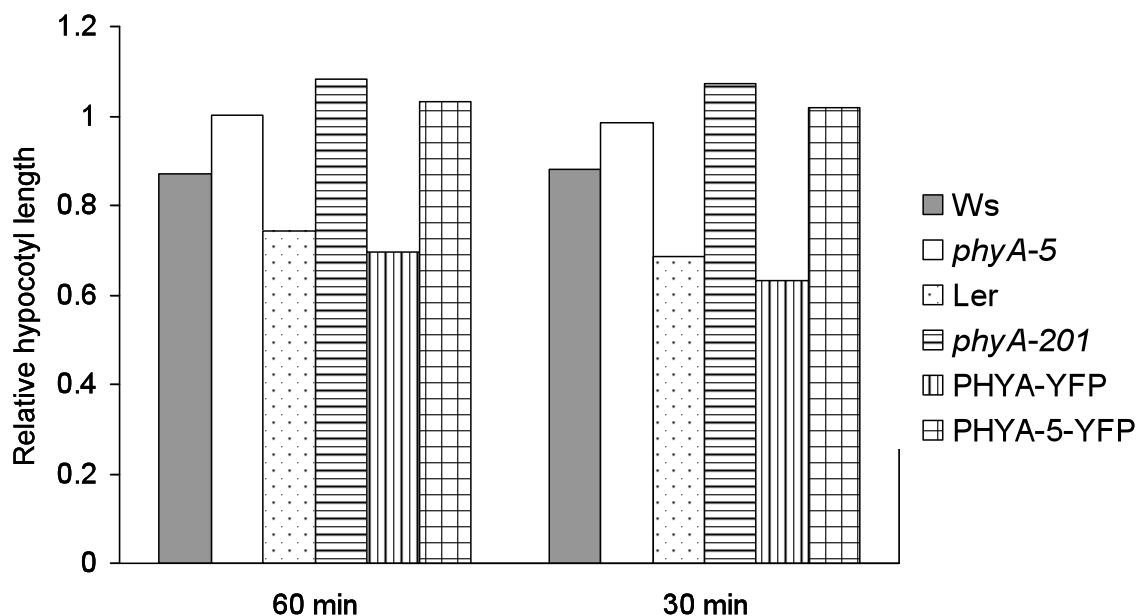


**Figure 8.** The effect of rare FR pulses on hypocotyl elongation inhibition. 2.5 min pulses of FR light ( $6 \mu\text{mol m}^{-2}\text{s}^{-1}$ ) were applied every 60 (left panel) or 30 min (right panel).

Analyzed genotypes: Ws: Wassilewskaya; *phyA-5* mutant (ecotype Ws); Ler: Landsberg erecta, *phyA-201* (ecotype Ler); *PHYA-YFP*: *PHYA:PHYA-YFP* in *phyA-201* background; *PHYA-5-YFP*: *PHYA:PHYA-5-YFP* in *phyA-201* background.

The results shown in Figure 7 and Figure 8 suggest that the *phyA-5* mutation alters the normal VLFR.

To investigate further the effect of the *phyA-5* mutation on VLFR, the ability of *phyA-5* to induce response at the gene expression level was studied. The transcript level of *PRR9* (*PSEUDO RESPONSE REGULATOR 9*, At2g49790) is upregulated by light, which is mediated predominantly by *phyA* during initial exposure to R light, with *phyB* playing only a minor role in this process in the presence of *phyA* (Tepperman *et al.*, 2006). This gene can be used as a marker to examine VLFR.

4-day-old etiolated seedlings were irradiated with a single R light pulse (0.01 or 10  $\mu\text{mol m}^{-2}\text{s}^{-1}$ ) for 1 min and were transferred to darkness for 60 min before sample collection. The mRNA level was determined by qRT-PCR. Data were normalized to the corresponding dark levels and *TUBULIN2/3* mRNA transcript (Figure 9).

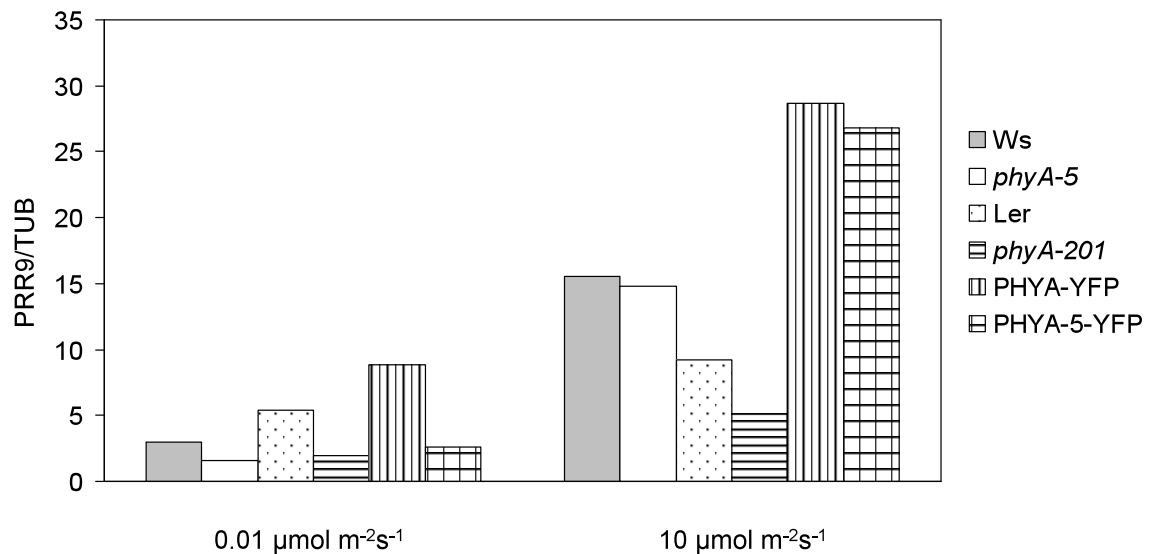


**Figure 9.** Light-inducible induction of *PRR9* transcription

Expression level of *PRR9*, induced by 1 min irradiation with 0.01  $\mu\text{mol m}^{-2}\text{s}^{-1}$  (left panel) or 10  $\mu\text{mol m}^{-2}\text{s}^{-1}$  (right panel) of R light.

Analyzed genotypes: Ws: Wassilewskaya; *phyA-5* mutant (ecotype Ws); Ler: Landsberg erecta, *phyA-201* (ecotype Ler); PHYA-YFP: *PHYA:PHYA-YFP* in *phyA-201* background; PHYA-5-YFP: *PHYA:PHYA-5-YFP* in *phyA-201* background.

The results revealed that *PRR9* mRNA induction by very low intensity R light is impaired in *phyA-5* and transgenic line expressing PHYA-5-YFP similarly to the null

## RESULTS

mutant *phyA-201*. A strong R pulse induces *PRR9* expression equally in *phyA-5* and WT. Similar results were obtained for transgenic lines harboring *PHYA:PHYA-YFP* and *PHYA:PHYA-5-YFP* transgenes in *phyA-201*. However, the *phyA-201* null mutant exhibited reduction in the expression of *PRR9* not as markedly as after a weak R pulse. Increased induction of *PRR9* expression after a strong R pulse in *phyA-201* can be explained by phyB action.

These experimental data confirmed that the *phyA-5* mutation affects VLRf at both physiological and genetical levels.

### 3.3 *PhyA-5* transcription analysis

Expression of *PHYA* is repressed by light (Hennig *et al.*, 1999). Upon constant FR irradiation phytochrome A alone mediates all light responses, therefore, under these conditions *phyA* down-regulates its own expression. Mutation in the *PHYA* gene may affect *PHYA* promoter control, followed by disruptions in *PHYA* expression. Changes in *PHYA* expression level in *phyA-5* mutant compared to wild-type can explain the observed hyposensitive phenotype of the mutant.

The mRNA level of *PHYA* in *phyA-5* and wild-type was determined in order to examine the possibility of impaired *PHYA* expression. Wild-type (Ws) and *phyA-5* seedlings were grown in darkness, constant weak FR light ( $1 \mu\text{mol m}^{-2}\text{s}^{-1}$ ) or strong FR light ( $10 \mu\text{mol m}^{-2}\text{s}^{-1}$ ) for 4 days. mRNA levels were determined by qRT-PCR. Data normalized to *TUBULIN2/3* levels are shown in Figure 10.

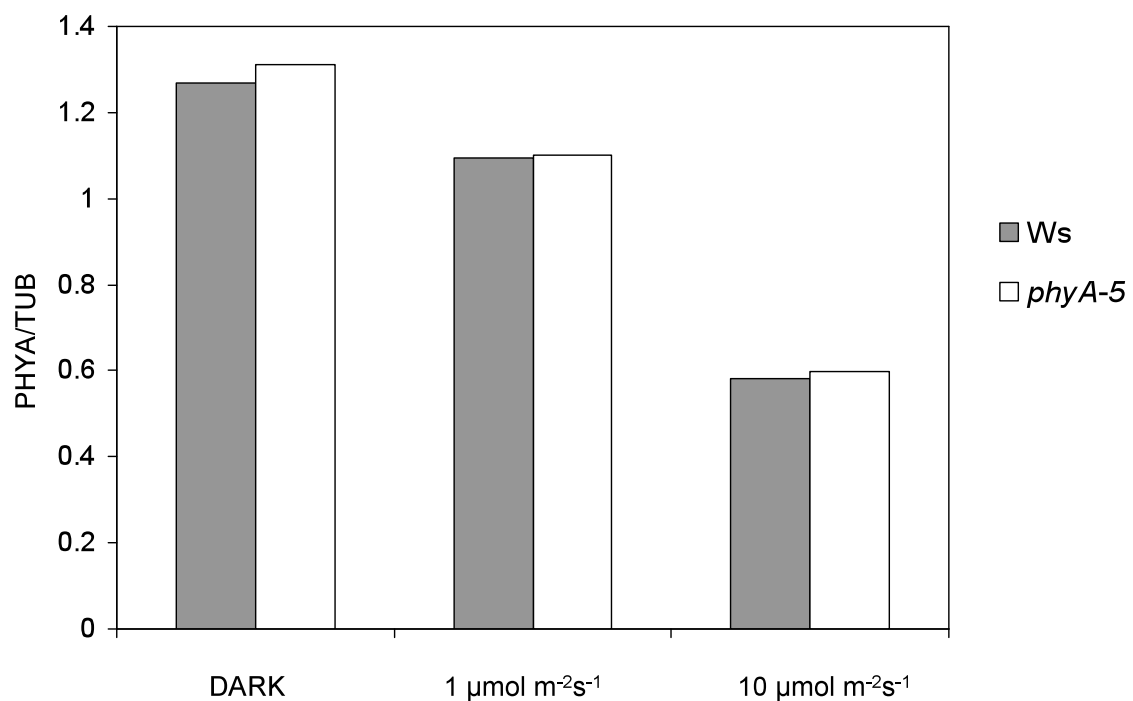


**Figure 10.** *PHYA* and *PHYA-5* transcription level

*PHYA* transcript levels in 4-day-old wild-type (white columns) or *phyA-5* (grey columns) seedlings was obtained using qRT-PCR analysis. Seedlings were grown in the dark, weak FR light ( $1 \mu\text{mol m}^{-2}\text{s}^{-1}$ ) or strong FR light ( $10 \mu\text{mol m}^{-2}\text{s}^{-1}$ ) prior to RNA isolation.

## RESULTS

The results showed light-dependent reduction in transcript level of both *PHYA* and *PHYA-5*. No detectable difference can be observed between *PHYA* and *PHYA-5* transcript levels in FR grown seedlings, suggesting that the feedback loop between phyA-5 protein and *PHYA* is not disrupted and phyA-5 is a functional regulator of its own expression.

### 3.4 PhyA-5 protein level analysis

In order to investigate whether the hyposensitive phenotype of *phyA-5* mutant can be explained by changes in protein stability, several experiments were performed.

PHYA and PHYA-5 protein levels were determined in dark-grown 4-day-old seedlings treated with  $25 \mu\text{mol m}^{-2}\text{s}^{-1}$  R light for different time periods. Western blot analysis was performed on total protein extracts, isolated from wild-type or *phyA-5* etiolated seedlings using PHYA or actin specific antiserum (Figure 11A).

It was known from previous studies that the highest levels of phyA can be measured in etiolated seedlings, and the light-induced degradation of phyA is triggered by the Pr-Pfr transition of the photoreceptor (Hennig *et al.*, 1999). In the experiments performed in this study the phyA-5 protein level in darkness does not differ from that of wild-type phyA (Figure 11 A, lanes 1, 7). There is also no difference between red light induced degradation of phyA and phyA-5 protein (Figure 11, A, lanes 2-6 and 8-12 respectively). The obtained results suggest that strong R light can activate Pfr formation of phyA-5 as effectively as that of wild-type phyA.

In the next set of experiments it was investigated whether the phyA-5 level differs from its wild-type counterpart under those conditions, when the mutant displays a hyposensitive phenotype (Figure 11B).

There was no detectable difference between the steady-state levels of phyA and phyA-5 in seedlings grown under strong FR light, which is consistent with the wild-type phenotype observed in the *phyA-5* mutant under these conditions. In 4-day-old weak FR-grown seedlings, however, phyA-5 exhibited detectable levels, whereas wild-type phyA remained below detection limit (Figure 11B, lines 5-8). The presented dataset also revealed that the levels of PHYA-YFP and PHYA-5-YFP fusion proteins are comparable to the level of endogenous phyA and phyA-5 protein, respectively, which, taken together with physiological studies (see chapter 3.2), confirms that transgenic PHYA-YFP fusion proteins are fully functional and correspond to their endogenous counterparts. It is also observable that the YFP tag slightly increases the stability of the photoreceptor, resulting in higher steady-state levels as compared to the corresponding non-tagged PHYAs. This observation is in good agreement with results published by Wolf *et al.* (2011).

Considering that the transcription level of *PHYA-5* is not altered upon FR light irradiation, the elevated protein level could be explained in terms of disrupted degradation due to insufficient Pr-Pfr transition under weak FR light. This explanation removes the apparent contradiction between elevated photoreceptor level and reduced responses.

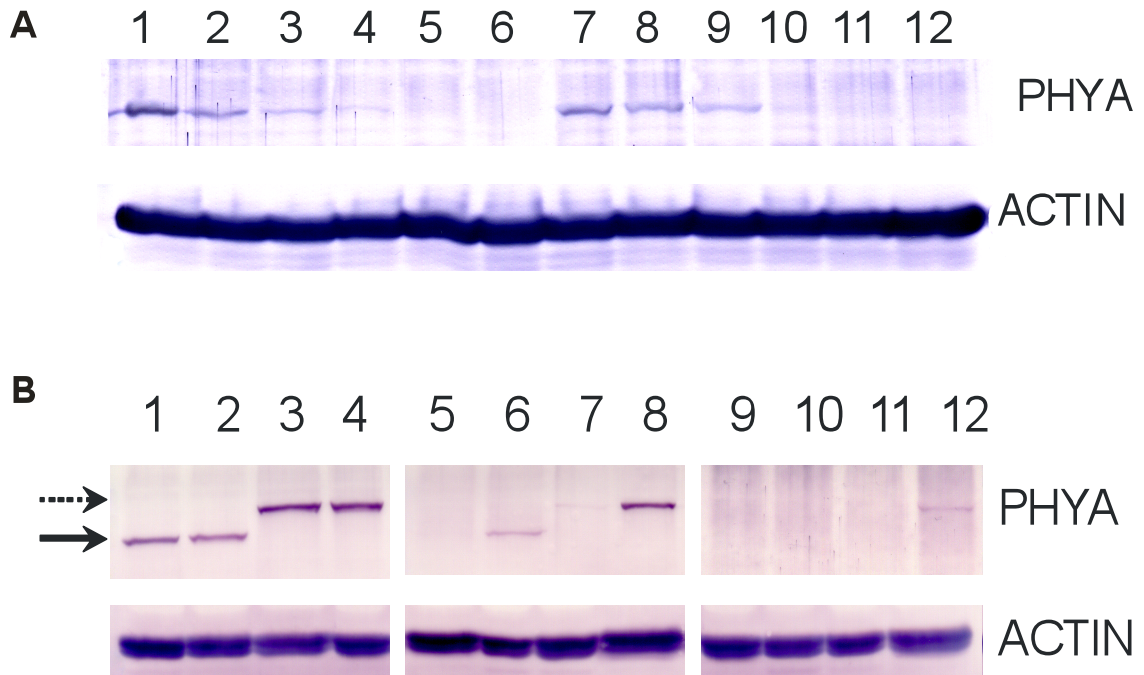


**Figure 11.** Light-dependent degradation of phyA-5

**A:** R light-induced degradation:

Total protein was isolated from 4-day-old etiolated seedlings, treated with  $25 \mu\text{mol m}^{-2}\text{s}^{-1}$  R light for different time periods and subjected to western blot analysis using PHYA or actin specific antiserum

0 h (lanes 1, 7), 1 h (lanes: 2, 8), 2 h (lanes 3, 9), 3 h (lanes 4, 10), 4 h (lanes 5, 11), 6 h (lanes 6, 12).

Ws: lanes 1-6; *phyA-5*: lanes 7-12.

**B:** FR light-induced degradation:

Total protein was isolated from 4-day-old seedlings, grown in darkness, and under constant irradiation of weak ( $1 \mu\text{mol m}^{-2}\text{s}^{-1}$ ) or strong ( $10 \mu\text{mol m}^{-2}\text{s}^{-1}$ ) FR light. Western blot analysis using PHYA (upper panels) or ACTIN specific (lower panel) antiserum was performed.

dark (lanes 1-4),  $1 \mu\text{mol m}^{-2}\text{s}^{-1}$  (lanes 5-8),  $10 \mu\text{mol m}^{-2}\text{s}^{-1}$  (lanes 9-12).

Ws (lanes: 1, 5, 9); *phyA-5* (lanes 2, 6, 10);

*PHYA:PHYA-YFP* in *phyA-201* (lanes 3, 7, 11); *PHYA:PHYA-5-YFP* in *phyA-201* in (lanes 4, 8, 12).

The continuous arrow marks the bands corresponding to endogenous PHYA, whereas the spotted arrow marks the PHYA-YFP specific band.

### 3.5 Subcellular localization of phyA-5 protein

Subcellular localization of the phyA-5 protein was studied in transgenic plants. The phyA-YFP and phyA-5-YFP fusion proteins were expressed under the control of the *PHYA* promoter in the *phyA-201* null mutant. Physiological studies (see chapter 3.2) had revealed that both phyA-YFP and phyA-5-YFP are functional photoreceptors.

All localization experiments were performed with etiolated seedlings of the homozygous transgenic lines. Seedlings were grown for 4 days in darkness, and light treated prior to epifluorescence microscopic analysis (Figure 12).

The light treatment was provided by irradiation of the samples with  $1 \mu\text{mol m}^{-2}\text{s}^{-1}$  or  $10 \mu\text{mol m}^{-2}\text{s}^{-1}$  far-red light for 4 h and 24 h. The results of microscopic studies revealed that strong FR light treatment of any duration does not lead to different localization patterns of phyA-5 compared to wild-type phyA. In weak FR light, however, the nuclear import of phyA-5-YFP is decreased below detection level.

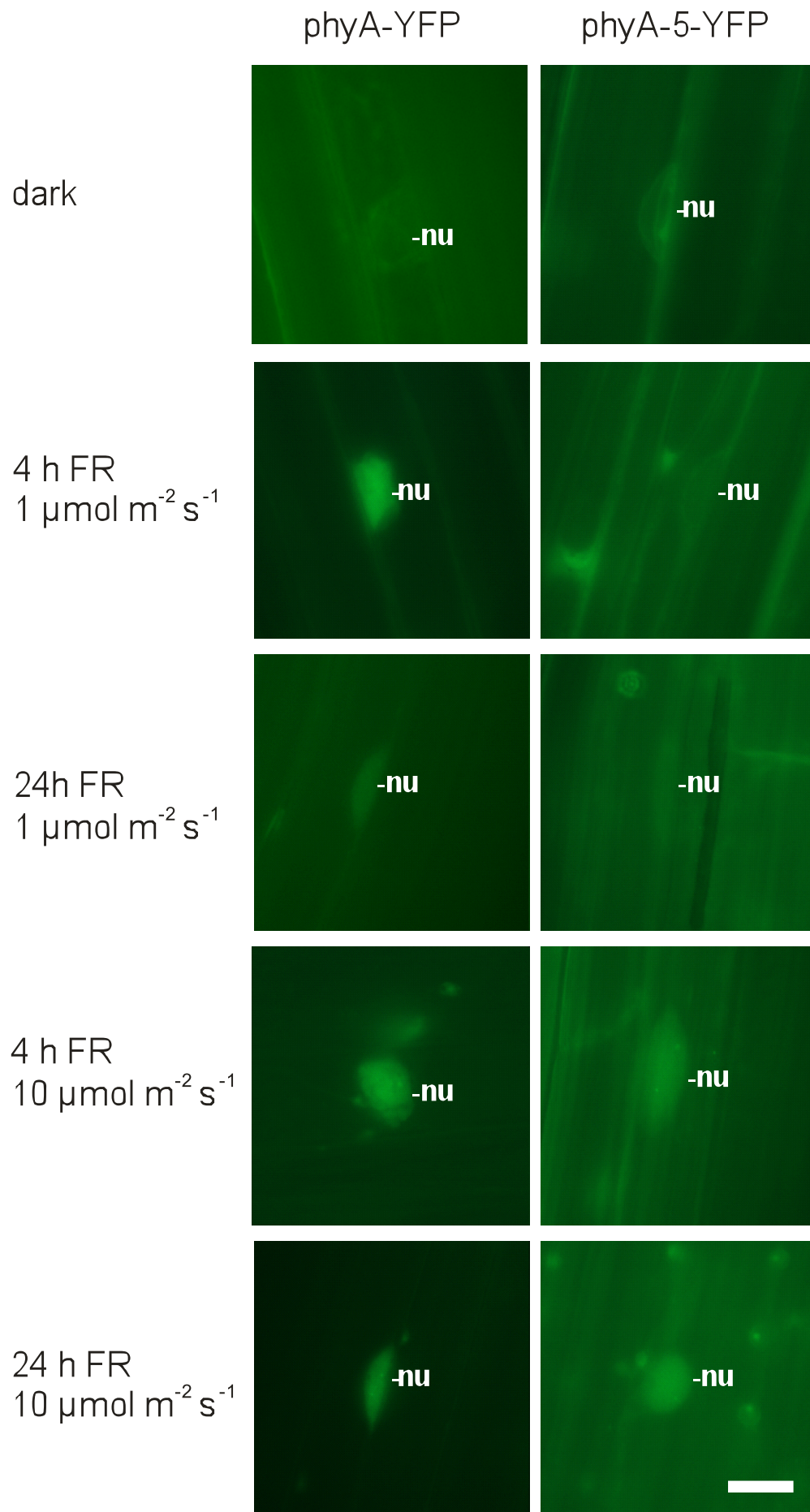
These data correlate with the observed hyposensitivity of the mutant in weak FR light and supports the idea that the observed phenotype is caused by a decreased level of nuclear phyA under this condition.

The efficiency of the nuclear import of phyA-5 was further examined by applying semi-quantitative epifluorescence microscopy (Figure 13). Etiolated seedlings expressing *PHYA:PHYA-YFP* and *PHYA:PHYA-5-YFP* in *phyA-201* were irradiated with 1 min R light pulse ( $0.2$  or  $5 \mu\text{mol m}^{-2}\text{s}^{-1}$ ).

**Figure 12.** Intracellular dynamics of phyA-YFP and phyA-5-YFP fusion proteins under different light treatments.

Cellular distribution of phyA-YFP (*PHYA:PHYA:YFP* in *phyA-201* background) and phyA-5-YFP (*PHYA:PHYA-5:YFP* in *phyA-201*) is shown in darkness and after 4 h or 24 h treatment of FR light ( $1 \mu\text{mol m}^{-2}\text{s}^{-1}$  or  $10 \mu\text{mol m}^{-2}\text{s}^{-1}$ ).

**nu** point to nuclei, white bar represents 10  $\mu\text{m}$ .



After a subsequent incubation of 5 min at 25°C, fluorescent images were taken (Figure 13A). The fluorescent signal was background corrected and normalized to the corresponding averaged dark control (Figure 13B).

The results indicate that a short pulse of strong ( $5 \mu\text{mol m}^{-2}\text{s}^{-1}$ ) red light promotes induction of the nuclear import of phyA and phyA-5 at the same level. On the contrary, nuclear accumulation of phyA-5 after a pulse of weak ( $0.2 \mu\text{mol m}^{-2}\text{s}^{-1}$ ) red light was significantly impaired as compared to the wild-type.

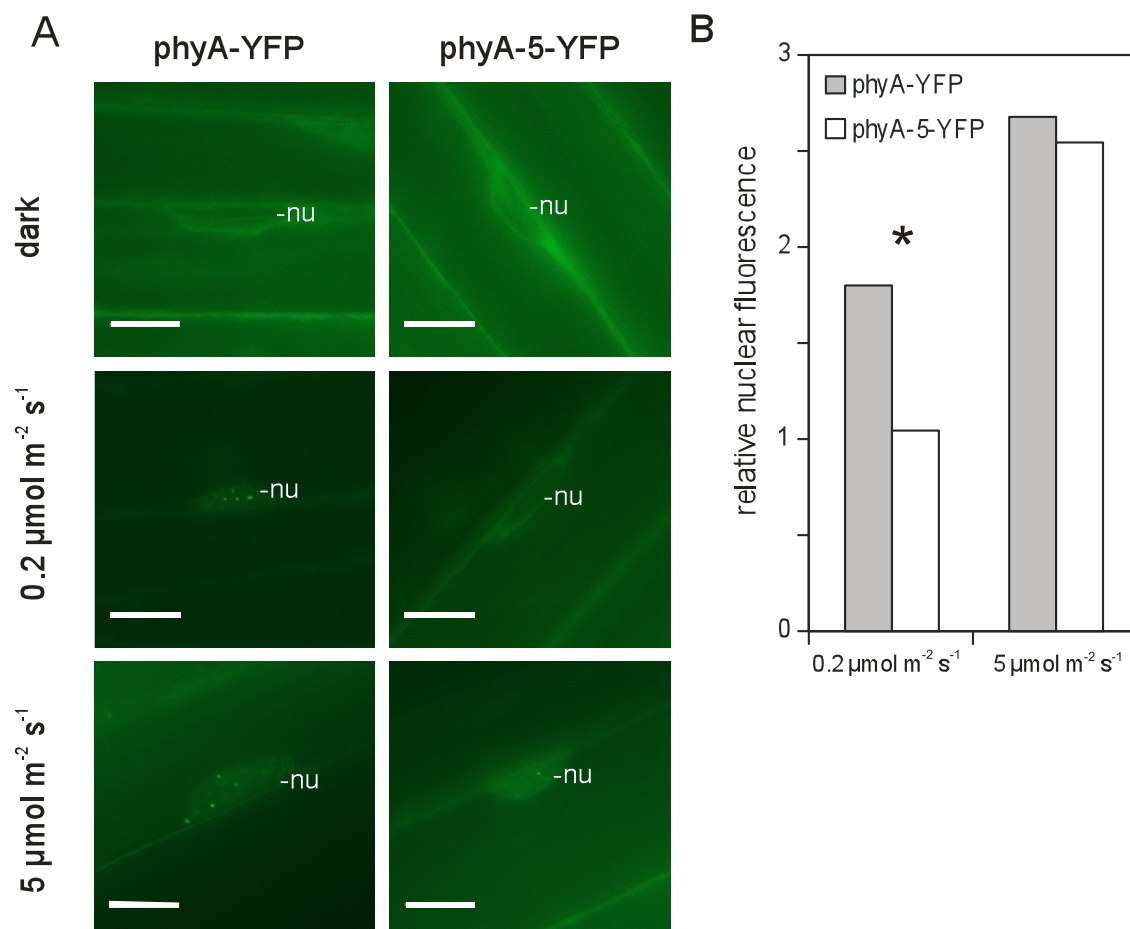


**Figure 13.** The phyA-5 nuclear import is impaired at lower fluences.

**A:** representative images used for semi-quantitative fluorescence microscopy shown in Figure 13B. nu: nucleus, scale bar represents  $10 \mu\text{m}$ .

**B:** Quantification of phyA-5 nuclear import after R light pulse of different intensities. Dark mean values were: phyA-YFP:  $9.23 \pm 1.72$ , phyA-5-YFP:  $8.00 \pm 1.53$ . Statistically significant difference between phyA-YFP and phyA-5-YFP signal was determined by Student's two-tailed heteroscedastic t-test: asterisk indicate sample sets where  $P < 0.001$ .

### 3.6 Molecular interaction of PHYA-5 with nuclear transport facilitators

No NLS motif has been identified in phyA, suggesting the existence of transport facilitators for phytochrome nuclear translocation. It was shown previously that nuclear accumulation of phyA is mediated by the small plant-specific proteins FHY1 and FHL (Hiltbrunner *et al.*, 2005, 2006) and that a shortened fragment of phytochrome A (phyA 1-406) is sufficient for light-induced binding to FHY/FHL1.

Yeast-2-hybrid assays were used to examine the binding affinity of phyA-5 to FHY and FHL. The *PHYA-5* coding sequence was fused to the GAL4 DNA-binding domain (BD), whereas *FHY1* and *FHL* coding sequences were fused to the GAL4 activation domain (AD). These fusion proteins were co-expressed in yeast cells growing on solid medium (Figure 14). The nonselective (L-W-) plates allow growth of yeast cells containing both AD and BD plasmids as growth control, whereas selective (L-W-H-) plates allow growth only of those cells in which the AD and BD tagged proteins directly interact with each other. To test whether the interaction of phyA and phyA-5 with FHY1/FHL is light-specific, phycocyanobilin chromophore (PCB) was added to the medium. This allows phyA to undergo Pr-Pfr transition after light treatment and promotes cell growth on the selective medium only when phyA Pfr is interacting with its partners.

After the dropping of 5  $\mu$ l yeast cultures, the plates were incubated at 28°C for two days under 1  $\mu$ mol m<sup>-2</sup>s<sup>-1</sup> red light (R), 10  $\mu$ mol m<sup>-2</sup>s<sup>-1</sup> far-red light (FR) or in darkness (D).

Efficient growth on the non-selective (L-W-) plates confirms the presence of the plasmids expressing the proteins participating in the assay (Figure 14). Colony growth on L-W-H- medium indicates interaction between the examined proteins. In cases when PCB was also added to the medium, phyA can exist in Pfr form in R light, whereas without R irradiation, most of the phyA molecules are present in Pr form. The yeast growth indicated that the FHY1/FHL proteins interact with phyA only under R light treatment, but not on dark or FR irradiated plates. This finding confirms that protein interaction of nuclear transport facilitators with phyA is Pfr-specific, as shown previously (Hiltbrunner *et al.*, 2006).

		H-L-W-				
		+PCB			-PCB	L-W-
		R	FR	D		
AD	BD					
AD	PHYA-BD					
AD	PHYA 5-BD					
AD	PHYA (1-406)-BD					
AD	PHYA-5 (1-406)-BD					
AD-FHY1	BD					
AD-FHY1	PHYA-BD					
AD-FHY1	PHYA-5-BD					
AD-FHY1	PHYA (1-406)-BD					
AD-FHY1	PHYA 5 (1-406)-BD					
AD-FHL	BD					
AD-FHL	PHYA-BD					
AD-FHL	PHYA 5-BD					
AD-FHL	PHYA (1-406)-BD					
AD-FHL	PHYA 5 (1-406)-BD					

**Figure 14.** Light-regulated interaction of FHY1, FHL and PHYA in yeast cells  
R:  $1 \mu\text{mol m}^{-2}\text{s}^{-1}$  red light; FR:  $10 \mu\text{mol m}^{-2}\text{s}^{-1}$  far-red light; D: darkness. AD: GAL4 activation domain; BD: GAL4 DNA-binding domain.  
Plates: non-selective (L-W-), selective (H-L-W-, containing 1 mM 3-aminotiazole).  
All plates contained PCB, unless otherwise indicated (-PCB).

The N-terminal 406-amino-acid fragment of phyA (1-406) exhibited normal interaction with FHY1/FHL (in good agreement with Hiltbrunner *et al.*, 2006), whereas phyA-5 (1-406) showed no detectable interaction with FHL and FHY1.

To investigate further the possible differences between the binding affinities of phyA Pfr and phyA-5 Pfr to the nuclear import facilitators, overnight cultures were diluted to the same optical density, OD = 1 (1x) and sets of dilutions (2x - 20x) were made. 5  $\mu$ l from each dilution were dropped on selective H-L-W- plates, supplied with 1 mM 3-aminotriazole and 10  $\mu$ M PCB. Plates were incubated for 2 days at 28 °C under 1  $\mu$ mol m<sup>-2</sup>s<sup>-1</sup> red light. The results (Figure 15) confirmed that the A30V mutation impairs phyA-5 binding to FHY1 and FHL as compared to wild-type phyA.

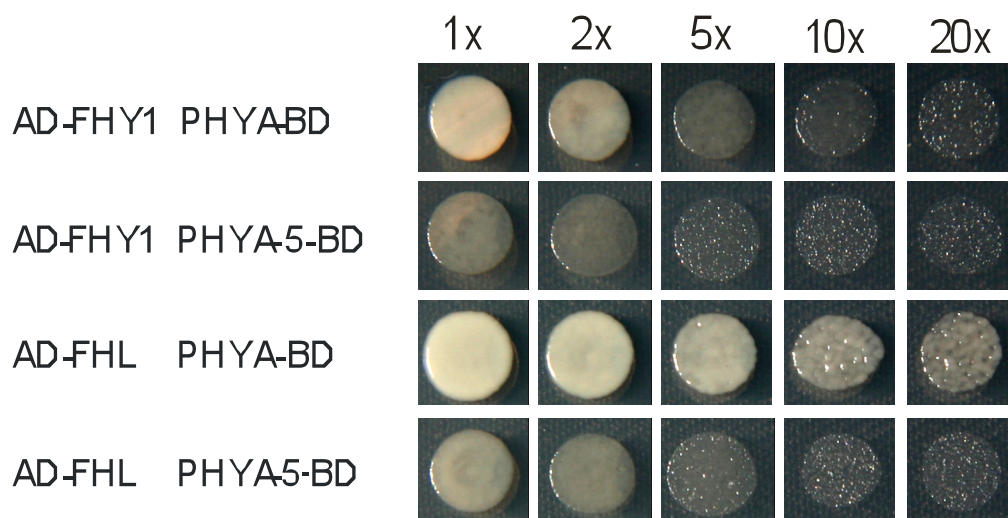


**Figure 15.** Binding affinity of phyA-5 to FHY1 and FHL in yeast cells  
AD: GAL4 activation domain; BD: GAL4 DNA-binding domain.  
Left panel indicates co-transformed plasmids.  
Upper line indicates dilution rates.

In order to quantify the level of protein interaction,  $\beta$ -galactosidase activity was determined (Figure 16). Yeast strain Y187 was co-transformed with the indicated plasmids. 0.5 ml liquid cultures were propagated in non-selective medium (L-W-) supplied with 20  $\mu$ M PCB overnight in the dark. Cultures were irradiated with 30  $\mu$ mol m<sup>-2</sup>s<sup>-1</sup> R for 5 min, either followed by 5 min irradiation with 20  $\mu$ mol m<sup>-2</sup>s<sup>-1</sup> FR (Pr), or not (Pfr). After light treatment, the cultures were incubated in dark for 4 h and  $\beta$ -galactosidase activity was measured.

The results of the assay confirm the results obtained by the plate growth assay. The interaction between FHY1/FHL and phyA is Pfr specific and this binding is impaired in the phyA-5 protein.

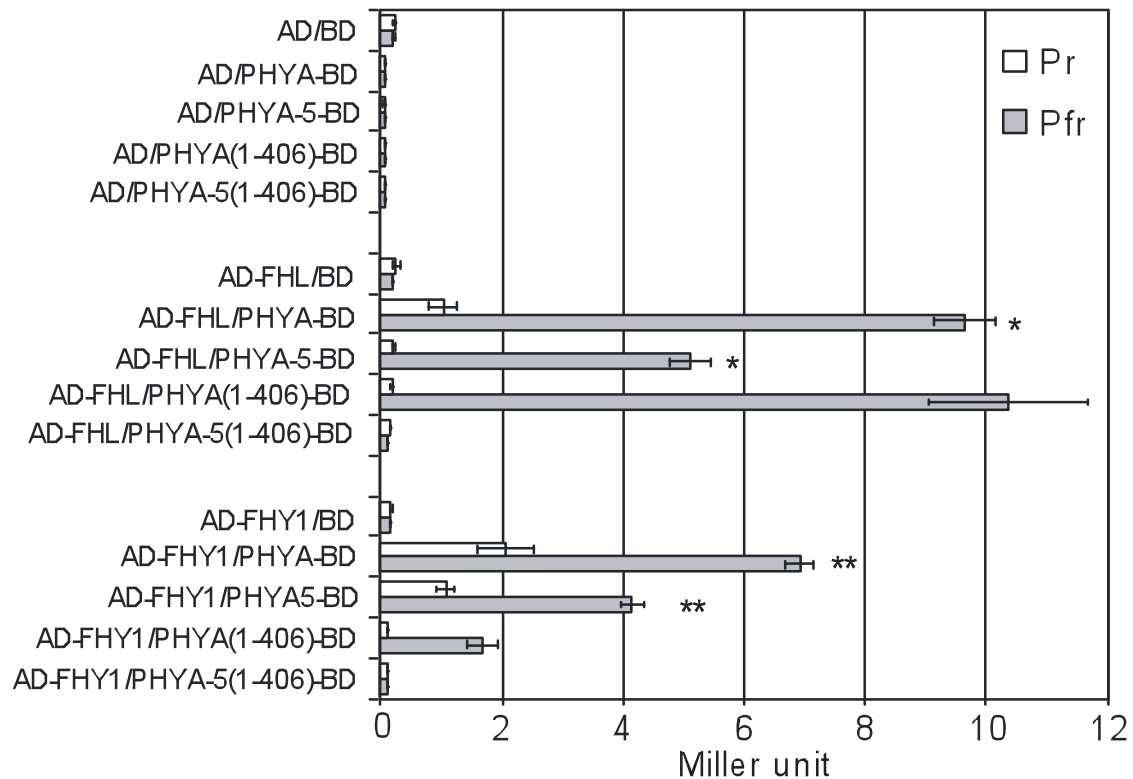


**Figure 16.** Quantification of protein interactions

AD: GAL4 activation domain; BD: GAL4 DNA-binding domain.

Left panel indicates the cotransformed plasmids. White and grey columns show the Pr and Pfr specific binding, respectively, of phyA to FHL and FHY1.

B-galactosidase activity was measured using ortho-Nitrophenyl-b-galactoside substrate. Triplicates were assayed and mean values are plotted. Error bars indicate standard error. Student's two-tailed heteroscedastic t test was used to determine the statistical significance of the difference between values indicated by 1 or 2 asterisks, respectively (each bar represents 20 replicates,  $P < 0.001$ ).

### 3.7 Complementation of the *phyA-201* mutant by phyA-5-YFP-NLS and phyA-YFP-NLS fusion proteins

In order to validate the conclusion that the phenotype of the *phyA-5* mutant is caused by insufficient nuclear import, the transgenic plants expressing the phyA-5 and WT phyA proteins fused to YFP and NLS driven by the PHYA promoter in *phyA-201* background were generated.

Resistance-based selection of transformants was performed and several T1 lines were tested for resistance-based segregation. Single copy homozygous transformed lines were tested by Western blot and lines with transgenic phyA levels similar to that of the endogenous phyA were selected for further analysis.

Subcellular localization experiments were performed with 4-day-old etiolated seedlings of the transgenic lines grown in darkness prior to epifluorescence microscopy.

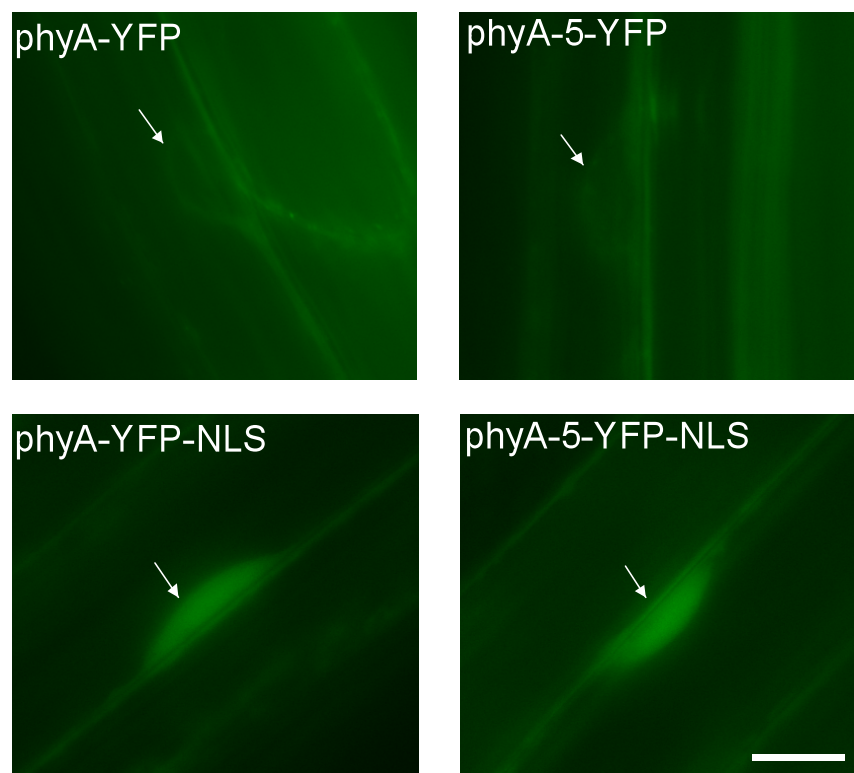


**Figure 17.** Subcellular localization of phyA-YFP-NLS and phyA-5-YFP-NLS. Cellular distribution of phyA-YFP (*PHYA:PHYA:YFP* in *phyA-201* background), phyA-5-YFP (*PHYA:PHYA-5:YFP* in *phyA-201*), phyA-YFP-NLS (*PHYA:PHYA:YFP:NLS* in *phyA-201*) and phyA-5-YFP-NLS (*PHYA:PHYA-5:YFP:NLS* in *phyA-201*) is shown in 4-days old etiolated seedlings.

White arrow point to nuclei, white scale bar represents 10  $\mu$ m.

The result of microscopic observations showed that, as expected, phyA-YFP-NLS and phyA-5-YFP-NLS proteins were constitutively localized in the nucleus (Figure 17).

Hypocotyl growth inhibition was determined for 4-day-old seedlings grown in  $1 \mu\text{mol m}^{-2}\text{s}^{-1}$  constant FR. The results of the analysis revealed that phyA-5-YFP-NLS complements the *phyA-201* mutant as effectively as phyA-YFP-NLS (Figure 18).

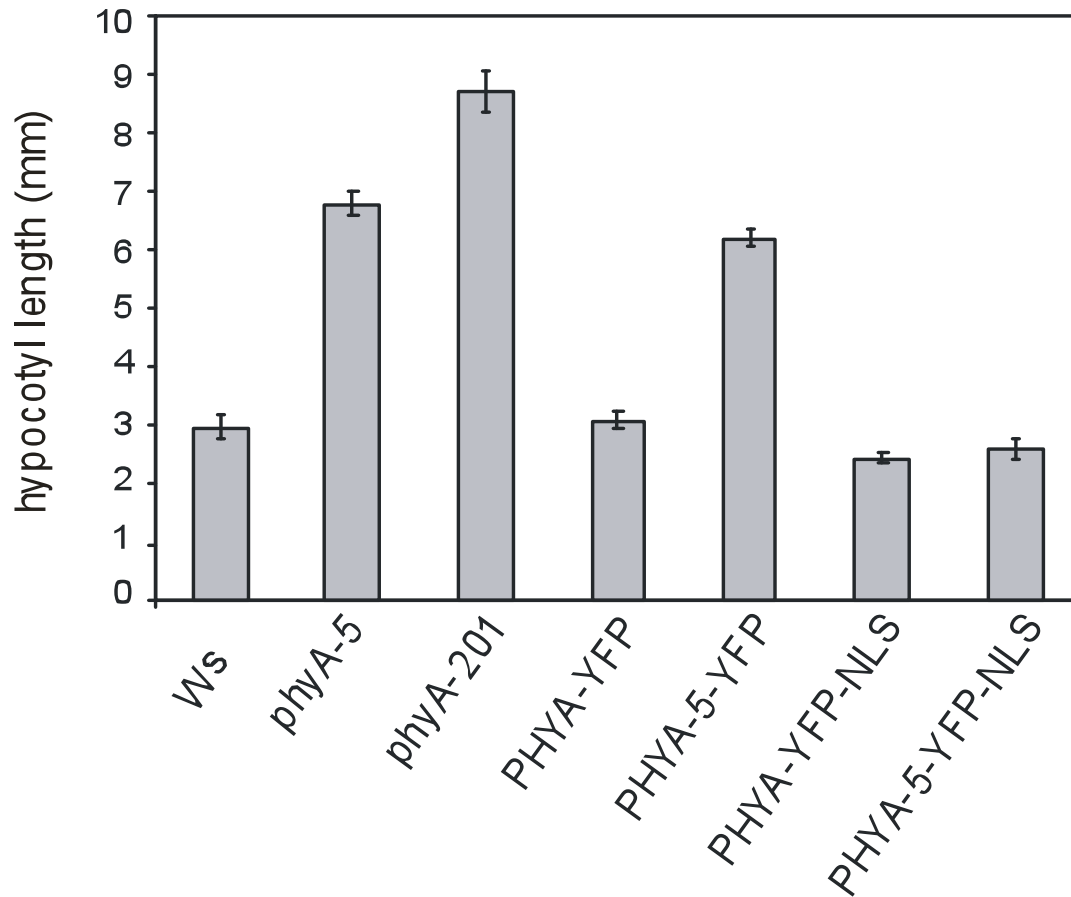


**Figure 18.** Complementation the *phyA-201* phenotype by PHYA-5-YFP-NLS. Hypocotyl lengths of seedlings grown under  $1 \mu\text{mol m}^{-2}\text{s}^{-1}$  constant FR light for 4 days were measured.

Analyzed genotypes: Ws: Wassilewskaya; *phyA-5* mutant (ecotype Ws); *phyA-201* (ecotype Ler); PHYA-YFP: *PHYA:PHYA-YFP* in *phyA-201* background; PHYA-5-YFP: *PHYA:PHYA-5-YFP* in *phyA-201* background; PHYA-YFP-NLS: *PHYA:PHYA-YFP-NLS* in *phyA-201* background; PHYA-5-YFP-NLS: *PHYA:PHYA-5-YFP-NLS* in *phyA-201* background.

Error bars indicate standard error.

The light-induced degradation of phyA-5-YFP-NLS was also studied. Seedlings grown in constant darkness or  $1 \mu\text{mol m}^{-2}\text{s}^{-1}$  constant FR were subjected to protein extraction and Western blot analysis. The experiment demonstrated that there is no difference in the light-induced degradation of the phyA-5-YFP-NLS and phyA-YFP-NLS fusion proteins (Figure 19).

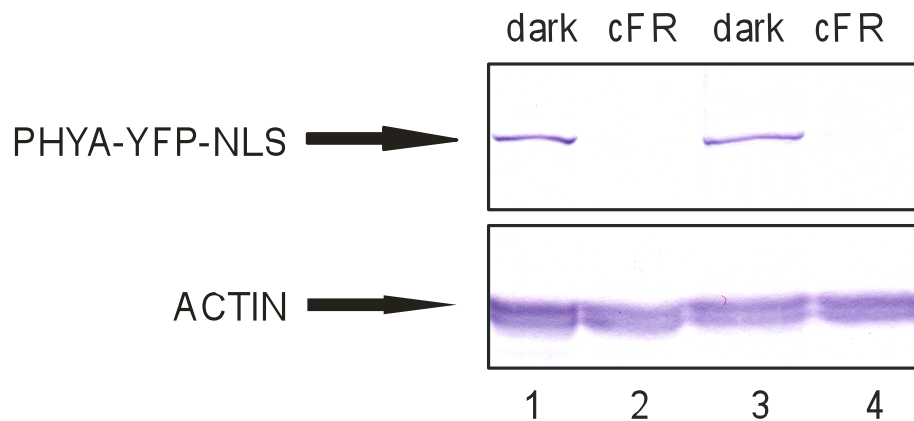


**Figure 18.** Light-induced degradation of phyA-5-YFP-NLS.

Seedlings grown for 4 days in the dark or under  $1 \mu\text{mol m}^{-2}\text{s}^{-1}$  FR light (indicated above) were subjected to total protein extraction and western blot hybridization applying PHYA (upper panel) or actin-specific antiserum (lower panel).

Analyzed genotypes: PHYA:PHYA-YFP-NLS in *phyA-201* background (lane 1, 2) and PHYA:PHYA-5-YFP-NLS in *phyA-201* (lane 3, 4).

The obtained data attest beyond the doubt that the constitutively nuclear phyA-5 can initiate proper signaling.

## 4. DISCUSSION

### **The hyposensitive, light-intensity dependent phenotype of the *psm* mutant is caused by a single amino acid change in the *PHYA* gene**

This study presents the identification and characterization of *psm* (the Phytochrome Signaling Mutant (*psm*)). *psm*, which was isolated in the laboratory of G. Whitelam, displays fluence-dependent far-red light-insensitive phenotype. *psm* seedlings grown under weak FR light exhibit a long hypocotyl phenotype similar to that observed in the *phyA* null mutant (Parks and Quail 1993, Nagatani *et al.*, 1993, Whitelam *et al.*, 1993), whereas under strong FR light irradiation the mutant displays a normal wild-type-like inhibition of hypocotyl elongation (Figures 1, 4, 5). The same pattern was observed in cotyledon expansion: under weak FR light the mutant exhibits cotyledons more closed than the wild-type, confirming hyposensitivity under these conditions. No difference compared to WT was observed in R light-grown seedlings, suggesting that the mutation affects only the phytochrome A signaling pathway.

The segregation analyses of the backcross population allowed characterizing the mutation as monogenic and recessive. The mapping analyses and sequencing of the respective gene revealed that the observed phenotype of the mutant is caused by the single C-T nucleotide exchange in the *PHYA* gene. This nucleotide substitution leads to exchange of alanine to valine at the amino acid position 30 (A30V). The new mutant allele of *PHYA* was named *phyA-5* as suggested by the guidelines described by Quail *et al.* (1994). Transgenic plants expressing *phyA-5* fused to the yellow fluorescent protein (YFP) under the control of the *PHYA* promoter were generated in the null mutant *phyA-201* to verify that the identified mutation is indeed responsible for the observed phenotype. The *PHYA-5*-YFP fusion protein re-established the intensity-dependent phenotype of the *phyA-5* mutant, demonstrating that the observed phenotype is caused by the A30V mutation in the *phyA* molecule (Figures 4, 5). The observed recessiveness of the phenotype is consistent with the loss-of-function nature of the mutation, i.e. complementation of the phenotype in heterozygous plants by the wild-type gene.

### **The *phyA-5* mutation alters the NTE domain essential for full biological activity and affects HIR and VLRF**

The A30V mutation is at a highly conserved position in the NTE domain of the phyA photoreceptor. The sequence alignment (Figure 3) shows that the mutated Ala residue is evolutionary conserved, being present in phytochromes isolated from different taxa. Furthermore, at this position the alanine residue is also conserved in all Type II *Arabidopsis* phytochromes. The functional importance of the domain has been discussed over decades.

Phytochrome A mediates two responses – HIR and VLFR, both of them characterized by a low Pfr/Ptot ratio (Schäfer and Bowler, 2002). The influence of the NTE domain on phyA-mediated responses has been demonstrated in several reports. Oat phyA deletions, which lack amino acids 7-69, were shown to be biologically inactive, although they could form dimers and autoligate chromophore. This truncated version of the photoreceptor also demonstrated a shift in action spectrum, having Pfr absorption maxima shifted to a shorter wavelength (Cherry *et al.*, 1992). It was shown in a similar study that oat phyA deletions  $\Delta 1-52$  were severely dysfunctional regarding FR-HIR response (Boylan *et al.*, 1994). The truncated deletions of oat phyA ( $\Delta 6-47$ ,  $\Delta 22-47$ ,  $\Delta 22-30$ ) expressed in tobacco were also shown to be inactive, especially under lower intensities of FR light. The spectral sensitivity of the photoreceptor was also shifted with each of the deletions towards shorter wavelengths (Jordan *et al.*, 1996, 1997). It is interesting to note that a deletion in the same domain ( $\Delta 6-57$ ) in phyB causes decreased phytochrome activity under weak R light, confirming that molecules missing this fragment are less sensitive to irradiation (Wagner *et al.*, 1996b).

This study has demonstrated that phytochrome A, which has a mutated highly conserved residue in the NTE domain, exhibits hyposensitivity in the inhibition of hypocotyl elongation and cotyledon opening upon constant irradiation by FR light. Further investigation of the effect of the mutation on HIR revealed strong reduction in this type of response, especially at higher FR wavelengths (Figure 6): *phyA-5* shows no detectable response at 742 nm FR light, suggesting complete insensitivity of the photoreceptor under these conditions. Additionally, the *phyA-5* mutation does not cause a shift in the action spectrum, unlike truncated versions of the photoreceptor investigated in

the above-mentioned studies (Cherry *et al.*, 1992; Boylan *et al.*, 1994; Jordan *et al.*, 1996, 1997).

The influence of the NTE domain on phyA-mediated responses has also been demonstrated by expressing the oat phyA molecule lacking amino acid residues 6-12 in *Arabidopsis* and tobacco. Expression of this modified photoreceptor caused alterations in VLFR or HIR (Casal *et al.*, 2002). More recently Trupkin *et al.* (2007) used *Arabidopsis* homologous system and found that  $\Delta$ 6-12 phyA signaling is reduced under continuous FR light and unaltered under FR pulses.

Experiments conducted as part of this study using short FR light pulses of different intensities and frequencies revealed that weak FR pulses do not induce the inhibition of hypocotyl elongation in *phyA-5*. This mutant exhibits a null phenotype under such conditions (Figure 7). Strong and frequent FR pulses induce a *phyA-5*-driven response. Such response was less pronounced as compared to the wild-type phyA, confirming the impaired VLFR in the mutant. Hypocotyls of *phyA-5* plants were longer than wild-type hypocotyls during prolonged dark phases (30 min and 60 min). These experiments led to the conclusion that the A30V amino acid exchange in the NTE domain also alters the VLFR, which is consistent with previously published studies.

*PRR9* gene expression exhibits acute induction after short exposure to the light. This response is mediated mostly by phyA (Tepperman *et al.*, 2001, 2006), which makes it a good marker for examination of phyA-mediated VLFR. The results of this study show that induction of *PRR9* expression by very low intensity R light is decreased in *phyA-5*, confirming the impaired VLFR in the mutant.

Impaired HIR at lower intensities of FR light and impaired VLFR induced by weak R pulse allow considering the possibility of insufficient phyA-5 Pfr formation, when weak light could not generate the necessary amount of Pfr. *phyA-5* still produces lower amounts of Pfr under strong light irradiation or pulses as compared to the WT. However, the overall ratio Pfr/Prtot is above the necessary threshold and the resulting Pfr is enough to trigger the response.

Previous work with the purified photoreceptor showed that the 6-kD domain (N-terminal 70 amino acids) is required for correct chromophore/apoprotein interactions and undergoes substantial conformational changes upon photoconversion of Pr to Pfr (Hahn *et al.*, 1984; Vierstra *et al.*, 1987), exhibiting  $\alpha$ -helical folding in the Pr-to-Pfr transformation (Deforce *et al.*, 1994). It has been suggested that these residues participate in the stabilization of Pfr conformation (Furuya and Song, 1994).

Protein structure analysis, performed with web-based software RaptorX revealed that alanine in position 30 is located in the core  $\alpha$ -helical structuralized region (see Appendix, Figure 19). Further analysis has shown that the amino acid switch in this position (A30V) leads not only to the structural changes in position 30, but also affects the surrounding amino acids. The region's secondary structure contains less  $\alpha$ -helical folding and more random coil; as a result, the region becomes more disordered and unstructured. Predicted probabilities of secondary structure for  $\alpha$ -helical folding are lower for the whole analyzed region, which also suggests that the A30V substitution destabilizes the NTE domain in terms of structured patterns. These data allow speculating that reorganization towards more random secondary structure leads to destabilization of Pfr conformation.

Thus, it could be concluded that the conserved alanine residue at position 30 of the phyA NTE is located at the highly conserved position of the region, which is responsible for the biological activity of phytochrome A and the conformational stability of Pfr.

### **The phyA-5 mutation does not cause changes in PHYA expression, but alters protein abundance in weak FR**

The observed hyposensitive mutant phenotype can be explained by: (i) changes in PHYA mRNA level; (ii) changes in phyA protein level; (iii) impaired functionality of the photoreceptor. To investigate the cause of the phenotype, a series of experiments were performed.

The activity of the *PHYA* promoter is negatively regulated by light (Hennig *et al.*, 1999). phyA alone mediates all light responses in FR light; thereby *PHYA* down-regulates its own expression under FR light irradiation. Mutations in the *PHYA* gene can cause disruptions in *PHYA* expression, thus the observed hyposensitive phenotype of *phyA-5* can be explained by this theory.

The level of *PHYA* transcription in *phyA-5* and wild-type was determined (Figure 10). The results show that the *PHYA* transcript level is not altered in *phyA-5* seedlings grown in darkness or under any intensity of FR light. This proves that the phyA-5 photoreceptor, like WT phyA, can down-regulate its own expression under FR irradiation.

Thus, it can be concluded that the negative feedback loop resulting in the down-regulation of *PHYA* promoter activity in constant FR is intact in the *phyA-5* mutant.

In order to investigate whether or not the photoreceptor protein level is affected in *phyA-5* because of the changes in accumulation, the degradation dynamics was measured applying western blot analysis. The results revealed that the level of phyA-5 is not altered as compared to phyA in etiolated seedlings. Similarly, the R light induced degradation of the mutant photoreceptor shows the same dynamics as the wild-type (Figure 11 A). The steady level of phyA-5 accumulation under continuous strong FR light does not differ from the wild-type either. However, the phyA-5 level is higher than the wild-type in weak FR light (Figure 11 B). The results were verified by studying the transgenic *PHYA*-YFP and *PHYA-5*-YFP fusion proteins, which showed levels comparable to their endogenous counterparts under each type of irradiation. The results presented also confirm the recent finding that the YFP tag slightly increases the stability of the fusion proteins, which results in higher *PHYA*-YFP and *PHYA-5*-YFP levels as compared to the corresponding endogenous counterparts (Wolf *et al.*, 2011).

A possible explanation of this finding could be that the degradation machinery has limited access to the phyA-5 Pfr molecules under low FR, whereas high FR or saturating R light can maintain wild-type-like phyA-5 levels through more effective degradation.

At this point it is necessary to advert to the apparent contradiction between high phyA-5 levels and a hyposensitive phenotype under weak FR light irradiation. The possible explanation of the phenomenon may be that the phyA-5 protein is stable, but functionally inactive under these conditions.

### **The missense mutation in *phyA-5* causes an altered subcellular localization of the photoreceptor in low-fluence FR light**

Abundance and distribution of phyA are regulated by light in multiple ways. The highest levels of phyA are observed in etiolated seedlings (Hennig *et al.*, 1999); the transition from darkness to light causes a rapid decrease in the *PHYA* mRNA level, leading to a decrease in the synthesis of the phyA apoprotein (Sharrock and Quail, 1989). As discussed above, the regulation of *PHYA* transcription is not altered in *phyA-5*. The transition from darkness to light also triggers the Pr-Pfr transition, leading to nuclear import (Kircher *et al.*, 1999, 2002) and rapid light-induced degradation (Hennig *et al.*,

1999; Sharrock and Clack, 2002). Recent research revealed that light-induced degradation of phyA takes place in both nucleus and cytosol, but the degradation in cytosol is slower (Debrieux and Fankhauser, 2010; Toledo-Ortiz *et al.*, 2010).

In light of the accumulated knowledge, data of this study suggest that phyA-5 mislocalization can be the reason for the observed phenotype. To examine this possibility, the intracellular localization of phyA-5-YFP was studied. It was confirmed that phyA-5-YFP and phyA-YFP fusion proteins are functional photoreceptors regarding physiological responses and abundance. Thus, their intracellular localization mimics the localization of their endogenous counterparts (Figures 4, 5). Microscopic data revealed that the nuclear import of phyA-5-YFP is decreased below detection level in weak FR light irrespective of the duration of the irradiation (Figure 12), whereas phyA-YFP showed normal nuclear import, confirming the previous data (Kim *et al.*, 2000, Kircher *et al.*, 1999, 2002). In contrast, strong FR light does not lead to different localization patterns of phyA-5 compared to the wild-type phyA, providing explanation for equal degradation of the mutant and the wild-type proteins under strong FR light irradiation. Short pulses of strong R light could induce the nuclear import and nuclear speckle formation of both PHYA-5-YFP and phyA-YFP proteins (Figure 13). A weak pulse, however, was significantly less effective in promoting phyA-5 nuclear accumulation. Our findings confirmed that the impaired nuclear import of phyA-5 is responsible for the higher phyA-5 level under these conditions, which is in consent with previously published data (Debrieux and Fankhauser, 2010; Toledo-Ortiz *et al.*, 2010).

### **Binding of phyA-5 to FHY1 and FHL is weaker than that of the WT**

Nuclear translocation of phyA is a key part of phyA-mediated signaling. PhyA, which lacks a nuclear location signal (NLS), requires transport facilitators for nuclear translocation. The small plant-specific proteins FHY1 and FHL were previously shown to assist the nuclear accumulation of phyA (Hiltbrunner *et al.*, 2005, 2006). FHY1 and FHL proteins can bind directly to the Pfr form of PHYA and specifically manage its import to the nucleus. The N-terminal 406 amino acids of phytochrome A (phyA 1-406) are sufficient for light-induced binding to FHY/FHL1 (Hiltbrunner *et al.*, 2005, 2006). This binding is an essential step in PHYA nuclear import and triggers PHYA-dependent nuclear signaling (Genoud *et al.*, 2008; Rausenberger *et al.*, 2011).

Yeast-two-hybrid assays demonstrated that the binding of phyA-5 Pfr to FHY1 and FHL proteins significantly decreased compared to phyA (Figure 14, Figure 15, Figure 16). phyA-5 (1-406) showed no detectable interaction with FHL and FHY1. Thus, it can be concluded that the A30V mutation affects the binding affinity of the phyA protein to the nuclear transport facilitators FHY1 and FHL, highlighting the importance of the NTE domain of PHYA in establishing an interaction with the FHY1/FHL system.

The decreased affinity of phyA-5 to the transport facilitators provides an explanation for the impaired nuclear import observed under weak FR irradiation. Strong R light irradiation provides a high Pfr/Pr ratio of phyA (Mancinelli, 1994), which results in sufficient nuclear import of phyA-5, leading to proper signaling despite its low affinity to FHY1/FHL system. Strong FR irradiation, despite providing lower Pfr/Pr than R light, still produces enough Pfr to induce nuclear import and signaling.

However, weak FR light results in a low Pfr/Pr ratio and a small amount of phyA-5 Pfr. Its impaired binding to the nuclear facilitators leads to insufficient signaling, causing the observed phenotype.

The same situation occurs under weak FR or R pulses, inducing the VLFR in the wild-type plants, but failing to do so in *phyA-5*, whereas strong light pulses reduce the difference between the effects of phyA and phyA-5.

### **Expression of PHYA-5-YFP-NLS complements the phyA-201 mutant**

It had been shown previously that the phyA-NLS fusion protein is constitutively present in the nucleus of the *phy1/phyA* double mutant, restoring responsiveness to FR (Genoud *et al.*, 2008). Several experiments were conducted in order to validate whether the observed phenotype is indeed caused by the weakened affinity of phyA-5 Pfr to FHY1 and FHL proteins, resulting in impaired nuclear transportation, or it is actually a result of alterations in nuclear signaling itself.

Analyses of the transgenic lines expressing phyA-YFP-NLS and phyA-5-YFP-NLS fusion proteins in *phyA-201* background revealed that phyA-5 and phyA localized in the nucleus can generate signaling with equal efficiency (Figure 18). Expression of phyA-5-YFP-NLS and phyA-YFP-NLS can fully complement the *phyA-201* mutant phenotype. In addition, both fusion proteins display normal wild-type-like light-induced degradation

(Figure 19). These facts confirm that the atypical phyA levels detected in the mutant in weak FR light are caused by the impaired nuclear import of phyA-5 Pfr.

Thus, it can be concluded that the NTE domain participates in regulating the nuclear import of phyA. Nuclear translocation of phyA-5 is impaired under conditions resulting in low Pfr, and the inadequate nuclear level of phyA-5 Pfr results in ineffective signaling, producing the hyposensitive phenotype. Accordingly, the bulk of phyA-5 is concentrated in the cytosol and is degraded slower than the nuclear pool (Toledo-Ortiz *et al.*, 2010; Debrieux and Fankhauser, 2010), resulting in higher steady-state level of protein. This explanation eliminates the apparent contradiction between high phyA-5 levels and a hyposensitive phenotype under low Pfr conditions.

The data of this study support recently published findings and mathematical modeling, which show that the appropriate stability of the phyA Pfr-FHY/FHL complex is essential for proper phyA nuclear import and signaling (Rausenberger *et al.*, 2011). This study proves that a slight alteration affecting the stability of the phyA Pfr-FHY/FHL complexes can significantly impair phyA signaling.

The data obtained in the current study underline the interconnection between phototransformation of phyA, its nuclear import, functioning and degradation.

## 5. SUMMARY - ZUSAMMENFASSUNG

### 5.1 Summary

As sessile and photoautotrophic organisms, plants require an explicit adjustment of the development processes with the prevailing environmental conditions. Light is the most important environmental factor, which acts not only as the energy source, but also as the regulation signal for numerous physiological processes in the plants. A set of photosensing molecules – photoreceptors – have been developed in plants to perceive light of different quality, intensity, direction and continuance.

Phytochromes are photoreceptors that perceive the red and far-red regions of the light spectrum (650 - 750 nm). In *Arabidopsis* the phytochrome gene family consists of five members (PHYA-E). Phytochromes can be divided into “light-labile” (phyA) and light-stable (phyB-E) types. Phytochromes mediate responses that can be categorized as follows: very low fluence responses (VLFR), low fluence responses (LFR) and high irradiance responses (HIR). The light-labile phyA mediates responses that are characterized by a low Pfr/Pr ratio and R/FR irreversibility, namely VLFR and FR-HIR.

This study describes the *Arabidopsis thaliana* mutant (*psm*, renamed *phyA-5*) showing a distinct photomorphogenic phenotype. Molecular mapping revealed a new missense mutation in the PHYA amino terminal extension (NTE) domain. The *phyA-5* mutant exhibits a hyposensitive phenotype in continuous low-intensity far-red light, whereas in high-intensity conditions the mutant resembles the wild-type. Both VLFR and HIR are reduced in the mutant. The mutation does not affect the expression level of PHYA. The dark-accumulated level of the mutated phyA-5 protein and R light-induced degradation were shown to be normal, whereas higher residual amounts of phyA-5 were detected in low FR.

It has been shown that the complex mutant phenotype and the abnormal stability of the mutated protein under low intensity of FR light are caused by the impaired nuclear import of the phyA-5 under these conditions, whereas high-fluence light induces normal nuclear import, resulting in a phenotype resembling the wild-type. Furthermore, it has been demonstrated that the reduced nuclear import of phyA-5 is caused by the decreased binding affinity of the mutant photoreceptor to the nuclear import facilitators FHY1 and FHL.

Studies on transgenic plants expressing phyA-5-YFP-NLS protein in *phyA-201* background provided evidence that phyA-5 behaves identically to wild-type phyA, i.e. it is constitutively localized in the nucleus.

To sum up, the data obtained show that the NTE domain influences the regulation of phyA nuclear import through participation in the assembling of the FHY1/FHL/PHYA Pfr complex and the resulting aberrant nucleo/cytoplasmic distribution impairs light-induced degradation of phyA. Results of this study underline the interconnection between phototransformation of phyA, its nuclear import, functioning and degradation.

### 5.2 Zusammenfassung

Als sessile und photoautotrophe Organismen müssen Pflanzen ihre Entwicklungsvorgänge genau an die bestehenden Umweltbedingungen anpassen. Licht ist einer der wichtigsten Umweltfaktoren, weil es nicht nur als Energiequelle dient, sondern auch als regulierendes Signal für eine Vielzahl von physiologischen Prozessen in Pflanzen agiert. Ein Set von photosensorischen Molekülen – die Photorezeptoren – haben sich in Pflanzen entwickelt um Licht unterschiedlicher Qualität, Intensität, Ausrichtung und Dauer wahrzunehmen.

Phytochrome sind Photorezeptoren, die die rote und dunkelrote Strahlung des Lichtspektrums wahrnehmen (650 – 750 nm). In *Arabidopsis* besteht die Familie der Phytochrome aus fünf Mitgliedern (PHYA-E). Man unterscheidet dabei lichtinstabile (phyA) und lichtstabile Typen (phyB-E). Phytochrome vermitteln Reaktionen, die sich wie folgt charakterisieren lassen: Reaktionen auf sehr niedrige Lichtfluenz (*very low fluence response*, VLFR), Reaktionen auf niedrige Lichtfluenz (*low fluence response*, LFR) und Reaktionen auf hohe Strahlungsintensität (*high irradiance response*, HIR). Das Licht-instabile phyA vermittelt Reaktionen, die durch eine niedrige Pfr/Pr Ratio und eine R/FR Irreversibilität gekennzeichnet sind, nämlich die VLFR und die FR-HIR Reaktionen.

Diese Doktorarbeit beschreibt eine *Arabidopsis thaliana* Mutante (*psm*, umbenannt in *phyA-5*), die einen charakteristischen photomorphogenetischen Phänotyp aufweist. Durch molekulares *Mapping* wurde eine neue *missense* Mutation in der aminoterminalen Extensionsdomäne (*amino terminal extension*, NTE) gefunden. Die PhyA-5 Mutante weist unter kontinuierlichem Licht des dunkelroten Spektrums bei

## SUMMARY - ZUSAMMENFASSUNG

geringer Lichtintensität einen hyposensitiven Phänotyp auf. Unter hoher Lichtintensität jedoch gleicht die Mutante dem Wildtyp. Die Mutation hat keine Auswirkungen auf das Expressionslevel von PHYA, da das Niveau des im Dunkeln akkumulierten phyA-5 Proteins und der durch rotes Licht vermittelte Abbau des Proteins normal sind. Allerdings wurden höhere Restmengen von phyA-5 Protein unter geringem dunkelrotem (*low FR*) gefunden.

Es konnte gezeigt werden, dass der komplexe mutante Phänotyp und die nicht normale Stabilität des mutanten Proteins unter dunkelrotem Licht mit geringer Intensität auf einen verminderten Transport des Proteins in den Kern zurückzuführen ist. Unter normaler Lichtfluenz jedoch ist auch der Transport in den Kern normal, was einen wildtypähnlichen Phänotyp zur Folge hat. Darüber hinaus konnte gezeigt werden, dass der verminderte Transport von phyA-5 in den Zellkern durch eine verminderte Bindungsaffinität des mutanten Photorezeptors an FHY1 und FHL – Komponenten, die den Kerntransport erleichtern - verursacht wird.

Untersuchungen an transgenen Pflanzen, die ein phyA-5-YFP-NLS Fusionsprotein in einem *phyA-201*-mutantem Hintergrund exprimieren, gaben Hinweise darauf, dass phyA-5 sich wie phyA im Wildtyp verhält und konstitutiv im Zellkern lokalisiert ist.

Zusammenfassend lässt sich sagen, dass die NTE-Domäne die Regulierung des Kerntransports von phyA durch die Bildung des FHY1/FHL/PHYA/Pfr Komplexes beeinflusst und die daraus resultierende, aberrante Kern- bzw. zytoplasmatische Verteilung des Proteins den lichtinduzierten Abbau von phyA stört. Die Ergebnisse dieser Studie betonen noch einmal die Wichtigkeit der Zusammenhänge der Phototransformation von PhyA mit dem Kerntransport, der Funktion und dem Abbau des Proteins.

**6. REFERENCES**

- Ahmad, M., Cashmore, A.R. (1993). HY4 gene of *A. thaliana* encodes a protein with characteristics of a blue-light photoreceptor. *Nature* 366, 162-166.
- Ahmad, M., Jarillo, J. A., Smirnova, O. and Cashmore, A. R. (1998). The CRY1 blue light photoreceptor of *Arabidopsis* interacts with phytochrome A in vitro. *Mol. Cell* 1, 939-948.
- Ahmad, M., Lin, C. and Cashmore, A.R. (1995). Mutations throughout an *Arabidopsis* blue-light photoreceptor impair blue-light-responsive anthocyanin accumulation and inhibition of hypocotyl elongation. *The Plant Journal* 8, 653-658.
- Al-Sady, B., Kikis, E.A., Monte, E., Quail, P.H. (2008). Mechanistic duality of transcription factor function in phytochrome signaling. *Proc Natl Acad Sci USA* 105, 2232-2237.
- Al-Sady, B., Ni, W., Kircher, S., Schäfer, E., Quail, P.H. (2006). Photoactivated phytochrome induces rapid PIF3 phosphorylation prior to proteasome-mediated degradation. *Mol Cell* 23, 439-446.
- Bae, G., Choi, G. (2008). Decoding of light signals by plant phytochromes and their interacting proteins. *Annu Rev Plant Biol* 59, 281-311.
- Bauer D., Viczián A., Kircher S., Nobis T., Nitschke R., Kunkel T., Panigrahi K.C., Adám E., Fejes E., Schäfer E., Nagy F. (2004). Constitutive photomorphogenesis 1 and multiple photoreceptors control degradation of phytochrome interacting factor 3, a transcription factor required for light signaling in *Arabidopsis*. *Plant Cell* 16, 1433-1445.
- Berendzen, K., Searle, I., Ravenscroft, D., Koncz, C, Batschauer, A., Coupland, G., Somssich, I.E., Ulker B. (2005). A rapid and versatile combined DNA/RNA extraction protocol and its application to the analysis of a novel DNA marker set polymorphic between *Arabidopsis thaliana* ecotypes Col-0 and Landsberg erecta. *Plant Methods* 23, 1:4.
- Birnboim, H.C., and Doly, J. (1979). A rapid alkaline extraction procedure for screening recombinant plasmid DNA. *Nucleic Acids Res* 7, 1513-1523.
- Botto, J.F., Sanchez, RA, Whitelam, G.C., Casal, J.J. (1996). Phytochrome A mediates the promotion of seed germination by very low fluences of light and canopy shade light in *Arabidopsis*. *Plant Physiology* 110, 439-444.
- Boylan, M., Douglas, N., and Quail, P.H. (1994). Dominant negative suppression of *Arabidopsis* photoresponses by mutant phytochrome A sequences identifies spatially discrete regulatory domains in the photoreceptor. *Plant Cell* 6, 449-460.
- Braslavsky, S.E., Gartner, W. and Schaffner, K. (1997). Phytochrome photoconversion. *Plant, Cell & Environment* 20, 700-706.
- Buche, C., Poppe, C., Schäfer, E., Kretsch, T. (2000). *eid1*: a new *Arabidopsis* mutant hypersensitive in phytochrome A-dependent high-irradiance responses. *Plant Cell* 12, 547-558.

## REFERENCES

- Butler, W.L., Norris, K.H., Siegelman, H.W., Hendricks, S.B. (1959). Detection, assay, and preliminary purification of the pigment controlling photoresponsive development of plants. *Proc Natl Acad Sci USA* 45, 1703-1708.
- Casal, J. J., Yanovsky, M.J., Luppi, J.P. (2000b). Two photobiological pathways of phytochrome A activity, only one of which shows dominant negative suppression by phytochrome B. *Photochem Photobiol* 71, 481-486.
- Casal, J.J. (2000a). Phytochromes, cryptochromes, phototropin: photoreceptor interactions in plants. *Photochem. Photobiol* 71, 1-11.
- Casal, J.J., Davis, S.J., Kirchenbauer, D., Viczián, A., Yanovsky, M.J., Clough, R.C., Kircher, S., Jordan-Beebe, E.T., Schäfer, E., Nagy, F. and Vierstra, R.D. (2002). The serine-rich N-terminal domain of oat phytochrome a helps regulate light responses and subnuclear localization of the photoreceptor. *Plant Physiol* 129,1127-1137.
- Casal, J.J., Sanchez, R.A., Yanovsky, M.J. (1997). The function of phytochrome A. *Plant, Cell & Environment* 20, 813-819.
- Cashmore, A., Jarillo, J. A., Wu Y. J., and Liu D. (1999). Cryptochromes: blue light receptors for plants and animals. *Science* 284, 760-765.
- Cerdan, P.D., Yanovsky, M.J., Reymundo, F.C., Nagatani, A., Staneloni, R.J., Whitelam, G.C. and Casal, J.J. (1999). Regulation of phytochrome B signaling by phytochrome A and FHY1 in *Arabidopsis thaliana*. *Plant J* 18, 499-507.
- Chen, H., Shen, Y., Tang, X., Yu, L., Wang, J., Guo, L., Zhang, Y., Zhang, H., Feng, S., Strickland, E., Zheng, N., and Deng, X.W. (2006). *Arabidopsis* CULLIN4 forms an E3 ubiquitin ligase with RBX1 and the CDD complex in mediating light control of development. *Plant Cell* 18, 1991-2004.
- Chen, M. (2008). Phytochrome nuclear body: an emerging model to study interphase nuclear dynamics and signaling . *Curr. Opin. Plant Biol* 11, 503 - 508 .
- Chen, M., Chory, J. and Fankhauser, C. (2004). Light signal transduction in higher plants. *Annu. Rev. Genet* 38, 87-117.
- Chen, M., Schwab, R., and Chory, J. (2003). Characterization of the requirements for localization of phytochrome B to nuclear bodies. *Proc. Natl Acad. Sci. USA* 100, 14493 - 14498 .
- Chen, M., Tao, Y., Lim, J., Shaw, A., Chory, J. (2005). Regulation of phytochrome B nuclear localization through light-dependent unmasking of nuclear-localization signals. *Curr. Biol* 15, 637-642.
- Cherry, J., Hondred, D., Walker, J. and Vierstra, R. (1992). Phytochrome requires the 6-kDa N-terminal domain for full biological activity. *Proc Natl Acad Sci USA* 89, 5039-5043.
- Cherry, J.R., Hondred, D., Walker, J.M., Keller, J.M., Hershey, H.P. and Vierstra, R.D. (1993). Carboxy-terminal deletion analysis of oat phytochrome A reveals the presence of separate domains required for structure and biological activity. *Plant Cell* 5, 565-575.
- Choi, G., Yi, H., Lee, J., Kwon, Y.K., Soh, M.S., Shin, B., Luka, Z., Hahn, T.R., Song, P.S. (1999). Phytochrome signalling is mediated through nucleoside diphosphate kinase 2. *Nature* 401, 610-613.

## REFERENCES

- Christie, J. M. and Briggs, W. R. (2001). Blue light sensing in higher plants, *J. Biol. Chem* 276, 11457-11460.
- Christie, J.M., Reymond, P., Powell, G.K., Bernasconi, P., Raibekas, A.A., Liscum, E., Briggs, W.R. (1998). Arabidopsis NPH1: a flavoprotein with the properties of a photoreceptor for phototropism. *Science* 282(5394), 1698-701.
- Clack, T., Mathews, S. and Sharrock, R.A. (1994). The phytochrome apoprotein family in Arabidopsis is encoded by five genes: the sequences and expression of PHYD and PHYE. *Plant Mol. Biol* 25, 413-427.
- Clough, R.C., Jordan-Beebe, E.T., Lohman, K.N., Marita, J.M., Walker, J.M., Gatz, C., and Vierstra, R.D. (1999). Sequences within both the N- and C-terminal domains of phytochrome A are required for Pfr ubiquitination and degradation. *Plant J* 17, 155-167.
- Clough, S.J. and Bent, A.F. (1998). Floral dip: a simplified method for Agrobacterium-mediated transformation of Arabidopsis thaliana. *Plant J* 16, 735-743.
- Debrieux, D. and Fankhauser, C. (2010). Light-induced degradation of phyA is promoted by transfer of the photoreceptor into the nucleus. *Plant Mol Biol* 73, 687-695.
- Deforce, L., Tokutomi, S., Song, P.S. (1994). Phototransformation of pea phytochrome A induces an increase in alpha-helical folding of the apoprotein: Comparison with a monocot phytochrome A and CD analysis by different methods. *Biochemistry* 33, 4918-4922.
- Desnos, T., Puente, P., Whitelam, G.C. and Harberd, N.P. (2001). FHY1: a phytochrome A-specific signal transducer. *Genes Dev* 15, 2980-2990.
- Devlin, P.F., Patel, S.R., Whitelam, G.C. (1998). Phytochrome E influences internode elongation and flowering time in Arabidopsis. *Plant Cell* 10, 1479-1487.
- Devlin, P.F., Robson, P.R., Patel, S.R., Goosey, L., Sharrock, R.A., Whitelam, G.C. (1999). Phytochrome D acts in the shade-avoidance syndrome in Arabidopsis by controlling elongation growth and flowering time. *Plant Physiology* 119, 909-915.
- Dieterle, M., Bauer, D., Buche, C., Krenz, M., Schäfer, E., Kretsch, T. (2005). A new type of mutation in phytochrome A causes enhanced light sensitivity and alters the degradation and subcellular partitioning of the photoreceptor. *Plant J* 41, 146-161.
- Dieterle, M., Zhou, Y.C., Schäfer, E., Funk, M. and Kretsch, T. (2001). EID1, an F-box protein involved in phytochrome A-specific light signalling. *Genes Dev* 15, 939-944.
- Duek, P.D., Elmer, M.V., van Oosten, V.R. and Fankhauser, C. (2004). The degradation of HFR1, a putative bHLH class transcription factor involved in light signaling, is regulated by phosphorylation and requires COP1. *Curr Biol* 14, 2296-2301.
- Duek, P.D., Fankhauser, C. (2005). bHLH class transcription factors take centre stage in phytochrome signalling. *Trends Plants Sci* 10, 51-54.
- Eichenberg, K., Hennig, L. and Schäfer, E. (2000). Variation in dynamics of phytochrome A in Arabidopsis ecotypes and mutants. *Plant Cell Environ* 23, 311-319.
- Fankhauser, C., Yeh, K.C., Lagarias, J.C., Zhang, H., Elich, T.D. and Chory, J. (1999). PKS1, a substrate phosphorylated by phytochrome that modulates light signaling in Arabidopsis. *Science* 284, 1539-1541.

## REFERENCES

- Franklin, K.A. and Whitelam, G.C. (2005). Phytochromes and shade avoidance responses in plants. *Ann Bot (Lond.)* 96, 169-175.
- Franklin, K.A., Davis, S.J., Stoddart, W.M., Vierstra, R.D., Whitelam, G.C. (2003). Mutant analyses define multiple roles for phytochrome C in Arabidopsis photomorphogenesis. *Plant Cell* 15,1981-1989.
- Furuya, M. (1989). Molecular properties and biogenesis of phytochrome I and II. *Adv Biophys* 25,133-167.
- Furuya, M., Song, P.S. (1994). Assembly and properties of holophytochrome. In: Kendrick, R.E., Kronenberg, G.H.M., editors. *Photomorphogenesis in Plants*. Ed 2. Dordrecht, The Netherlands: Kluwer Academic Publishers, 105-140.
- Genoud, T., Schweizer, F., Tscheuschler, A., Debrieux, D., Casal, J.J., Schäfer, E., Hiltbrunner, A., Fankhauser, C. (2008). FHY1 mediates nuclear import of the light-activated phytochrome A photoreceptor. *PLoS Genet* 4, e1000143.
- Gil, P., Kircher, S., Adam, E., Bury, E., Kozma-Bognar, L., Schäfer, E., Nagy, F. (2000). Photocontrol of subcellular partitioning of phytochrome-B:GFP fusion protein in tobacco seedlings. *The Plant Journal* 22, 135-145.
- Hahn, T.R., Song, P.S., Quail, P.H., Vierstra, R.D. (1984). Tetranitromethane oxidation of phytochrome chromophore as a function of spectral form and molecular weight. *Plant Physiol* 74, 755-758.
- Hamazato, F., Shinomura, T., Hanzawa, H., Chory, J., Furuya, M. (1997). Fluence and wavelength requirements for Arabidopsis CAB gene induction by different phytochromes. *Plant Physiol* 115, 1533-1540.
- Hennig, L., Buche, C., Eichenberg, K. and Schäfer, E. (1999). Dynamic properties of endogenous phytochrome A in Arabidopsis seedlings. *Plant Physiol* 121, 571-577.
- Hennig, L., Stoddart, W.M., Dieterle, M., Whitelam, G.C., Schäfer, E. (2002). Phytochrome E controls light-induced germination of Arabidopsis. *Plant Physiology* 128, 194-200.
- Hiltbrunner, A., Tscheuschler, A., Viczian, A., Kunkel, T., Kircher, R.S., Schäfer, E. (2006). FHY1 and FHL act together to mediate nuclear accumulation of the phytochrome A photoreceptor. *Plant Cell Phys* 47, 1023-1034.
- Hiltbrunner, A., Viczián, A., Bury, E., Tscheuschler, A., Kircher, S., Tóth, R., Honsberger, A., Nagy, F., Fankhauser, C., Schäfer, E. (2005). Nuclear accumulation of the phytochrome A photoreceptor requires FHY1. *Curr Biol* 15, 2125 - 2130.
- Hisada, A., Hanzawa, H., Weller, J.L., Nagatani, A., Reid, J.B., Furuya, M. (2000). Light-induced nuclear translocation of endogenous pea phytochrome A visualized by immunocytochemical procedures. *The Plant Cell* 12, 1063-1078.
- Hoecker, U. and Quail, P. H. (2001). The phytochrome A-specific signaling intermediate SPA1 interacts directly with COP1, a constitutive repressor of light signaling in Arabidopsis. *J Biol Chem* 276, 38173-38178.
- Hoecker, U., Tepperman, J. M. and Quail, P. H. (1999). SPA1: a WD-repeat protein specific to phytochrome A signal transduction. *Science* 284, 496-499.

## REFERENCES

- Huala, E., Oeller, P.W., Liscum, E., Han, I.S., Larsen, E., Briggs, W.R. (1997). Arabidopsis NPH1: a protein kinase with a putative redox-sensing domain. *Science* 278, 2120-2123.
- Hudson, M., Ringli, C., Boylan, M.T., Quail, P.H. (1999). The FAR1 locus encodes a novel nuclear protein specific to phytochrome A signaling. *Genes Dev* 13, 2017-27.
- Hudson, M.E., Lisch, D.R., Quail, P.H. (2003). The FHY3 and FAR1 genes encode transposase-related proteins involved in regulation of gene expression by the phytochrome A-signaling pathway. *Plant J* 34, 453-471.
- Jabben, M., Shanklin, J., and Vierstra, R.D. (1989a). Red light-induced accumulation of ubiquitin-phytochrome conjugates in both monocots and dicots. *Plant Physiol* 90, 380 - 384.
- Jabben, M., Shanklin, J., and Vierstra, R.D. (1989b). Ubiquitin-phytochrome conjugates: pool dynamics during in vivo phytochrome degradation. *J Biol Chem* 264, 4998 - 5005.
- Jander, G., Norris, S.R., Rounsley, S.D., Bush, D.F., Levin, I.M., Last, R.L. (2002). Arabidopsis map-based cloning in the post-genome era. *Plant Phys* 129, 440-450.
- Jang, I.C., Yang, J.Y., Seo, H.S., and Chua, N.H. (2005). HFR1 is targeted by COP1 E3 ligase for post-translational proteolysis during phytochrome A signaling. *Genes Dev* 19, 593-602.
- Jordan, E.T., Cherry, J.R., Walker, J.M. and Vierstra, R.D. (1996). The amino-terminus of phytochrome A contains two distinct functional domains. *Plant J* 9, 243-257.
- Jordan, E.T., Marita, J.M., Clough, R.C., Vierstra, R.D. (1997). Characterization of regions within the N-terminal 6-kilodalton domain of phytochrome A that modulate its biological activity. *Plant Physiol* 115, 693-704.
- Kalderon, D., Roberts, B.L., Richardson, W.D. and Smith, A.E. (1984). A short amino acid sequence able to specify nuclear location. *Cell* 39, 499-509.
- Kevei, E., Schäfer, E., Nagy, F. (2007). Light-regulated nucleo-cytoplasmic partitioning of phytochromes. *J Exp Bot* 58, 3113-3124.
- Khanna, R., Huq, E., Kikis, E.A., Al-Sady, B., Lanzatella, C., Quail, P.H. (2004). A novel molecular recognition motif necessary for targeting photoactivated phytochrome signaling to specific basic helix-loop-helix transcription factors. *Plant Cell* 16, 3033-3044.
- Kim, J., Yi, H., Choi, G., Shin, B., Song, P.S., Choi, G. (2003). Functional characterization of phytochrome interacting factor 3 in phytochrome-mediated light signal transduction. *Plant Cell* 15, 2399-2407.
- Kim, L., Kirche, S., Toth, R., Adam, E., Schäfer, E., Nagy, F. (2000). Light-induced nuclear import of phytochrome-A:GFP fusion proteins is differentially regulated in transgenic tobacco and Arabidopsis. *Plant J* 22, 125-133.
- Kircher, S., Gil, P., Kozma-Bognar, L., Fejes, E., Speth, V., Husselstein-Muller, T., Bauer, D., Adam, E., Schäfer, E., Nagy, F. (2002). Nucleocytoplasmic partitioning of the plant photoreceptors phytochrome A, B, C, D, and E is regulated differentially by light and exhibits a diurnal rhythm. *The Plant Cell* 14, 1541-1555.

- Kircher, S., Kozma-Bognar, L., Kim, L., Adam, E., Harter, K., Schäfer, E., Nagy, F. (1999). Light quality-dependent nuclear import of the plant photoreceptors phytochrome A and B. *Plant Cell* 11, 1445-1456.
- Koncz, C., Martini, N., Szabados, L., Hrouda, M., Bachmair, A., Schell, J. (1994). Specialized vectors for gene tagging and expression studies. in *Plant Molecular Biology Manual* 2. edition, editors: Gelvin, S.B., Schilperoort, R.A., Kluwer Academic Publishers, Dordrecht, 2, 1-22.
- Koncz, C., Schell, J. (1986). The promoter of T-DNA gene 5 controls the tissue-specific expression of chimaeric genes carried by a novel type of *Agrobacterium* binary vector. *Mol Gen Genet* 204, 383-396.
- Kretsch T, Poppe C, Schäfer, E. (2000). A new type of mutation in the plant photoreceptor phytochrome B causes loss of photoreversibility and an extremely enhanced light sensitivity. *Plant J.* 22:177-86
- Lapko, V.N., Jiang, X.Y., Smith, D.L. and Song, P.S. (1997). Posttranslational modification of oat phytochrome A: phosphorylation of a specific serine in a multiple serine cluster. *Biochemistry* 36, 10595-10599.
- Lapko, V.N., Jiang, X.Y., Smith, D.L. and Song, P.S. (1998). Surface topography of phytochrome A deduced from specific chemical modification with iodoacetamide. *Biochemistry* 37, 12526-12535.
- Lapko, V.N., Jiang, X.Y., Smith, D.L. and Song, P.S. (1999). Mass spectrometric characterization of oat phytochrome A: isoforms and posttranslational modifications. *Protein Sci* 8, 1032-1044.
- Lee, J., He, K., Stolc, V., Lee, H., Figueroa, P., Gao, Y., Tongprasit, W., Zhao, H., Lee, I., and Deng, X.W. (2007). Analysis of transcription factor HY5 genomic binding sites revealed its hierarchical role in light regulation of development. *Plant Cell* 19, 731-749.
- Leivar, P., Quail, P.H. (2011). PIFs: pivotal components in a cellular signaling hub. *Trends Plant Sci.* 16, 19-28.
- Leivar, P., Tepperman, J.M., Monte, E., Calderon, R.H., Liu, T.L., Quail, P.H. (2009). Definition of early transcriptional circuitry involved in light-induced reversal of PIF-imposed repression of photomorphogenesis in young *Arabidopsis* seedlings. *Plant Cell* 21, 3535-3553
- Li, J., Li, G., Gao, S., Martinez, C., He, G., Zhou, Z., Huang, X., Lee, J.H., Zhang, H., Shen, Y., Wang, H., Deng, X.W. (2010). *Arabidopsis* transcription factor ELONGATED HYPOCOTYL5 plays a role in the feedback regulation of phytochrome A signaling. *Plant Cell*, 22, 3634-3649.
- Lin, C., Ahmad, M., Cashmore, A.R. (1996). *Arabidopsis* cryptochrome 1 is a soluble protein mediating blue light-dependent regulation of plant growth and development. *Plant J* 10, 893-902.
- Lin, C., Yang, H., Guo, H., Mockler, T., Chen, J., Cashmore, A.R. (1998). Enhancement of blue light sensitivity of *Arabidopsis* seedlings by a blue light receptor cryptochrome 2. *Proc Natl Acad Sci USA* 95, 7686-7699.

## REFERENCES

- Lin, R., Ding, L., Casola, C., Ripoll, D.R., Feschotte, C., Wang, H. (2007). Transposase-derived transcription factors regulate light signaling in Arabidopsis. *Science* 318, 1302-1305.
- Lorrain, S., Allen, T., Duek, P.D., Whitelam, G.C., Fankhauser, C. (2008). Phytochrome-mediated inhibition of shade avoidance involves degradation of growth-promoting bHLH transcription factors. *Plant J* 53:312-323.
- Lorrain, S., Genoud, T. and Fankhauser, C. (2006). Let there be light in the nucleus! *Curr Op Plant Biol* 9, 509-514.
- Lukowitz, W., Gillmor, C.S., Scheible, W.R. (2000). Positional cloning in Arabidopsis. Why it feels good to have a genome initiative working for you. *Plant Phys* 123, 795-805.
- Maloof, J.N., Borevitz, J.O., Dabi, T., Lutes, J., Nehring, R.B., Redfern, J.L., Trainer, G.T., Wilson, J.M., Asami, T., Berry, C.C., Weigel, D., Chory, J. (2001). Natural variation in light sensitivity of Arabidopsis. *Nat Genet* 29, 441-446.
- Mancinelli, A. (1994). In *Photomorphogenesis in plants - 2nd Edition*. Kendrick RE, Kronenberg. GMH. Kluwer Academic Publishers.
- Mandoli, D.F., Briggs, W.R. (1981). Phytochrome control of two low-irradiance responses in etiolated oat seedlings. *Plant Physiol* 67, 733-739.
- Martínez-García, J.F., Huq, E. and Quail, P.H. (2000). Direct targeting of light signals to a promoter element-bound transcription factor. *Science* 288, 859-863.
- Mathews, S., Sharrock, R.A. (1997). Phytochromes gene diversity. *Plant Cell Environment* 20, 666-671.
- Matsushita, T., Mochizuki, N., Nagatani, A. (2003). Dimers of the N-terminal domain of phytochrome B are functional in the nucleus. *Nature* 424, 571-574.
- McCurdy, D.W., Pratt, L.H. (1986). Immunogold electron microscopy of phytochrome in *Avena*: identification of intracellular sites responsible for phytochrome sequestering and enhanced pelletability. *The Journal of Cell Biology* 103, 2541-2550.
- Møller, S.G., Ingles, P.J. and Whitelam, G.C. (2002). The cell biology of phytochrome signaling. *New Phytol* 154, 553-590.
- Monte, E., Tepperman, J.M., Al-Sady, B., Kaczorowski, K.A., Alonso, J.M., Ecker, J.R., Li, X., Zhang, Y., Quail, P.H. (2004). The phytochrome-interacting transcription factor, PIF3, acts early, selectively, and positively in light-induced chloroplast development. *Proc Natl Acad Sci USA* 101, 16091-16098.
- Nagatani, A. (2004). Light-regulated nuclear localization of phytochromes. *Curr Opin Plant Biol* 7, 708-711.
- Nagatani, A., Reed, J. W., Chory J. (1993). Isolation and Initial Characterization of Arabidopsis Mutants That Are Deficient in Phytochrome A. *Plant Physiol* 102, 269-277.
- Nagy, F., Schäfer, E. (2002). Phytochromes control photomorphogenesis by differentially regulated, interacting signaling pathways in higher plants. *Annu Rev Plant Biol* 53, 329-355.

## REFERENCES

- Ni, M., Tepperman, J.M. and Quail, P.H. (1998). PIF3, a phytochrome-interacting factor necessary for normal photoinduced signal transduction, is a novel basic helix-loop-helix protein. *Cell* 95, 657-667.
- Ni, M., Tepperman, J.M. and Quail, P.H. (1999). Binding of phytochrome B to its nuclear signalling partner PIF3 is reversibly induced by light. *Nature* 400, 781-784.
- Oka, Y., Matsushita, T., Mochizuki, N., Suzuki, T., Tokutomi, S., Nagatani, A. (2004). Functional analysis of a 450-amino acid N-terminal fragment of phytochrome B in *Arabidopsis*. *Plant Cell* 16, 2104-2116.
- Osterlund, M.T., Ang, L.H. and Deng, X.W. (1999). The role of COP1 in repression of *Arabidopsis* photomorphogenic development. *Trends Cell Biol* 9, 113-118.
- Osterlund, M.T., Hardtke, C.S., Wei, N. and Deng, X.W. (2000a). Targeted destabilization of HY5 during light-regulated development of *Arabidopsis*. *Nature* 405, 462-466.
- Osterlund, M.T., Wei, N., and Deng, X.W. (2000b). The roles of photoreceptor systems and the COP1-targeted destabilization of HY5 in light control of *Arabidopsis* seedling development. *Plant Physiol* 124, 1520-1524.
- Oyama, T., Shimura, Y., and Okada, K. (1997). The *Arabidopsis* HY5 gene encodes a bZIP protein that regulates stimulus-induced development of root and hypocotyl. *Genes Dev* 11, 2983-2995.
- Palágyi, A., Terecskei, K., Adám, E., Kevei, E., Kircher, S., Mérai, Z., Schäfer, E., Nagy, F. and Kozma-Bognár, L. (2010). Functional analysis of amino-terminal domains of the photoreceptor phytochrome B. *Plant Physiol* 153, 1834-1845.
- Park, E., Kim, J., Lee, Y., Shin, J., Oh, E., Chung, W.I., Liu, J.R., Choi, G. (2004). Degradation of phytochrome interacting factor 3 in phytochrome-mediated light signaling. *Plant Cell Physiol* 136, 968-975.
- Parks, B.M., Quail, P.H. (1993). hy8, a new class of *Arabidopsis* long hypocotyl mutants deficient in functional phytochrome A. *Plant Cell* 1993 5, 39-48.
- Pratt, L.H. (1994). Distribution and localisation of phytochrome within the plant. In: Kendrick RE, Kronenberg GHM, eds. *Photomorphogenesis in plants*, 2nd edn. Dordrecht, The Netherlands: Kluwer Academic Publishers, 163-185.
- Qin, M., Khun, R., Moran, S., Quail, P.H. (1997). Overexpressed phytochrome C has similar photosensory specificity to phytochrome B but a distinctive capacity to enhance primary leaf expansion. *Plant J* 12, 1163-1172.
- Quail, P. H. (2000). Phytochrome interacting factors. *Semin Cell Dev Biol* 11, 457-466.
- Quail, P.H. (1997). An emerging map of the phytochromes. *Plant Cell Environ* 20, 657-665
- Quail, P.H. (2002). Phytochrome photosensory signalling networks. *Nat Rev Mol Cell Biol* 3, 85-93.
- Quail, P.H., Briggs, W.R., Chory, J., Hangarter, R.P., Harberd, N.P., Kendrick, R.E., Koornneef, M., Parks, B., Sharrock, R.A., Schäfer, E., Thompson, W.F., Whitelam, G.C. (1994). Spotlight on Phytochrome Nomenclature. *Plant Cell* 6, 468-471.

- Rausenberger, J., Tscheuschler, A., Nordmeier, W., Wüst, F., Timmer, J., Schäfer, E., Fleck, C. and Hiltbrunner, A. (2011). Photoconversion and Nuclear Trafficking Cycles Determine Phytochrome A's Response Profile to Far-Red Light. *Cell* 146, 813-825.
- Rizzini, L., Favory, J.J., Cloix, C., Faggionato, D., O'Hara, A., Kaiserli, E., Baumeister, R., Schäfer, E., Nagy, F., Jenkins, G.I., Ulm, R. (2011). Perception of UV-B by the Arabidopsis UVR8 protein, *Science*. 332, 103-106.
- Rösler, J., Klein, I. and Zeidler, M. (2007). Arabidopsis *fhl/fhy1* double mutant reveals a distinct cytoplasmic action of phytochrome A. *Proc Natl Acad Sci USA* 104, 10737 - 10742.
- Saijo, Y., Sullivan, J.A., Wang, H., Yang, J., Shen, Y., Rubio, V., Ma, L., Hoecker, U., Deng, X.W. (2003). The COP1-SPA1 interaction defines a critical step in phytochrome A-mediated regulation of HY5 activity. *Genes Dev* 17, 2642-2647.
- Saijo, Y., Zhu, D., Li, J., Rubio, V., Zhou, Z., Shen, Y., Hoecker, U., Wang, H. and Deng, X.W. (2008). Arabidopsis COP1/SPA1 complex and FHY1/FHY3 associate with distinct phosphorylated forms of phytochrome A in balancing light signaling. *Mol Cell* 31, 607-613.
- Sakai, T., Kagawa, T., Kasahara, M., Swartz, T.E., Christie, J.M., Briggs, W.R., Wada, M., Okada, K. (2001). Arabidopsis *nph1* and *npl1*: blue light photoreceptors that mediate both phototropism and chloroplast relocation. *Proc Natl Acad Sci USA* 98, 6969-6974.
- Sakamoto, K. and Nagatani, A. (1996). Nuclear localization activity of phytochrome B. *Plant J* 10, 859-868.
- Sambrook, J., Fritsch, E.F., and Maniatis, T. (1989). *Molecular Cloning: A Laboratory Manual*. NY: Cold Spring Harbor Laboratory Press.
- Schäfer E. and Bowler C. (2002). Phytochrome-mediated photoperception and signal transduction in higher plants. *EMBO Rep* 3, 1042-1048.
- Schäfer, E. and Nagy, F. (Eds.). (2005). *Photomorphogenesis in Plants and Bacteria*, 3rd Edition. Dordrecht, The Netherlands, Springer.
- Schäffner, W. and Weissmann, C. (1973). A rapid, sensitive, and specific method for the determination of protein in dilute solution. *Anal Biochem* 56, 502-514.
- Schneider-Poetsch, H.A., Braun, B., Marx, S. and Schaumburg, A. (1991). Phytochromes and bacterial sensor proteins are related by structural and functional homologies: hypothesis on phytochrome-mediated signal transduction. *FEBS Lett* 281, 245-249.
- Schwechheimer, C., and Deng, X.W. (2000). The COP/DET/FUS proteins-Regulators of eukaryotic growth and development. *Semin Cell Dev Biol* 11, 495-503.
- Seo, H.S., Watanabe, E., Tokutomi, S., Nagatani, A., and Chua, N.H. (2004). Photoreceptor ubiquitination by COP1 E3 ligase desensitizes phytochrome A signaling. *Genes Dev* 18, 617-622.
- Sharrock, R.A. and Clack, T. (2002). Patterns of expression and normalized levels of the five Arabidopsis phytochromes. *Plant Physiol* 130, 442 - 456.
- Sharrock, R.A. and Clack, T. (2004). Heterodimerization of type II phytochromes in Arabidopsis. *Proc Natl Acad Sci U S A*. 101, 11500-11505.

## REFERENCES

- Sharrock, R.A. and Quail, P.H. (1989). Novel phytochrome sequences in *Arabidopsis thaliana*: structure, evolution, and differential expression of a plant regulatory photoreceptor family. *Genes Dev* 3, 1745-1757.
- Shen, H., Zhu, L., Castillon, A., Majee, M., Downie, B., Huq, E. (2008). Light-indicated phosphorylation and degradation of the negative regulator PHYTOCHROME INTERACTING FACTOR 1 from *Arabidopsis* depend upon its direct physical interactions with photoactivated phytochromes. *Plant Cell* 20, 1586-1602.
- Shen, Y., Zhou, Z., Feng, S., Li, J., Tan-Wilson, A., Qu, L.J., Wang, H. and Deng, X.W. (2009). Phytochrome A mediates rapid red light-induced phosphorylation of *Arabidopsis* FAR-RED ELONGATED HYPOCOTYL1 in a low fluence response. *Plant Cell* 21, 494-506.
- Shimizu-Sato, S., Huq, E., Tepperman, J.M., Quail, P.H. (2002). A light-switchable gene promoter system. *Nature Biotechnology* 20, 1041-1044.
- Shinomura, T., Nagatani, A., Hanzawa, H., Kubota M., Watanabe, M., Furuya, M. (1996). Action spectra for phytochrome A- and B-specific photoinduction of seed germination in *Arabidopsis thaliana*. *Proc Natl Acad Sci USA* 93, 8129-8133.
- Shinomura, T., Uchida, K., Furuya, M. (2000). Elementary processes of photoperception by phytochrome A for high-irradiance response of hypocotyl elongation in *Arabidopsis*. *Plant Physiol* 122, 147-156.
- Sineshchekov, V.A. (1995). Photobiophysics and photobiochemistry of the heterogenous phytochrome system. *Biochimica Biophysica Acta* 1228, 125-164.
- Singh, B.R., and Song, P.S. (1989). Interactions between native oat phytochrome and tetrapyrroles. *Biochim Biophys Acta* 996, 62-69.
- Singh, B.R., and Song, P.S. (1990). A differential molecular topography of the Pr and Pfr forms of native oat phytochrome as probed by fluorescence quenching. *Planta* 181, 263-267.
- Singh, B.R., Chai, Y.G., Song, P.S., Lee, J., Robinson, G.W. (1988). A photoreversible conformational change in 124 kDa *Avena* phytochrome. *Biochim Biophys Acta* 936, 395-405.
- Singh, B.R., Choi, J., Kwon, T., Song, P.S. (1989). Use of bilirubin oxidase for probing chromophore topography in tetrapyrrole proteins. *J Biochem Biophys Methods* 18, 135-148.
- Smith, H. (2000). Phytochromes and light signal perception by plants - an emerging synthesis. *Nature* 407, 585-591.
- Smith, H., and Whitelam, G.C. (1990). Phytochrome, a family of photoreceptors with multiple physiological roles. *Plant, Cell and Environment* 13, 695-707.
- Speth, V., Otto, V., Schäfer, E. (1986). Intracellular localisation of phytochrome in oat coleoptiles by electron microscopy. *Planta* 168, 299-304.
- Stockhaus, J., Nagatani, A., Halfter, U., Kay, S., Furuya, M., Chua, N.H. (1992). Serine-to-alanine substitutions at the aminoterminal region of phytochrome A result in an increase in biological activity. *Genes Dev* 6, 2364-2372.
- Strasser, B., Sánchez-Lamas, M., Yanovsky, M.J., Casal, J.J., Cerdán, P.D. (2010). *Arabidopsis thaliana* life without phytochromes. *Proc Natl Acad Sci U S A* 107, 4776-4781.

- Tepperman, J.M., Hwang, Y.S., Quail, P.H. (2006). *phyA* dominates in transduction of red-light signals to rapidly responding genes at the initiation of Arabidopsis seedling de-etiolation. *Plant J* 48, 728-742.
- Tepperman, J.M., Zhu, T., Chang, H.S., Wang, X., Quail, P.H. (2001). Multiple transcription-factor genes are early targets of phytochrome A signaling. *Proc Natl Acad Sci U S A*. 98, 9437-9442.
- Tokuhsa, J.G., Daniels, S.M., Quail, P.H. (1985). Phytochrome in green tissue: spectral and immunochemical evidence for two distinct molecular species of phytochrome in lightgrown *Avena sativa* L. *Planta* 164, 321-32.
- Toledo-Ortiz, G., Kiryu, Y., Kobayashi, J., Oka, Y., Kim, Y., Nam, H.G., Mochizuki, N., Nagatani, A. (2010). Subcellular sites of the signal transduction and degradation of phytochrome A. *Plant Cell Physiol* 51, 1648-1660.
- Trupkin, S.A., Debrieux, D., Hiltbrunner, A., Fankhauser, C. and Casal, J.J. (2007). The serine-rich N-terminal region of Arabidopsis phytochrome A is required for protein stability. *Plant Mol Biol* 63, 669-678.
- Ulm, R., Baumann, A., Oravec, A., Mate, Z., Adam, E., Oakeley, E.J., Schäfer, E., and Nagy, F. (2004). Genome-wide analysis of gene expression reveals function of the bZIP transcription factor HY5 in the UV-B response of Arabidopsis. *Proc Natl Acad Sci USA* 101, 1397- 1402.
- Vierstra, R. and Quail, P. (1983). Purification and initial characterization of 124-Kilodalton phytochrome from *Avena*. *Biochemistry* 22, 3290-3295.
- Vierstra, R., Quail, P., Hahn, T., Song, PS. (1987). Comparison of the protein conformations between different forms (Pr and Pfr) of native (124 kDa) and degraded (118/114 kDa) phytochromes from *Avena sativa*. *Photochem Photobiol* 45, 429-432.
- Wagner, D., Fairchild, C.D., Kuhn, R.M. and Quail, P.H. (1996a). Chromophore-bearing NH2-terminal domains of phytochromes A and B determine their photosensory specificity and differential light lability. *Proc Natl Acad Sci. USA* 93, 4011-4015.
- Wagner, D., Koloszvari, M., and Quail, P.H. (1996b). Two Small Spatially Distinct Regions of Phytochrome B Are Required for Efficient Signaling Rates. *The Plant Cell* 8, 859-871.
- Wang, H. and Deng, X.W. (2002). Arabidopsis FHY3 defines a key phytochrome A signaling component directly interacting with its homologous partner FAR1. *EMBO J* 21, 1339-1349.
- Whitelam, G.C., Johnson, E., Peng, J., Carol, P., Anderson, M.L., Cowl, J.S. and Harberd, N.P. (1993). Phytochrome A null mutants of Arabidopsis display a wild-type phenotype in white light. *Plant Cell* 5, 757-768.
- Wolf, I., Kircher, S., Fejes, E., Kozma-Bognar, L., Schäfer, E., Nagy, F., Adam, E. (2011). Light-regulated nuclear import and degradation of Arabidopsis phytochrome-A N terminal fragments. *Plant Cell Physiol* 52, 361-372.
- Wu, S.H., Lagarias, J.C. (2000). Defining the bilin lyase domain: lessons from the extended phytochrome superfamily. *Biochemistry* 39, 13487-13495.

- Xu, Y., Parks, B.M., Short, T.W. and Quail, P.H. (1995). Missense mutations define a restricted segment in the C-terminal domain of phytochrome A critical to its regulatory activity. *Plant Cell* 7, 1433-1443.
- Yamaguchi, R., Nakamura, M., Mochizuki, N., Kay, S.A., Nagatani, A. (1999). Light-dependent translocation of a phytochrome B-GFP fusion protein to the nucleus in transgenic *Arabidopsis*. *J. Cell Biol* 145, 437-445.
- Yamaguchi, S., Smith, M.W., Brown, R.G., Kamiya, Y., Sun, T. (1998). Phytochrome regulation and differential expression of gibberellin 3beta-hydroxylase genes in germinating *Arabidopsis* seeds. *Plant Cell* 10, 2115-2126.
- Yanagawa, Y., Sullivan, J.A., Komatsu, S., Gusmaroli, G., Suzuki, G., Yin, J., Ishibashi, T., Saijo, Y., Rubio, V., Kimura, S., Wang, J., and Deng, X.W. (2004). *Arabidopsis* COP10 forms a complex with DDB1 and DET1 in vivo and enhances the activity of ubiquitin conjugating enzymes. *Genes Dev* 18, 2172-2181.
- Yang, S.W., Jang, I.C., Henriques, R. and Chua, N.H. (2009). FAR-RED ELONGATED HYPOCOTYL1 and FHY1-LIKE associate with the *Arabidopsis* transcription factors LAF1 and HFR1 to transmit phytochrome A signals for inhibition of hypocotyl elongation. *Plant Cell* 21, 1341-1359.
- Yanovsky, M.J., Casal, J.J., Luppi, J.P. (1997). The VLF loci, polymorphic between ecotypes *Landsberg erecta* and *Columbia*, dissect two branches of phytochrome A signal transduction that correspond to very-lowfluence and high-irradiance responses. *Plant J* 12, 659-667.
- Yanovsky, M.J., Casal, J.J., Whitelam, G.C. (1995). Phytochrome A, phytochrome B and HY4 are involved in hypocotyl growth responses to natural radiation in *Arabidopsis*: weak de-etiolation of the phyA mutant under dense canopies. *Plant, Cell and Environment* 18, 788-794.
- Yanovsky, M.J., Luppi, J.P., Kirchbauer, D., Ogorodnikova, O.B., Sineshchekov, V.A., Adam, E., Kircher, S., Staneloni, R.J., Schäfer, E., Nagy, F., and Casal, J.J. (2002). Missense mutation in the PAS2 domain of phytochrome A impairs subnuclear localization and a subset of responses. *Plant Cell* 14, 1591-1603.
- Yeh, K.C. and Lagarias, J.C. (1998). Eukaryotic phytochromes: light-regulated serine/threonine protein kinases with histidine kinase ancestry. *Proc Natl Acad Sci USA* 95, 13976-13981.
- Yi, C., and Deng, X.W. (2005). COP1 - From plant photomorphogenesis to mammalian tumorigenesis. *Trends Cell Biol* 15, 618-625.
- Zeidler, M., Zhou, Q., Sarda, X., Yau, C.P. and Chua, N.H. (2004). The nuclear localization signal and the C-terminal region of FHY1 are required for transmission of phytochrome A signals. *Plant J* 40, 355-365.
- Zhou, Q., Hare, P.D., Yang, S.W., Zeidler, M., Huang, L.F. and Chua, N.H. (2005). FHL is required for full phytochrome A signaling and shares overlapping functions with FHY1. *Plant J* 43, 356-370.
- Zhu, D., Maier, A., Lee, J.H., Laubinger, S., Saijo, Y., Wang, H., Qu, L.J., Hoecker, U., Deng, X.W. (2008). Biochemical characterization of *Arabidopsis* complexes containing CONSTITUTIVELY PHOTOMORPHOGENIC1 and SUPPRESSOR OF PHYA proteins in light control of plant development. *Plant Cell* 20, 2307-2323.

## REFERENCES

- Zhu, Y., Tepperman, J. M., Fairchild, C. D. and Quail, P. (2000). Phytochrome B binds with greater apparent affinity than phytochrome A to the basic helix-loop-helix factor PIF3 in a reaction requiring the PAS domain of PIF3. *Proc Natl Acad Sci USA* 97, 13419-13424.

AA #	17	18	19	20	21	22	23	24	25	26	27	28	29	30	31	32	33	34	35	36
<b>AA Wt</b>	<b>R</b>	<b>H</b>	<b>S</b>	<b>A</b>	<b>R</b>	<b>I</b>	<b>I</b>	<b>A</b>	<b>Q</b>	<b>T</b>	<b>T</b>	<b>V</b>	<b>D</b>	<b>A</b>	<b>K</b>	<b>L</b>	<b>H</b>	<b>A</b>	<b>D</b>	<b>F</b>
<b>SS</b>	C	C	H	H	H	H	H	H	H	C	C	C	C	H	H	H	H	C	C	C
H	0.306	0.359	0.49	0.548	0.561	0.576	0.572	0.535	0.414	0.353	0.318	0.392	0.389	0.499	0.489	0.476	0.415	0.391	0.339	0.395
E	0.024	0.041	0.09	0.168	0.267	0.335	0.332	0.288	0.233	0.21	0.174	0.132	0.058	0.062	0.239	0.285	0.225	0.182	0.135	0.099
C	0.67	0.6	0.42	0.284	0.172	0.09	0.097	0.177	0.354	0.438	0.508	0.476	0.553	0.439	0.271	0.238	0.36	0.427	0.526	0.506
<b>AA phyA-5</b>	<b>R</b>	<b>H</b>	<b>S</b>	<b>A</b>	<b>R</b>	<b>I</b>	<b>I</b>	<b>A</b>	<b>Q</b>	<b>T</b>	<b>T</b>	<b>V</b>	<b>D</b>	<b>V</b>	<b>K</b>	<b>L</b>	<b>H</b>	<b>A</b>	<b>D</b>	<b>F</b>
<b>SS</b>	C	C	C	H	H	H	H	H	C	C	C	C	C	C	H	H	C	C	C	C
H	0.245	0.304	0.391	0.454	0.464	0.49	0.488	0.458	0.335	0.276	0.247	0.299	0.296	0.409	0.405	0.395	0.344	0.346	0.304	0.364
E	0.035	0.051	0.103	0.196	0.33	0.414	0.408	0.356	0.287	0.255	0.22	0.176	0.093	0.116	0.316	0.352	0.271	0.217	0.161	0.112
C	0.72	0.644	0.505	0.35	0.206	0.097	0.103	0.187	0.379	0.469	0.534	0.524	0.611	0.475	0.279	0.253	0.385	0.437	0.535	0.524

Figure 19. Predicted protein structure of phyA

AA# - amino acid number; AA Wt, AA phyA-5 – amino acid sequences of wild-type and mutated phyA, respectively; SS – predicted secondary structure; H, E, C - probabilities of  $\alpha$ -helical folding,  $\beta$ -sheet and random coil, respectively. Yellow marking indicates the amino acid in position 30, mutated in phyA-5. Grey color selections indicate the predicted  $\alpha$ -helical structure.

## ACKNOWLEDGEMENTS

I would like to express my deepest gratitude to the following:

**Prof. Dr. Ferenc Nagy**, for giving me a possibility to be a part of a wonderful group, for pushing me over my limits, for being an exceptional role model;

**Prof. Dr. George Coupland** and **Dr. Seth Devis** for presenting me with the opportunity to participate in ADOPT;

**Dr. Laszlo Kozma-Bognar**, for the never-ceasing optimism, for moral support and for being always available to help me;

**Dr. Andras Viczian**, for the scientific guidance, for the critical reading of my PhD manuscript, and for being an example of the devoted scientist;

**Dr. Erzsébet Fejes**, for incredible and constant assistance with all the administrative troubles over the years, for reviewing my manuscript and for sharing my passion about the opera;

**Dr. Eva Adam**, for the ability to answer any question at any time;

**Peter Gyula**, **Balazs Feher**, **Anita Hajdu**, **Kata Terecskei** and **Janos Bindics**, for being great colleagues and teammates;

**Ralf Petri**, for invaluable support and good advises during my first and the toughest year of PhD;

**Dr. Nora Bujdoso**, for great help with application, translations and bureaucracy.

**Amanda Devis**, for taking good care of me during my visit to Cologne and making me feel welcome.

**Petro Khoroshyy**, **Leyla Abasova**, **Zinaida Yudina**, for being great friends, for sharing with me the best, the worst and the funniest moments of an incredible “let’s get a PhD” experience!

To my parents, brother and my husband: I’m grateful for your support, your patience and your faith in me.

## LEBENS LAUF

Name: Vladyslava Sokolova  
Anschrift: 03134 G-Barski str-3, app 268, Kiew, Ukraine  
Geburtsdatum: 13.07.1981  
Geburtsort: Kiew, Ukraine  
Staatsangehörigkeit: ukrainisch  
Familienstand: verheiratet

Bildung und Beruf:

1995-1998: Polytechnischen Lyzeum, Kiew (chemisch-Biologischen Fakultät)

1998-2002: Nationale Technische Universität der Ukraine "KPI", Fakultät für Biotechnologie und Biotechnik  
Bachelor für Chemische Engineering und Technologie

2002-2004: Nationale Technische Universität der Ukraine "KPI", Fakultät für Biotechnologie und Biotechnik  
Biotechnologie, MSc  
Titel der Diplomarbeit: Photoperiod-mediated regulation of flowering time genes CO and FT in Arabidopsis

2004 - 2007 Doktorandin im Fach Botanik an der Universität zu Köln; Experimentelle Arbeit durchgeführt am Biological Research Center of the Hungarian Academy of Science (Szeged, Hungary), gefördert durch ADOPT-Programm

2007-2011 Biological Research Center of the Hungarian Academy of Science (Szeged, Hungary)  
Wissenschaftlicher Mitarbeiterin

## **EIDESSTATTLICHE ERKLÄRUNG**

Ich versichere, daß die von mir vorgelegte Dissertation selbständig angefertigt, die benutzten Quellen und Hilfsmittel vollständig angegeben und die Stellen der Arbeit - einschließlich Tabellen, Karten und Abbildungen -, die anderen Werken im Wortlaut oder dem Sinn nach entnommen sind, in jedem Einzelfall als Entlehnung kenntlich gemacht habe; daß diese Dissertation noch keiner anderen Fakultät oder noch nicht veröffentlicht worden ist sowie, daß ich eine solche Veröffentlichung vor Abschluß des Promotionsverfahrens nicht vornehmen werde. Die Bestimmungen dieser Promotionsordnung sind mir bekannt. Die von mir vorgelegte Dissertation ist von Prof. Dr. George Coupland betreut worden.

Teilpublikation:

Sokolova V, Bindics J, Kircher S, Adám E, Schäfer E, Nagy F, Viczián A. Missense Mutation in the N Terminal of Phytochrome A Disrupts the Nuclear Import of the Photoreceptor. *Plant Physiol.* 2011 Oct 10.